# SANDIA REPORT

SAND2005-1548
Unlimited Release
Printed March 2005

# Low-Cost Inertial Measurement Unit

T. J. Deyle

Prepared by
Sandia National Laboratories
Albuquerque, New Mexico 87185 and Livermore, California 94550

Sandia is a multiprogram laboratory operated by Sandia Corporation,
a Lockheed Martin Company, for the United States Department of Energy's
National Nuclear Security Administration under Contract DE-AC04-94AL85000.



Sandia National Laboratories

Issued by Sandia National Laboratories, operated for the United States Department of Energy
by Sandia Corporation.



Available to DOE and DOE contractors from
U.S. Department of Energy
Office of Scientific and Technical Information
P.O. Box 62
Oak Ridge, TN 37831

Telephone: (865)576-8401
Facsimile: (865)576-5728
E-Mail: reports@adonis.osti.gov
Online ordering: http://www.osti.gov/bridge

Available to the public from
U.S. Department of Commerce
National Technical Information Service
5285 Port Royal Rd
Springfield, VA 22161

Telephone: (800)553-6847
Facsimile: (703)605-6900
E-Mail: orders@ntis.fedworld.gov
Online order: http://www.ntis.gov/help/ordermethods.asp?loc=7-4-0#online

SAND 2005-1548
Unlimited Release
Printed March 2005

# Low-Cost Inertial Measurement Unit

Travis J. Deyle

Sandia National Laboratories
PO Box 969
Livermore, CA 94551-0969

## ABSTRACT

Sandia National Laboratories performs many expensive tests using inertial measurement units (IMUs) – systems that use accelerometers, gyroscopes, and other sensors to measure flight dynamics in three dimensions. For the purpose of this report, the metrics used to evaluate an IMU are cost, size, performance, resolution, upgradeability and testing. The cost of a precision IMU is very high and can cost hundreds of thousands of dollars. Thus the goals and results of this project are as follows:

1.) Examine the data flow in an IMU and determine a generic IMU design.

2.) Discuss a high cost IMU implementation and its theoretically achievable results.

3.) Discuss design modifications that would save money for suited applications.

4.) Design and implement a low cost IMU and discuss its theoretically achievable results.

5.) Test the low cost IMU and compare theoretical results with empirical results.

6.) Construct a more stream-lined printed circuit board design—reducing noise, increasing capabilities, and constructing a self-contained unit.

Using these results, we can compare a high cost IMU versus a low cost IMU using the metrics from above. Further, we can examine and suggest situations where a low cost IMU could be used instead of a high cost IMU for saving cost, size, or both.

## Acknowledgements

I would like to extend a special thanks to my mentor Rene Bierbaum. Her guidance and assistance has been greatly appreciated in completing this project and writing this paper.

## Table of Contents

## Table of Figures



## Table of Tables



## Table of Appendices

# I. INTRODUCTION

When performing a flight test, we collect data on many aspects of the flight. Flight path and the forces the object undergoes are particularly important aspects of the flight. To analyze such high-level data, some fundamental information is required. Typically this includes things such as velocity, acceleration, and rotation in all three axes, as well as a sense of overall position. There are many different and independent methods of gathering such data and often such methods are used in tandem. One method is the Global Positioning System (GPS) to gather the precise location using satellites. Another method is to use an Inertial Measurement Unit (IMU) to gather the data and then extract a flight path and location via dead reckoning. These can also be used together, with the GPS providing a periodic and accurate determination of position, while the IMU is used to interpolate between these GPS points using dead reckoning.

When designing an IMU, there are generally two key factors that must be considered: 1.) cost and 2.) resolution/capability. Unfortunately, the two are directly correlated. A higher cost IMU correlates directly to more capabilities and higher resolution. My task was to design a low-cost IMU and to evaluate the capabilities of such a system. In addition, I explored the use of a reconfigurable system that allowed for a wide range of performance/cost tradeoffs to be explored by varying the sensor selections.

# II. GENERIC IMU

An IMU is basically a collection of sensors whose output is used to determine the motion characteristics of a body. Therefore, it is more-or-less a specialized datalogger-transmitter. The basic flow of data in an IMU is shown in Figure 1 below.

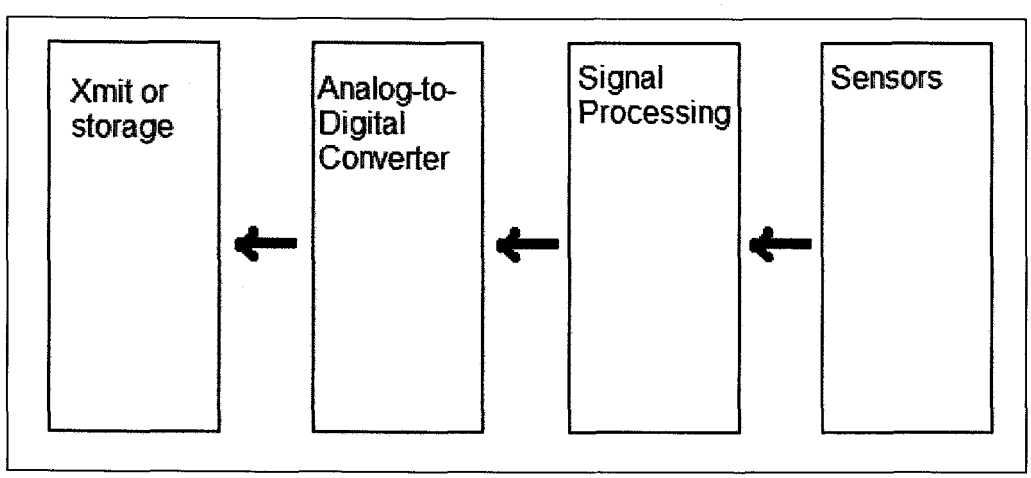


**Figure 1: Data Flow in the IMU**

The sensors and their signal processing are very system-dependent. They are dictated by the required resolution and precision for a particular scenario. However, it is simple to create a generic Analog-to-Digital Converter (ADC) and transmit or storage unit. For example, a microprocessor with on-board ADC could be used to perform the conversion and transmit or store the data. If more resolution is required, dedicated ADCs could be controlled via a microcontroller, which could then control transmission or storage. Alternatively, field programmable gate arrays (FPGA) or digital signal processors (DSP) could be used to develop this system. The important thing is that the system be reconfigurable and upgradeable.

By making the system reconfigurable and upgradeable, different sensors can be tested and validated by a single IMU unit. Further, additional sensors or inputs can be added for different measurements.

# III. HIGH COST IMU

As one would expect, a high cost IMU features high-precision and high-resolution components. Information from manufacturers regarding such an IMU's components is typically rather limited (due to export controls). However, by doing some internet searches, I was able to find a few devices that would work in such a system. The IMU discussed below is entirely theoretical and just serves as an example for price vs. capability comparisons.

## *A. IMPLEMENTATION & CAPABILITIES*

For the high-resolution and high-precision IMU, we will look at the following sensors:

| Sensor | Photograph | Cost & Size | Basic Properties |
|---|---|---|---|
| Honeywell QA3000 Single-Axis Accelerometer | 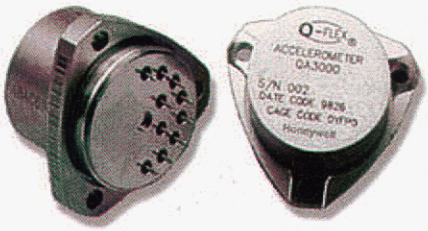 | Between $7,500-$15,000<br><br>> 1 $in^3$ | Resolution: < 1µg<br>Range: ±60g<br>Bandwidth: > 300 Hz<br>Noise: < 7 µg-rms |
| Honeywell GG440 Single-Axis Rate-Gyroscope | 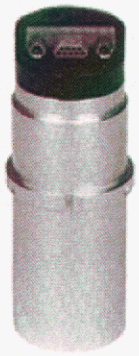 | Unknown (estimated $1000's)<br><br>1" diameter by 2.6" length | Resolution: < 0.02°/sec<br>Range: ±1200°/sec<br>Bandwidth: > 400 Hz |
| Honeywell HMC2003 Three-Axis Magnetometer | 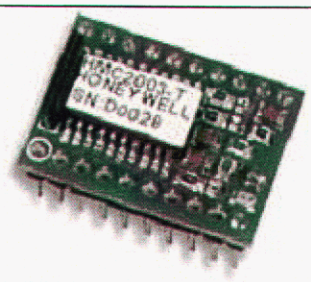 | $200<br><br>20-pin Wide DIP Package | Resolution: < 40 µgauss<br>Range: ± 2 gauss<br>Bandwidth: 1 kHz |

**Table 1: High-Precision IMU Components**

Note that since the accelerometers and rate gyroscopes are single-axis devices, three of them must be used to measure the dynamics of a body. This effectively triples the dollar amounts given above.

For our theoretical high-cost IMU, assume a sampling rate of 800 Hz — thus the analog bandwidth is 400 Hz by the Nyquist Theorem. This data rate is adequate to measure many of the flight characteristics of interest. The 400 Hz analog bandwidth is feasible with all of the devices in Table 1. Further, assume that the ADC being used operates off a +5V power supply.

Let's consider the capability of the accelerometer. The QA3000 has an output from ±10V with a ±60g range spread over the output voltage (assuming perfect linearity). Since the ADCs work off 5V, the output needs to go through some signal processing to be between 0 and 5V. Consider the following generic circuit in Figure 2 below.

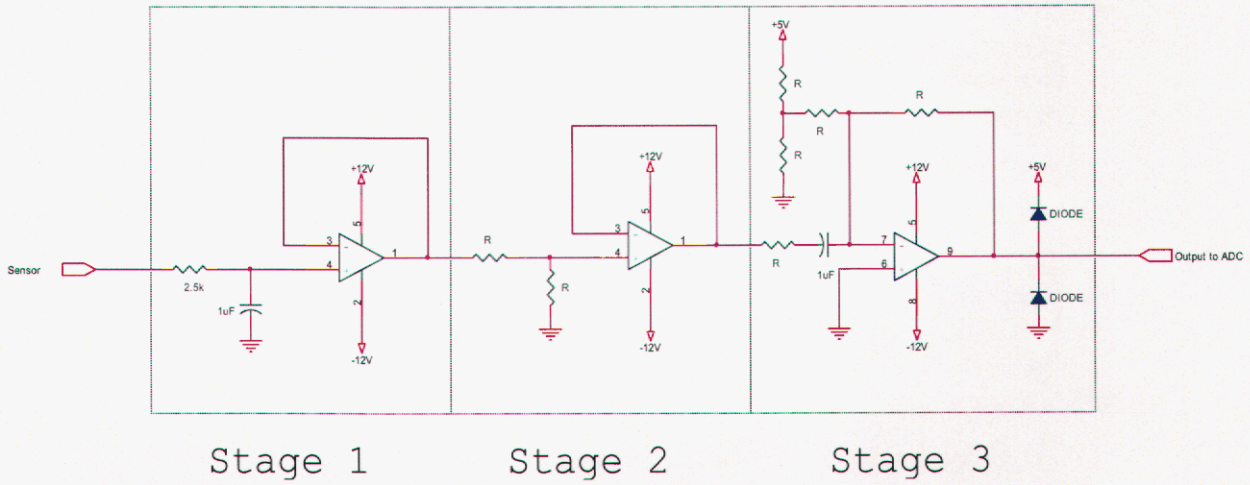


**Figure 2: Sample Signal Processing**

The op-amps are powered off ±12V while all other supplies are +5V. The signal processing realized in the above circuit has a variety of important functions, which are summarized below by stages.

1. Stage 1 is a simple low-pass filter tuned for 400 Hz. This stage has two purposes. First, it eliminates possible aliasing when the signal is sampled. Second, the band-limiting helps eliminate some of the Additive White Gaussian Noise (AWGN), which is dependent on bandwidth, in the sensor output to provide better noise characteristics. The output is buffered to the next stage.

2. Stage 2 attenuates the ±12V signal from Stage 1 to ±2.5V using a voltage divider. The output is then buffered to the next stage.

3. Stage 3 sums the output from Stage 2 with a +2.5V reference at the input of the op-amp. This adjusts the signal range to be between 0 and 5V for the ADC. The diodes clamp the op-amp output to 0 to 5V to prevent spurious signals from damaging the ADC. This stage also acts as a buffer between the signal processing and the ADC.

It should be noted that the full sensor output range is present at the output of Stage 3. The sensitivity of the output is dependent on the ADC being used. For a given ADC, we can increase sensitivity (within noise constraints) at the expense of the output range. For example, consider an amplifying stage between Stages 1 and 2. If the gain is two, the Stage 3 output range is now ±30g and the sensitivity/resolution is doubled. Thus, we can add some functionality by using a variable gain stage, as the range and resolution could be dynamically altered. Overall, this is an important tradeoff between sensor range and required ADC resolution. Another option is just to use an ADC with sufficient resolution to perform over the entire range and sensitivity of the sensor. When such high bandwidth links are available, the added ADC bits may be the best option. However, when communication bandwidth is at a premium, the variable gain stage may be the best option.

Now we can determine the resolution and required ADC capabilities. From the specification of the QA3000, the noise floor is approximately 7μg-rms. Thus, we should target an ADC that gives this same resolution per digit as well as covering the entire operational range of the sensor (i.e. ±60g from the signal processing using unity gain in an optional amplifier between Stages 1 and 2). The signal has the following property:

$$\frac{5.00}{\pm 60}\frac{V}{g} = \frac{5.00}{120}\frac{V}{g} = 0.042\frac{V}{g} = 0.042\frac{\mu V}{\mu g}$$

As an example, consider a 24-bit ADC. From a 24-bit ADC, we have a resolution of:

$$\frac{5.00}{2^{24}}\frac{V}{digits} = 0.298\frac{\mu V}{digit}$$

Thus our system has a resolution of:

$$0.298\frac{\mu V}{digit} \times \frac{1}{0.042}\frac{\mu g}{\mu V} = 7.09\frac{\mu g}{digit}$$

Since our noise is basically the same magnitude (7μg-rms), the last bit can be attributed to noise.

The above calculations show that a 24-bit ADC would in fact be perfect. The Texas Instruments ADS1211 4-channel 24-bit Analog-to-Digital Converter (≈ $15) would fit this requirement. It supports sampling of 16,000 samples/second (or 4,000 samples/second/channel). For transmission purposes, it may be possible to discard some

of the upper bits of the signal (depending on the desired range), allowing for fewer bits to be transmitted. Note too that there is no advantage to using an ADC with more bits since we already have a resolution that extends to the noise floor.

Performing similar calculations for the other two devices shows us that the same ADC (and similar signal conditioning) would work for the rate-gyroscopes and the magnetometer. These would yield resolutions at or near their noise floors. Further, a single ADC could be used and the analog signals could be time-division multiplexed via an analog multiplexer.

### *B. PRACTICAL PROBLEMS*

When dealing with such high resolution parts, there are a variety of very difficult hurdles when it comes to both construction and testing. What follows is a discussion of a few of these problems.

The first practical consideration is placement of parts on a device. For example, consider the accelerometers. Their *desired* function is to measure the linear acceleration of the body. If the accelerometers are placed near the edge of the flight body, then as the body begins rotating, the accelerometers would measure the angular acceleration of the body—but angular motion is the responsibility of the rate-gyroscopes! Further, the effect increases with increasing distance from the body's center of mass. The influence of this variable can be minimized by placing the accelerometers as close as possible to the body's center of mass. But with such sensitive sensors, this may not be enough. The accelerometers may need to compensate (either directly or during post-processing) for this rotational effect.

Another practical consideration involves construction. When mounting components, it is necessary to know their exact orientation. It is most desirable to mount them orthogonally to avoid post-processing calculations. The construction tolerances for mounting these devices must be *very* tight. To give some indication of just how tight, consider the accelerometers. Our bodies are accustomed to the constant 1g acceleration from the Earth's gravitational field. It is not uncommon for us to experience accelerations from 0g to 3g (roller coasters, for example). When sitting stationary, a sensor would feel the 1g acceleration when mounted parallel to the Earth's gravitational field, 0g when mounted perpendicularly, or some intermediate value when mounted at an angle. This is the notion of a tilt sensor depicted in Figure 3 below.

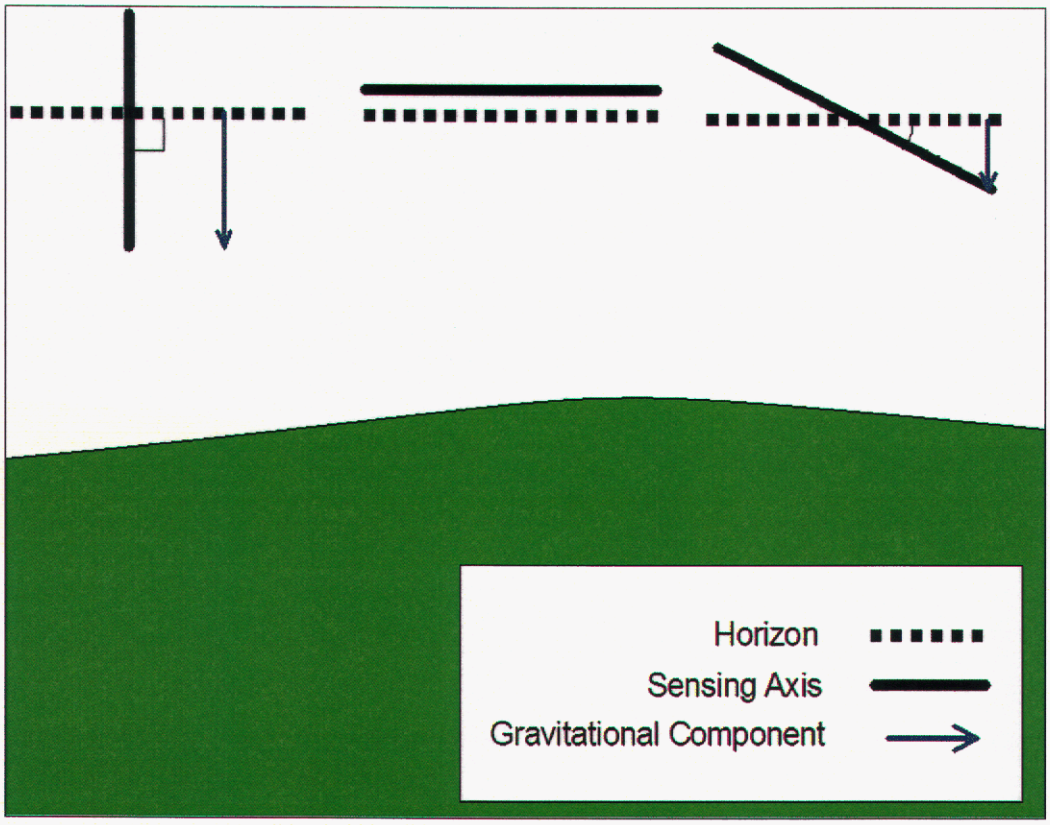


**Figure 3: Tilt Sensor Concept**

Using basic vector physics, we can calculate the component acceleration felt by the stationary sensor due to tilt. Consider the following drawing in Figure 4.

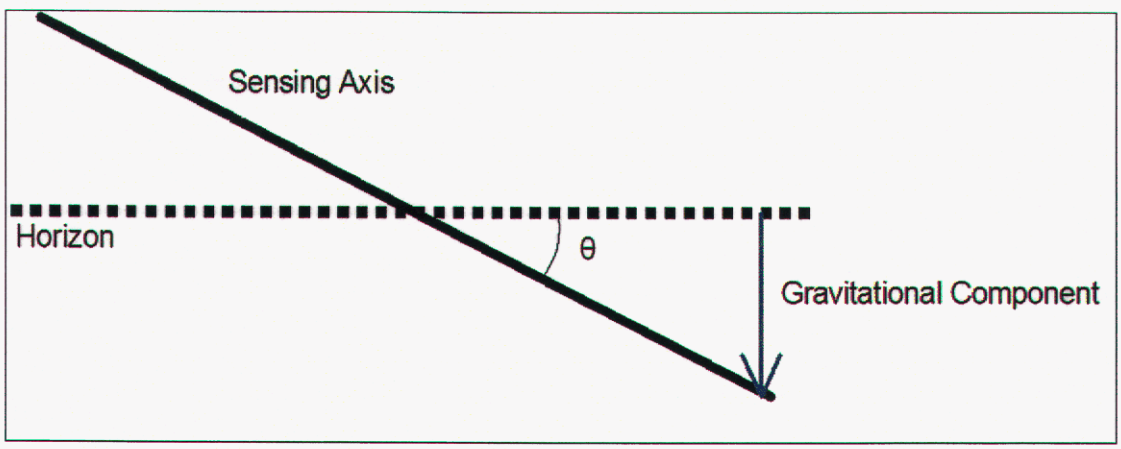


**Figure 4: Acceleration Computation Graphic**

The acceleration felt by the stationary sensor is given by:

$$A = 1g \times \sin(\theta^\circ)$$

Recalling from above that the QA3000 can easily distinguish 14μg, we can solve for the angle of tilt that corresponds to this acceleration.

$$\theta^\circ = \arcsin\left(14\mu g / 1g\right) = 0.0008^\circ$$

Thus a tilt of less than 1 milli-degree from the horizontal will adversely affect the accelerometers. This could be caused by something as small as tightening one screw more than another.

It should be noted that 14μg resolution represents a tilt from the vertical of approximately 0.3°. However, we are more concerned with the 'worst-case' scenario represented by a small tilt from the horizontal.

Note that the lack of orthogonality could perhaps be calibrated out, assuming that it was a constant effect. However, with such a small degree of tilt being considered, even the mounting in the testing bracket will have adverse affects. Problems are compounded if the sensor housings become loose.

### *C. TESTING CONSIDERATIONS*

Luckily, the practical problems with construction give some insight to possible testing methods. Using a 3-D gimbal to induce small amounts of tilt is probably the most straightforward, at least for the accelerometers. Recalling from above that the sensor can detect an incline of a mere 0.0008° rules out using hobby servo motors which only realistically provide 8 to 16 bits of resolution (not even close to the required 24). However, a mounting that uses gear-reduced stepper motors may work. Each step would correspond to a very small (and calculable) tilt. All that is necessary is to level the mounting to a known (and accurate) starting position. In this way, a very small and very accurate tilt is achievable to test our accelerometers' orthogonality. A similar system can be used to test both the magnetometer and rate gyroscopes.

# IV. LOW-COST IMU

In designing the low-cost IMU, the same generic principles discussed earlier come into play. The design is based on readily-available low-cost parts which allowed for flexibility and rapid design. The first step was to construct the prototype (wire-wrapped) shown in Figure 5 below.

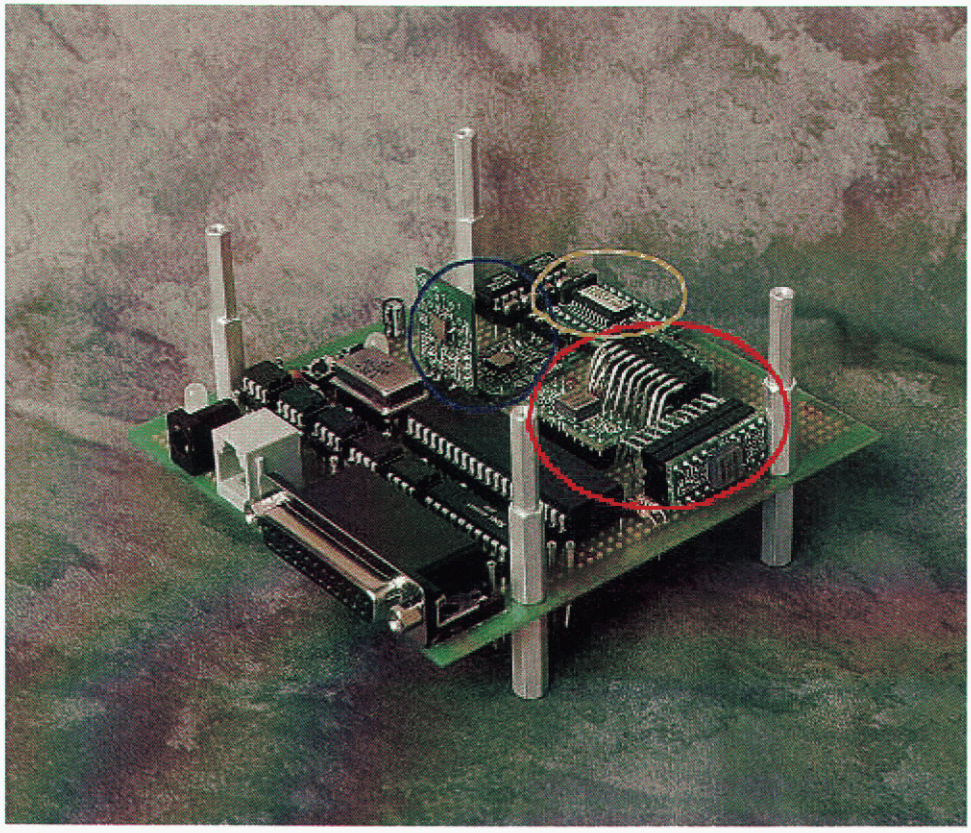

**Figure 5: Low-Cost IMU**

The prototype pictured above uses gyroscopes (red), accelerometers (blue), and a magnetometer (yellow) to measure acceleration, rotation, and orientation relative to Earth's magnetic field, respectively. The signals from these sensors (a total of 9 channels—3 axes for each of the 3 device types) are sampled by a microcontroller with onboard analog-to-digital converter. The digital values are then stored in EEPROMs for later retrieval and processing. After the sampling has completed (approximately 20 seconds of acquisition at 800 samples/channel/second), the data is sent to a PC for post processing via a serial connection. The attributes of these components is discussed subsequently.

*A. SENSORS*

In the robotics and hobby community, there are several vendors of low-cost Micro-Electro-Mechanical Systems (MEMS) accelerometers and rate gyroscopes. These MEMS devices are very capable, small, durable, and best of all, inexpensive. Further, the same magnetometer as the high-cost IMU can be used. It is a very capable and relatively inexpensive component. A summary of the devices used is contained in Table 2 below.

| Sensor | Photograph | Cost & Size | Basic Properties |
|---|---|---|---|
| Memsic MXR2312ML Dual-Axis Accelerometer | 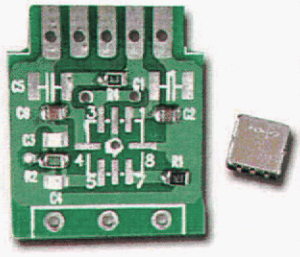 | $13<br><br>5 mm x 5 mm x 2 mm | Resolution: 1 mg<br>Range: ±2.0g<br>Bandwidth: 100 Hz<br>Sensitivity: 312 mV/g |
| Analog Devices ADXL203 Dual-Axis Accelerometer | 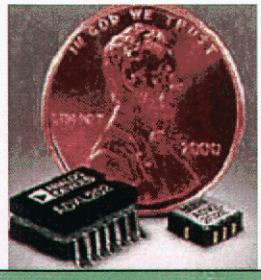 | $25<br><br>5 mm x 5 mm x 2 mm | Resolution: 1 mg<br>Range: ±1.7g<br>Bandwidth: 2.5 kHz<br>Sensitivity: 1000 mV/g |
| Analog Devices ADXRS300 Single-Axis Rate-Gyroscope | 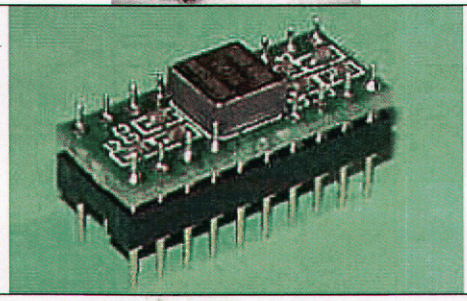 | $50<br><br>7 mm x 7 mm x 3 mm | Resolution: 0.1°/sec<br>Range: ±300°/sec<br>Bandwidth: 400 Hz<br>Sensitivity: 5 mV/°/sec |
| Honeywell HMC2003 Three-Axis Magnetometer | 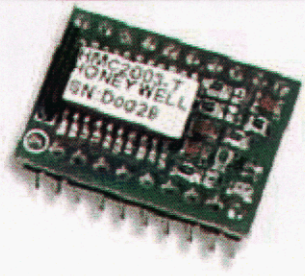 | $200<br><br>20-pin Wide DIP Package | Resolution: < 40 µgauss<br>Range: ± 2 gauss<br>Bandwidth: 1 kHz<br>Sensitivity: 1.0 V/gauss |

**Table 2: Low-Cost IMU Components**

It should be noted that the maximum theoretical resolution specified is not at the indicated bandwidth for the MEMS devices. They have Additive White Gaussian Noise (AWGN) characteristics, so the noise floor (and thus resolution) is dependent on the bandwidth. The bandwidth is adjusted via external filtering, which is discussed in more detail later.

## i. ACCELEROMETERS

MEMS sensors such as Memsic MXR2312 and Analog Devices' ADXL203 are quite a technological accomplishment. The simple physics and methods used to construct these devices is rather interesting, thus some additional information about these devices is contained in Appendix A In particular the appendix contains the accelerometer datasheets as well as a document which describes their internal structure (specifically for the ADXL202, though the discussion is also applicable to the ADXL203).

The Memsic was originally selected due to the easily assembled carrier board and was used in the first prototype in Figure 5. However, the sensitivity, bandwidth, temperature drift, and noise floor are all superior in the ADXL203. Thus, it will be used on the final production version and its theoretical performance is discussed below.

As a quick summary, the ADXL203 is a dual-axis ±1.7g device with a resolution of 1mg at 60Hz. Further, it is powered directly off of +5V and has a ratiometric output voltage (centered at 2.5V when at 0g). Its sensitivity (output swing) is 1000 mV/g. Best of all, the cost is approximately $25 per device and only two are required to cover all three axes. The output noise from the sensor is AWGN, and when band-limited, the noise floor is given by the equation:

$$Noise = 110\frac{\mu g - rms}{\sqrt{Hz}} \times \sqrt{BW \times 1.6}$$

The peak noise is four times the RMS value with a 95% confidence that the noise value is below the peak.

For this application, we can set the bandwidth to 50 Hz via an external 0.1μF capacitor (an easily obtainable value). Performing the calculation yields an average noise value of 0.98 mg-rms with a peak value of approximately 3.9 mg. This will help us determine the number of bits required to accurately measure the signal coming from the accelerometers. Ideally, the ADC should have a resolution better than both the peak and average noise. Recall that the accelerometer under consideration specifies an output sensitivity of 1000 mV/g. Thus, the ADC's ideal resolution should be better than the peak and average noise, which is given by the following:

$$3.9mg \times 1000\frac{mV}{g} = 3.9mV \text{ peak and } 0.98mg \times 1000\frac{mV}{g} = 0.98mV \text{ average.}$$

To get a resolution less than the average noise, a 13-bit ADC would be required. However, most ADCs integrated with a microcontroller have a 10-bit precision. A 10-bit ADC operating from 0 V to 5 V should be sufficient for the value of peak noise:

$$\frac{5.0V}{2^{10} digits} = 4.88\frac{mV}{digit}$$

Since our peak noise has similar amplitude, the last bit can be attributed to noise. Thus even in the presence of noise (meaning even under peak noise conditions) the resolution would be:

$$\left(1/1000\right)\frac{g}{mV} \times 4.88\frac{mV}{digit} = 4.88\frac{mg}{digit}$$

Using the same method as for the high-cost IMU calculations, this equates to a tilt of about 0.25°. This is less resolution than the high-resolution system previously discussed by a factor of about 650. However, at only $50 for all three axes, these sensors are cheaper by a factor of at least 500, not even considering the added difficulty of mounting, calibration, and testing the high-cost sensors!

ii. GYROSCOPES

Just as with the accelerometers, the simple physics and methods used to construct these devices are rather interesting, thus more about these devices is included in Appendix B In particular the appendix contains the rate gyroscope datasheet as well as a document which describes their internal structure.

As a brief summary, the ADXRS300 is a single-axis ±300 °/sec device (extendable up to ±1200 °/sec) with a resolution of sub °/sec. Further, it is powered directly off of 5V, and has a ratiometric output voltage (centered at 2.5V when at 0 °/sec). For simplicity, the sensor will be used in the default ±300 °/sec setting. Its sensitivity (output swing) is 5mV/°/sec. The output noise from the sensor is AWGN, and when band-limited, the noise floor in rms is given by the equation:

$$Noise = 0.1\frac{°/\sec}{\sqrt{Hz}} \times \sqrt{BW \times 1.6}$$

For this application, we set the bandwidth to 40 Hz via an external 22nF capacitor (an easily obtained value). Performing the calculation yields a noise value of 0.8 °/sec.

This will help us determine the number of bits required to accurately measure *this* signal coming from the gyroscopes.

From the specification, the output has a sensitivity of 5 mV/°/sec. Thus the sensor exhibits a noise floor of:

$$0.8°/\text{sec} \times 5\frac{mV}{°/\text{sec}} = 4.0mV$$

Again, a 10-bit ADC powered off 5V provides a resolution of:

$$\frac{5V}{2^{10} digits} = 4.88\frac{mV}{digit}$$

Since our noise is basically the same amount as a single digit, the last bit can be attributed to noise. This equates to an overall system resolution of:

$$\left(\frac{1}{5}\right)\frac{°/\text{sec}}{mV} \times 4.88\frac{mV}{digit} = 0.976\frac{°/\text{sec}}{digit}$$

Just as with the accelerometers, this is a significant decline in achievable resolution compared with the high-cost sensors. However, it is also a significant decline in cost as well.

iii. MAGNETOMETER

The magnetometer is used to measure the intensity of nearby magnetic fields. In particular, it can tell us our compass heading using the Earth's magnetic field. The device is discussed (datasheet and application note) for this use in Appendix C Following similar calculations as above, the 10-bit ADC provides a resolution of

$$\frac{5V}{2^{10} digits} = 4.88\frac{mV}{digit}$$

The sensitivity of the magnetometer (from the datasheet in the appendix) is 1000 mV/gauss. Using this, our device can resolve:

$$\left(\frac{1}{1000}\right)\frac{gauss}{mV} \times 4.88\frac{mV}{digit} = 4.88\frac{milli-gauss}{digit}$$

To put this into perspective, the Earth's magnetic field has a magnitude of about 0.6 gauss. This should be more than sufficient to provide us with the desired compass

headings and three dimensional orientation. Note that the device resolution given in Table 2 as 40 μguass is significantly lower than this value—meaning all 10 bits represent data approximately without noise.

It should be noted that if a more accurate heading were desired, a higher precision (more bits) ADC should be used. In fact, a 17-bit ADC would reach the noise floor of the device. Thus, the 24-bit ADC discussed for the High-Cost IMU would be more than sufficient to provide full range and resolution.

Also note that there are many sources of possible errors with magnetometers compared to the other sensors. Such sources include any nearby ferrous materials or fluctuations in the Earth's magnetic field over time. In particular, the ferrous material factor needs to be taken into account when constructing the mounting for the device. Further, large magnetic fields (i.e. those created by electromagnets) can throw the device's internal measurements out of alignment. For this reason, a Set/Reset circuit (contained in the application notes) may need to be employed before making measurements.

### *B. SIGNAL CONDITIONING & PROCESSING*

Luckily, the sensors discussed above all have outputs that work sufficiently with a 10-bit ADC with voltages from 0V to 5V. Because of this, we only need to worry about filtering, and possibly buffering to the ADC. Thus, only Stage 1 from Figure 2 is necessary for the prototype in Figure 5. The addition of a buffer would be beneficial as it would provide lower output impedance to the ADC and thus improve the sample-hold characteristics of the ADC. This simple addition is reserved for future prototype incarnations.

### *C. MICROCONTROLLER & COMMUNICATIONS*

The prototype performs some very simple operations but uses some complex techniques to accomplish them. The microcontroller used is the PIC18F4320. A synopsis of the features used is contained below in Figure 6.

PIC18F4320 Features Used:

- 10-bit, 13-channel ADC with programmable acquisition time.
- Addressable USART (Universal Synchronous Asynchronous Receiver Transmitter) supporting RS232 serial communication.
- 2 levels of interrupt priorities.
- Master Synchronous Serial Port (MSSP) supports both $I^2C$ and SPI serial protocols for peripherals.
- 4 x 16-bit timers.
- 256 bytes of on-board EEPROM storage space.
- Clocked at 40 MHz for an instruction speed of 10 million instructions per second.

**Figure 6: PIC Microcontroller Features**

The microcontroller waits for input from an external switch to begin sampling. The sensors are sampled for 20+ seconds (the capacity of the external storage EEPROMS, as discussed below). The prototype is then connected to a PC and the information is transferred off the EEPROMs. The data can then be graphed or undergo other post processing.

The code to control this behavior is rather complex. It uses priority interrupts to take ADC samples and store them in the EEPROMs. Due to timing, the data must be written in 128-byte pages to the EEPROMs for writing. This forces the use of a large circular buffer to store the samples. The code is contained in Appendix D

The system also uses a variety of communication mechanisms. The first form of communication is transmitting the digital sample values. For the prototype, the PIC transmits the samples to the external EEPROMs via an $I^2C$ bus. However, it would be desirable in many systems to have the data transmitted in real-time – by a SPI bus for example – without storing the data in the EEPROMs. This is entirely feasible since the $I^2C$ bus uses the same pins on the PIC as the on-chip SPI does. Thus, $I^2C$ can be used during testing, then disabled (to the EEPROMs) to allow SPI for real-time data transmission. This is an extremely useful feature as it allows flexibility during development and for final applications. This feature may be added in the next prototype incarnation.

The small 8-pin DIP packages in Figure 5 are the $I^2C$ EEPROMS. There are five of these EEPROMs, each with 64KB storage space. The sampling rate is 800 samples per second per channel. Since there are 9 sensors (3 per axis times 3 types of devices), the PIC is recording 7200 samples per second. The samples are each 10 bits, and the channel number is another 4 bits. Thus, each sample is effectively 2 bytes. The EEPROMs can store data for at most:

$$(5)EEPROM \times 64\frac{KB}{EEPROM} \times \left(1/2\right)\frac{sample}{bytes} \times \left(1/7200\right)\frac{\sec}{samples} = 22.75\sec$$

This amount of time gives adequate opportunity to perform various flight-like maneuvers during testing.

The final communication protocol used is the RS232 via the USART. This is the basic serial communication port contained on the back of most personal computers. The data is transferred from the EEPROMs via a terminal program (hyperterminal in Windows for example) or via other software. The data can then be analyzed on a PC.

*D. POST PROCESSING*

This is probably the most important step, from both a user and management perspective. It shows 'what the data means.' I used MatLab to analyze the data. I wrote a function that allows me to graph the data in various ways. The code to perform this is contained in Appendix E. For example, consider the actual data in Figure 13. The analysis of these data is discussed in detail in the following section.

*E. CAPABILITIES AND TESTING*

The following setup has been constructed to test the IMU. From this setup, we can test all three of the component types. The tilt mechanism allows for evaluation of the accelerometers, while the panning can be used to examine performance of the rate gyros. Motion of both of these axes will allow for testing of the magnetometer.

In the test setup images, you can see that there is a compass. This will be used to quantitatively test the magnetometer's accuracy. The laser pointer and the servo (tilt) in the vice are used to quantitatively test the accelerometers. Finally, the servo programmed for full rotation (pan) will allow us to verify that the rate gyros are working (though it will only verify one axis and not provide any quantitative analysis).

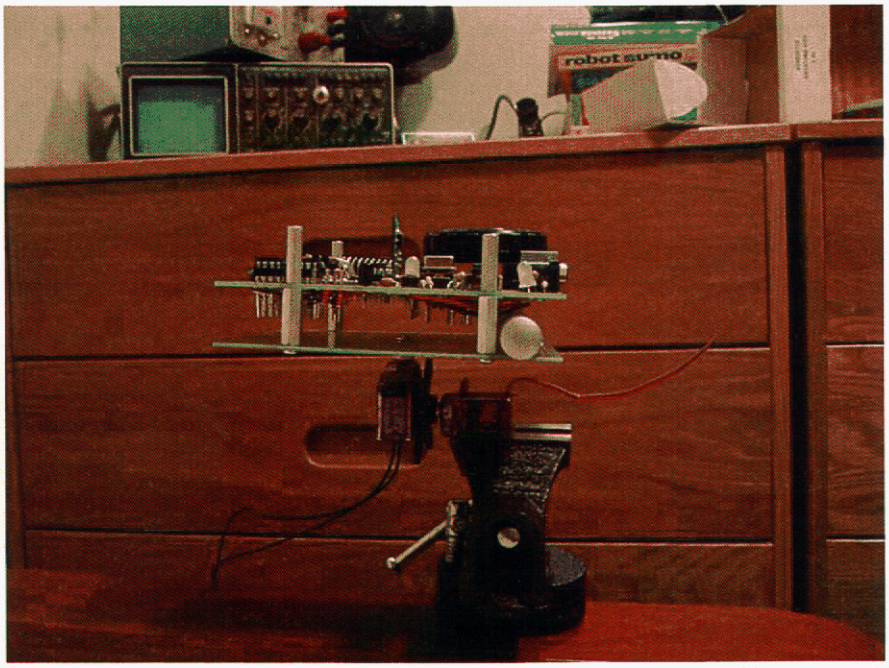


**Figure 7: Test Setup (Pan and Tilt Mechanism)**

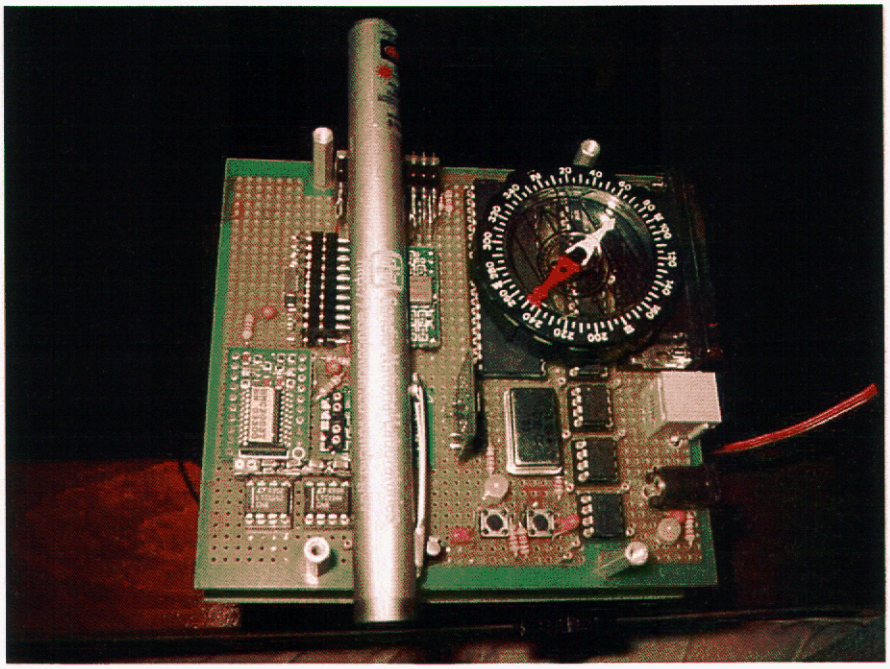

**Figure 8: Test Setup (Laser Pointer and Compass)**

i. ACCELEROMETER

The laser pointer shown in Figure 8 is mounted horizontal to the sensing axis, and then a yardstick helps determine the angle of tilt, as shown below.

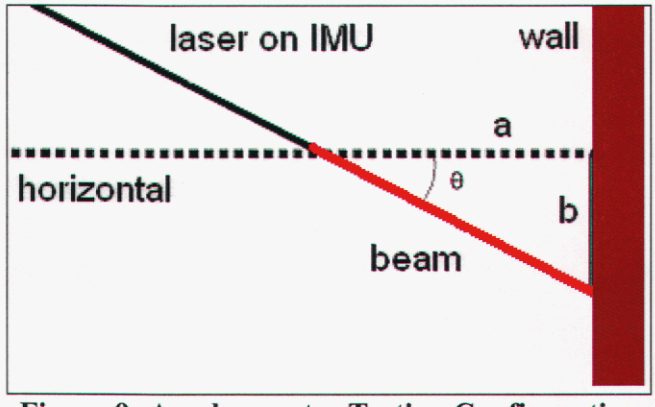


**Figure 9: Accelerometer Testing Configuration**

Using geometry to calculate the angle, $\theta = \tan^{-1}(b/a)$. Note that the gravitation force that *should* be sensed is given by $A = 1 * \sin(\theta)$, as discussed previously for the high-cost IMU (see Figure 4).

For the testing scenarios, five angles were chosen.

| Angle # | a | b | θ |
|---|---|---|---|
| 1 | 72.0 cm | +23.4 cm | +18.0° |
| 2 | 72.0 cm | +12.0 cm | +9.5° |
| 3 | 72.0 cm | +0.8 cm | +0.6° |
| 4 | 72.0 cm | -11.6 cm | - 9.1 |
| 5 | 72.0 cm | -23.3 cm | - 17.9 |

**Table 3: Accelerometer Testing Reference Angles**

When the data was captured, it was found that the noise performance of the accelerometer was not very good in this setup. Then again, the analog bandwidth of the MEMs is much lower than the 400 Hz bandwidth being sampled (by a factor of 16 in the case of the Memsic accelerometers, which are band-limited to 25 Hz). Thus, I decided to implement a software running-average, low-pass filter by this factor (16 point running-average filter) to get a better handle on the data.

Some suggestions for improving the noise performance are to decrease the sampling rate to more closely match the analog bandwidth, use op-amps to amplify prior to sampling, better analog/digital ground separation, or even use digital filtering as in this case.

Figure 10 and Figure 11 show the results from the IMU (via the MatLab code in Appendix E). The numerical values are given in Table 4 and were determined by

examining Figure 11 (using MatLab's zoom functionality and then averaging by eye). We can see that all the measured values were within about a degree and a half of the actual tilt. This is considered to be reasonable given that the Memsic accelerometer tested was noted in the datasheet to provide about 1° resolution. Hopefully the ADXL203 will perform to the standards calculated earlier (0.25° resolution).

| Test Angle | Expected acceleration (in milli-g) | Actual acceleration (in milli-g) | Actual Angle (Calculated using Arcsine) |
|---|---|---|---|
| +18.0° | 309 | 325 | +19.0° |
| +9.5° | 165 | 182 | +10.5° |
| +0.6° | 10 | 17 | +1.0° |
| - 9.1 | -158 | -165 | - 9.5 |
| - 17.9 | -307 | -325 | - 19.0 |

**Table 4: Accelerometer Testing Results**

Testing was performed on only one axis. The other axes should perform similarly.

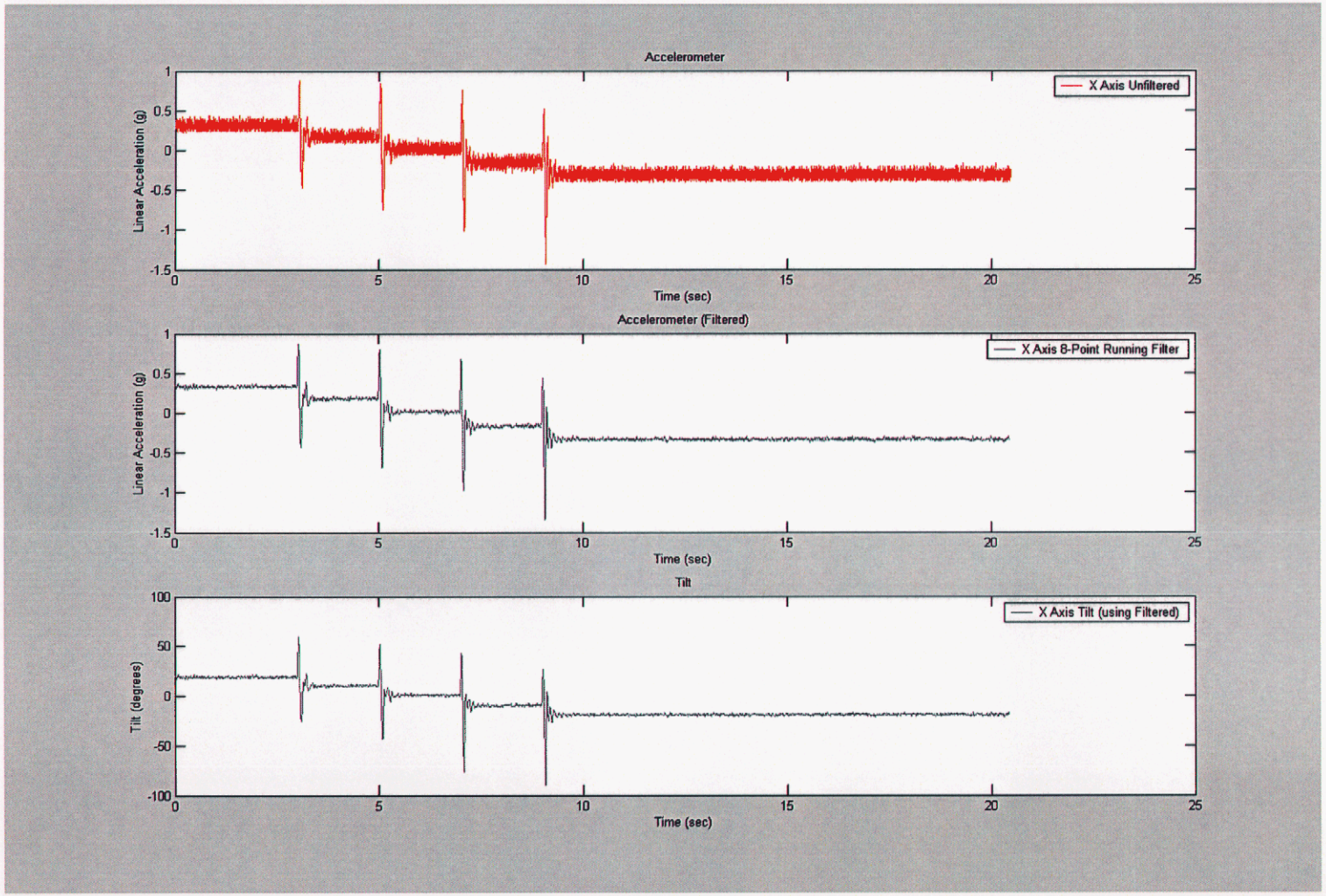


**Figure 10: Accelerometer Test Results**

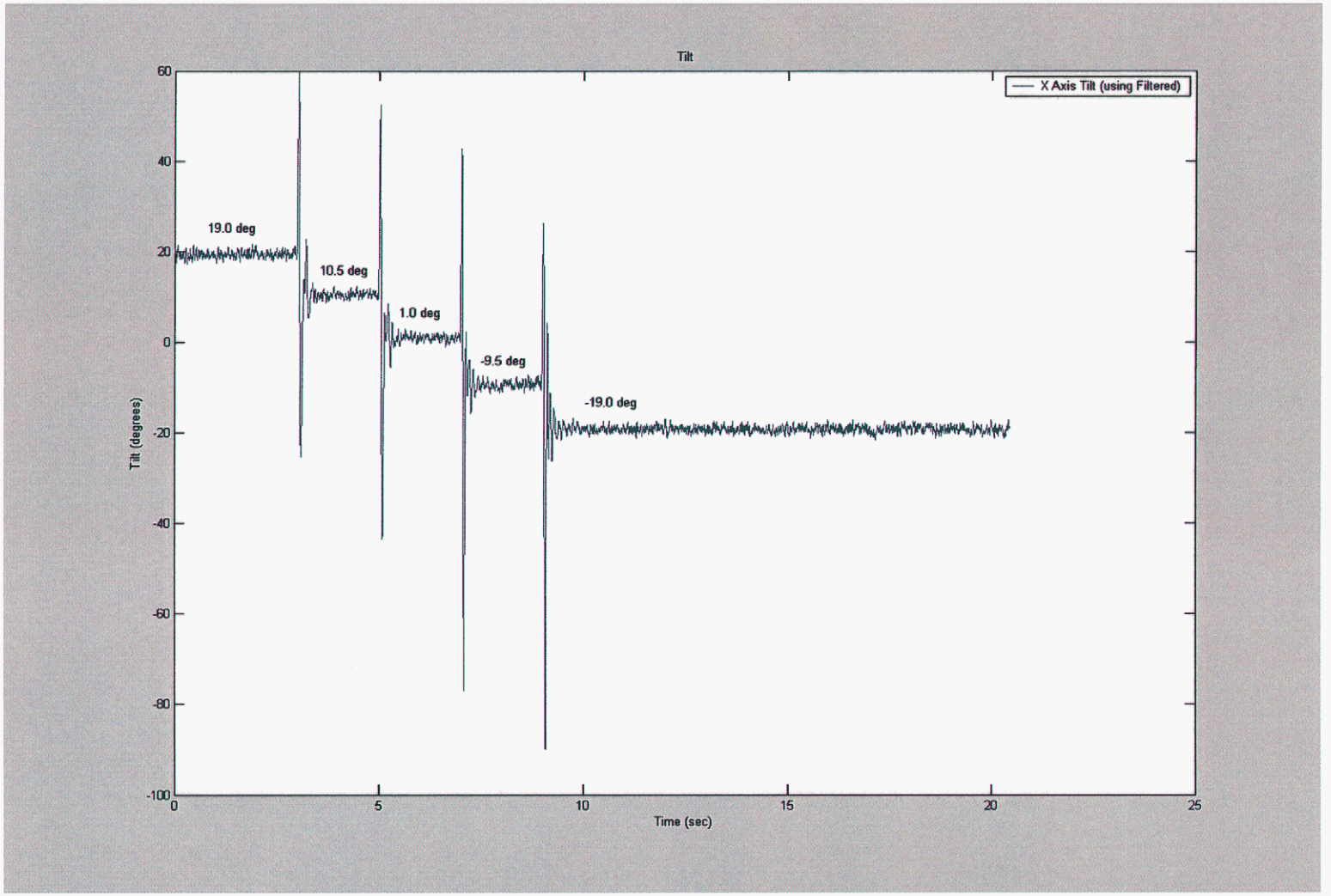


**Figure 11: Zoomed Tilt Results**

### ii. GYROSCOPE

To test the gyroscopes, I simply spun the board about its vertical (Z) axis. First, it was spun clockwise, then counter-clockwise, then clockwise again. These movements can easily be seen in Figure 12. Note that the angular velocity is given in degrees per second. This represents the actual rate of rotation of the board. Again, the other axes should perform similarly.

### iii. COMPLEX MOVEMENTS

Using what was learned from the testing, it is now possible to understand more complex movements. Consider the movements shown in Figure 13. We can see three distinct events. We can see from the gyroscopes that the first movement was a counter-clockwise rotation about the Y-axis, so that the X-axis was facing down. It also moved back to the original position (a rotation clockwise about the Y-axis). The second event was exactly the same, except that its rotation was about the X-axis (which caused the Y-axis accelerometer to be pointed up, as dictated by its orientation on the board). The final event was four rotations: clockwise, then counter-clockwise, then clockwise, then counter-clockwise. As expected, the accelerometers experienced very little change (mostly spurious noise due to small movements when being moved by my hands).

Note the magnetometer changes during the third event. It should be possible to determine the compass heading based on these readings. However, the reference voltages are not connected to the ADC, making it extremely difficult to determine the true offset voltage. This means that the set/reset circuit really is a necessity. The offsets (for this and all the other sensors) should probably be used so that this problem can be averted. Due to these issues, no quantitative measurements were verified. Qualitatively, the magnetometer appears to be working correctly.

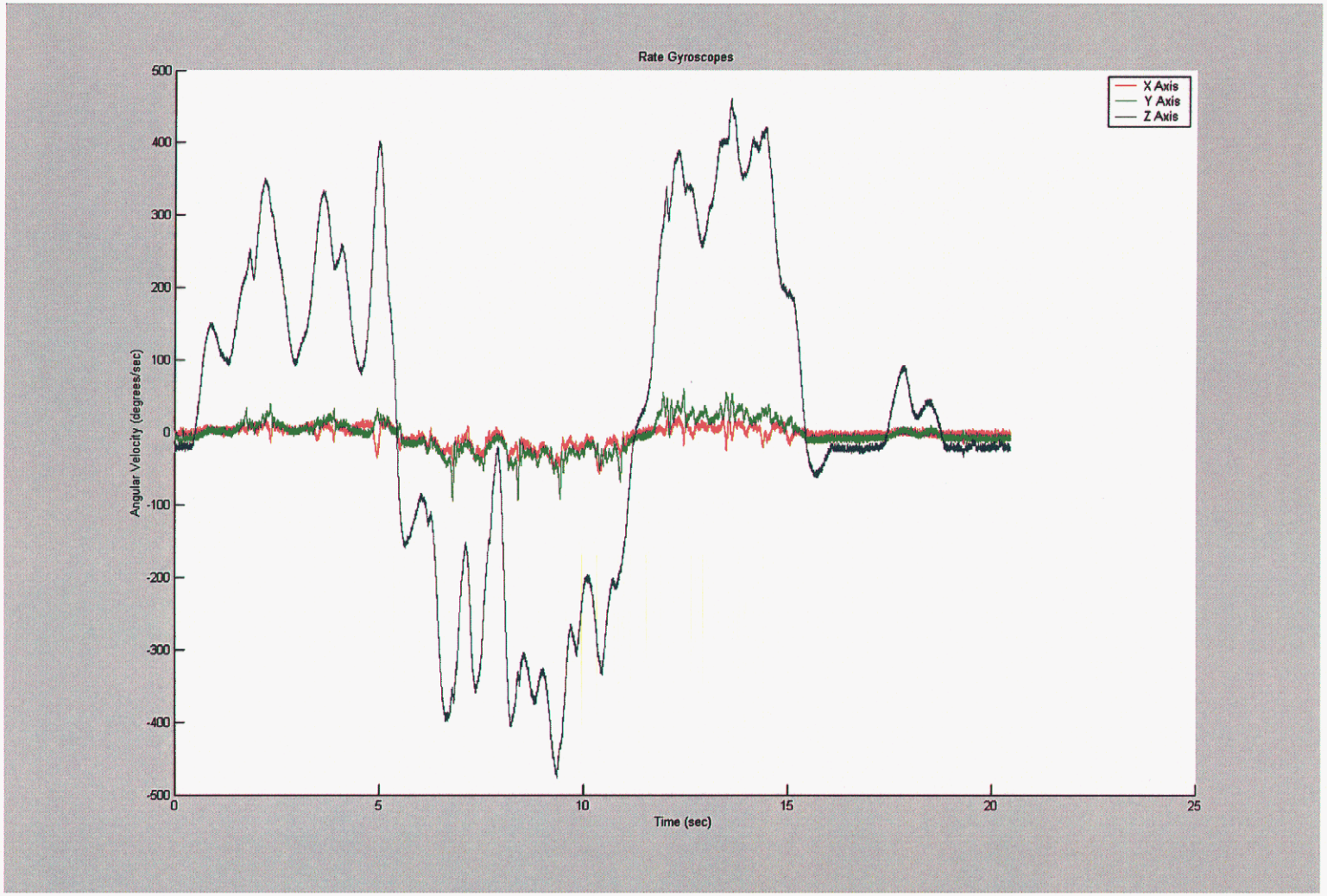


**Figure 12: Rate Gyro Testing Results**

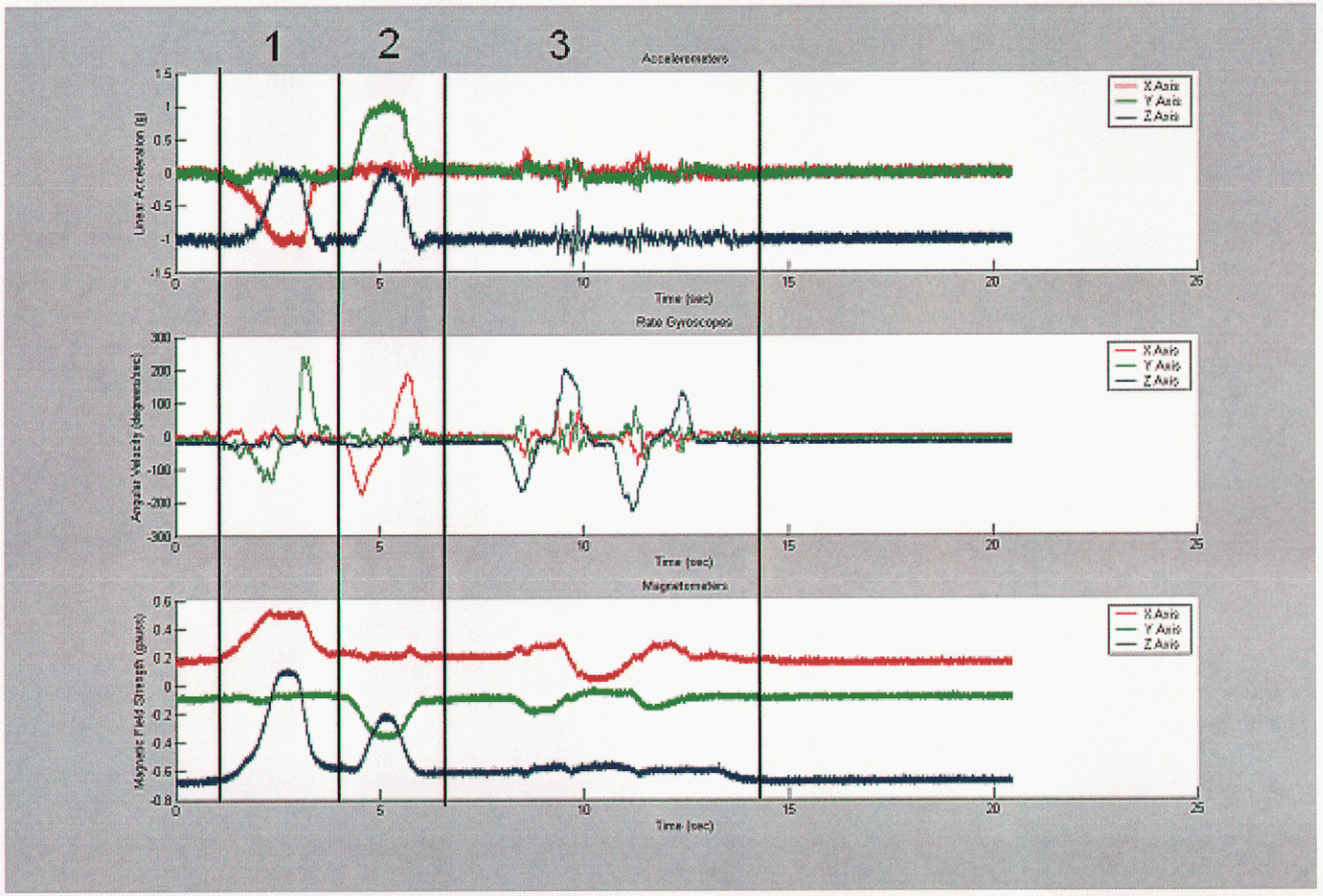


**Figure 13: Sensor Outputs (3 Events)**

# V. PRINTED CIRCUIT BOARD

After all the work in creating and testing a prototype, it was time to apply previously mentioned improvements. Thus, a new prototype on a printed circuit board was constructed (see Figure 14). A Printed Circuit Board (PCB) allows us to apply the following improvements:

- Op-amp buffering before the ADC for improved sample-hold noise performance.
- Isolated digital and analog grounds to remove power supply noise sources.
- Shorter traces (improves noise) and reduced board space.
- Reconfigurable ADC channels and a "sandbox" area for future prototyping.
- Jumpers to select either storage on EEPROMs via $I^2C$ or real-time SPI transmission.
- More stable mountings (especially for the vertical sensor boards) and a more professional/reproducible look.

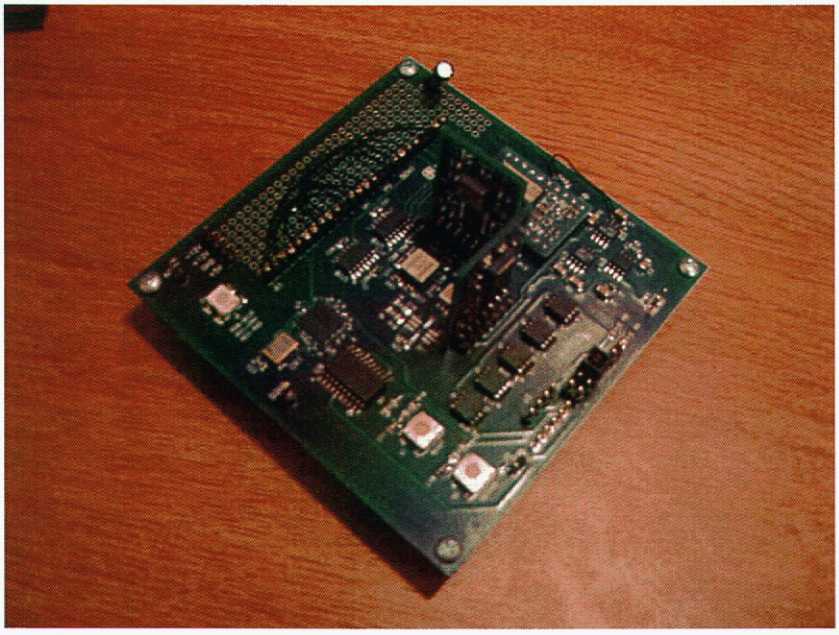

**Figure 14: IMU Printed Circuit Board**

The initial PCB implementation had two problems. First, one of the voltage converter chips was not connected to ground, and thus -12V was not generated (instead it put out +12V). This resulted in an inability to bias the op-amps properly. The error was due to the fact that Orcad doesn't include Vcc and ground connections on the chip schematics it inserts. This problem was fixable by soldering a jumper wire from the appropriate pin to one of the other ground contacts. However, it highlights a lesson learned for future use of Orcad. Also, it was discovered that the pinouts for the MAX233 RS232 chip are substantially different for the surface mount package and thus the board was incorrectly laid out. Although some transmit functionality is available, the data credibility are of concern. This may also be the cause of noise spikes that are observed in the data. Another version of this board has not yet been acquired, although these problems are both readily fixable.

# VI. CONCLUSION

In this project, the feasibility of developing a low cost IMU was explored. A prototype was built and a test setup was designed to characterize the prototype's performance. Although much of the characterization was qualitative, the quantitative assessment of accelerometer performance indicated that the sensor performed as expected. It appears that the magnetometer is not usable without the reset circuit present. Its performance was the most difficult to understand and characterize, and further work remains to explore this issue.

A Printed Circuit Board instantiation of the low cost IMU was also developed. Due to design defects, I was not able to characterize its performance. However, the defects could easily be fixed in a new iteration of the board.

The modularity of the design and communication protocol should allow other users to change or expand the capability of this IMU through selection of different sensors. It is also expected that more capable sensors and microprocessors would allow for improved resolution in the future.

Finally, it should be noted that this low-cost system could not replicate the capabilities of the high-cost systems. Rather, the low-cost system should be a viable solution for many applications and is flexible enough to allow for multiple uses.

**Distribution**

| | | |
|---|---|---|
| 1 | MS 9013 | R.E. Oetken, 8231, ATTN: K. Berger |
| 1 | MS 9014 | K.R. Hughes, 8242 |
| 1 | MS 9101 | J.C. Lund, 8232 |
| 1 | MS 9102 | A.L. Hull, 8233 |
| 1 | MS 9102 | P.Y. Yoon, 8235 |
| 1 | MS 9153 | D.R. Henson, 8200 |
| 1 | MS 9153 | G.A. Thomas, 8220 |
| 1 | MS 9153 | R.G. Miller, 8230 |
| 1 | MS 9153 | B.K. Damkroger, 8240 |
| 1 | MS 9202 | R.D. Monson, 8205 |
| 3 | MS 9202 | R.L. Bierbaum, 8205 |
| 10 | | Travis Deyle<br>6241 South 170$^{th}$ Street<br>Omaha, Nebraska 68135 |
| 3 | MS 9018 | Central Technical Files, 8945-1 |
| 1 | MS 0899 | Technical Library, 9616 |
| 1 | MS 9021 | Classification Office, 8511<br>DOE/OSTI via URL |

# Appendix A – MEMS Accelerometers

Datasheets:

A. **ADXL203 Precision ±1.7 *g* Dual Axis Accelerometer** by Analog Devices

B. **MXR2312ML Improved, Ultra Low Noise ±2.0 *g* Dual Axis Accelerometer with Ratiometric Outputs** by Memsic

Further Information:

C. **Dual Axis, Low *g*, Fully Integrated Accelerometers** by Harvey Weinberg (from Analog Dialogue 33-1)

# Precision ±1.7 *g* Single/Dual Axis Accelerometer

# ADXL103/ADXL203

## FEATURES

**High performance, single/dual axis accelerometer on a single IC chip**
**5 mm × 5 mm × 2 mm LCC package**
**1 mg resolution at 60 Hz**
**Low power: 700 µA at $V_S$ = 5 V (typical)**
**High zero *g* bias stability**
**High sensitivity accuracy**
**–40°C to +125°C temperature range**
**X and Y axes aligned to within 0.1° (typical)**
**BW adjustment with a single capacitor**
**Single-supply operation**
**3500 *g* shock survival**

## APPLICATIONS

**Vehicle Dynamic Control (VDC)/Electronic Stability Program (ESP) systems**
**Electronic chassis control**
**Electronic braking**
**Platform stabilization/leveling**
**Navigation**
**Alarms and motion detectors.**
**High accuracy, 2-axis tilt sensing**

## GENERAL DESCRIPTION

The ADXL103/ADXL203 are high precision, low power, complete single and dual axis accelerometers with signal conditioned voltage outputs, all on a single monolithic IC. The ADXL103/ADXL203 measures acceleration with a full-scale range of ±1.7 *g*. The ADXL103/ADXL203 can measure both dynamic acceleration (e.g., vibration) and static acceleration (e.g., gravity).

The typical noise floor is 110 µg/√Hz, allowing signals below 1 mg (0.06° of inclination) to be resolved in tilt sensing applications using narrow bandwidths (<60 Hz).

The user selects the bandwidth of the accelerometer using capacitors $C_X$ and $C_Y$ at the $X_{OUT}$ and $Y_{OUT}$ pins. Bandwidths of 0.5 Hz to 2.5 kHz may be selected to suit the application.

The ADXL103 and ADXL203 are available in 5 mm × 5 mm × 2 mm, 8-pad hermetic LCC packages.

## FUNCTIONAL BLOCK DIAGRAM

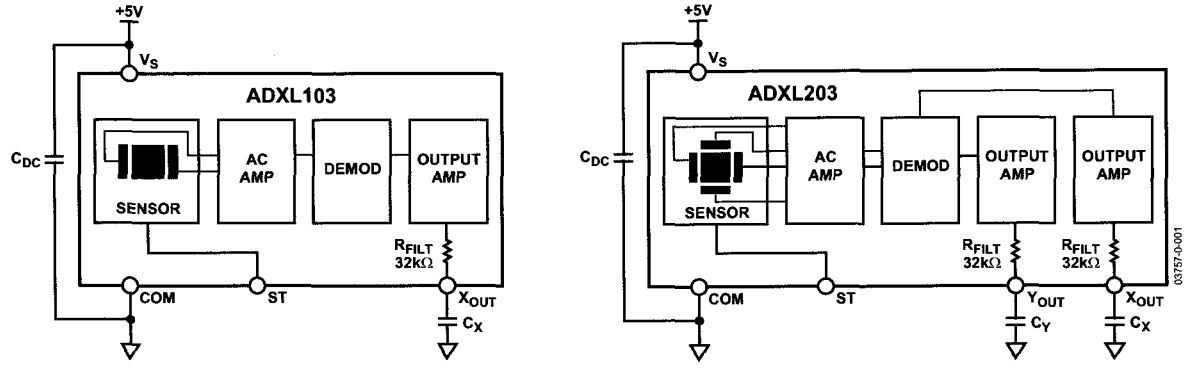


*Figure 1. ADXL103/ADXL203 Functional Block Diagram*



**One Technology Way, P.O. Box 9106, Norwood, MA 02062-9106, U.S.A.**
**Tel: 781.329.4700** **www.analog.com**
**Fax: 781.326.8703** 

# TABLE OF CONTENTS



## REVISION HISTORY

Revision 0: Initial Version

# SPECIFICATIONS

**Table 1. $T_A$ = −40°C to +125°C, $V_S$ = 5 V, $C_X$ = $C_Y$ = 0.1 µF, Acceleration = 0 *g*, unless otherwise noted.**

| Parameter | Conditions | Min | Typ | Max | Unit |
|---|---|---|---|---|---|
| SENSOR INPUT | Each Axis | | | | |
| Measurement Range[1] | | ±1.7 | | | *g* |
| Nonlinearity | % of Full Scale | | ±0.5 | ±2.5 | % |
| Package Alignment Error | | | ±1 | | Degrees |
| Alignment Error (ADXL203) | X Sensor to Y Sensor | | ±0.1 | | Degrees |
| Cross Axis Sensitivity | | | ±2 | ±5 | % |
| SENSITIVITY (Ratiometric)[2] | Each Axis | | | | |
| Sensitivity at $X_{OUT}$, $Y_{OUT}$ | $V_S$ = 5 V | 940 | 1000 | 1060 | mV/*g* |
| Sensitivity Change due to Temperature[3] | $V_S$ = 5 V | | ±0.3 | | % |
| ZERO *g* BIAS LEVEL (Ratiometric) | Each Axis | | | | |
| 0 *g* Voltage at $X_{OUT}$, $Y_{OUT}$ | $V_S$ = 5 V | 2.4 | 2.5 | 2.6 | V |
| Initial 0 *g* Output Deviation from Ideal | $V_S$ = 5 V, 25°C | | ±25 | | *mg* |
| 0 *g* Offset vs. Temperature | | | ±0.1 | | *mg*/°C |
| NOISE PERFORMANCE | | | | | |
| Output Noise | < 4 kHz, $V_S$ = 5 V, 25°C | | 1 | 6 | mV rms |
| Noise Density | @25°C | | 110 | | µg/√Hz rms |
| FREQUENCY RESPONSE[4] | | | | | |
| $C_X$, $C_Y$ Range[5] | | 0.002 | | 10 | µF |
| $R_{FILT}$ Tolerance | | 24 | 32 | 40 | kΩ |
| Sensor Resonant Frequency | | | 5.5 | | kHz |
| SELF TEST[6] | | | | | |
| Logic Input Low | | | | 1 | V |
| Logic Input High | | 4 | | | V |
| ST Input Resistance to Ground | | 30 | 50 | | kΩ |
| Output Change at $X_{OUT}$, $Y_{OUT}$ | Self Test 0 to 1 | 400 | 750 | 1100 | mV |
| OUTPUT AMPLIFIER | | | | | |
| Output Swing Low | No Load | | 0.3 | | V |
| Output Swing High | No Load | | 4.5 | | V |
| POWER SUPPLY | | | | | |
| Operating Voltage Range | | 3 | | 6 | V |
| Quiescent Supply Current | | | 0.7 | 1.1 | mA |
| Turn-On Time[7] | | | 20 | | ms |

[1] Guaranteed by measurement of initial offset and sensitivity.
[2] Sensitivity is essentially ratiometric to $V_S$. For $V_S$ = 4.75 V to 5.25 V, sensitivity is 186 mV/V/*g* to 215 mV/V/*g*.
[3] Defined as the output change from ambient-to-maximum temperature or ambient-to-minimum temperature.
[4] Actual frequency response controlled by user-supplied external capacitor ($C_X$, $C_Y$).
[5] Bandwidth = 1/(2 × π × 32 kΩ × C). For $C_X$, $C_Y$ = 0.002 µF, Bandwidth = 2500 Hz. For $C_X$, $C_Y$ = 10 µF, Bandwidth = 0.5 Hz. Minimum/maximum values are not tested.
[6] Self-test response changes cubically with $V_S$.
[7] Larger values of $C_X$, $C_Y$ will increase turn-on time. Turn-on time is approximately 160 × $C_X$ or $C_Y$ + 4 ms, where $C_X$, $C_Y$ are in µF.

All minimum and maximum specifications are guaranteed. Typical specifications are not guaranteed.

# ABSOLUTE MAXIMUM RATINGS

**Table 2. ADXL103/ADXL203 Stress Ratings**

| Parameter | Rating |
|---|---|
| Acceleration (Any Axis, Unpowered) | 3,500 *g* |
| Acceleration (Any Axis, Powered) | 3,500 *g* |
| Drop Test (Concrete Surface) | 1.2 m |
| $V_S$ | −0.3 V to +7.0 V |
| All Other Pins | (COM − 0.3 V) to ($V_S$ + 0.3 V) |
| Output Short-Circuit Duration (Any Pin to Common) | Indefinite |
| Operating Temperature Range | −55°C to +125°C |
| Storage Temperature | −65°C to +150°C |

Stresses above those listed under Absolute Maximum Ratings may cause permanent damage to the device. This is a stress rating only; functional operation of the device at these or any other conditions above those indicated in the operational section of this specification is not implied. Exposure to absolute maximum rating conditions for extended periods may affect device reliability.

**Table 3. Package Characteristics**

| Package Type | $\theta_{JA}$ | $\theta_{JC}$ | Device Weight |
|---|---|---|---|
| 8-Lead CLCC | 120°C/W | 20°C/W | <1.0 gram |

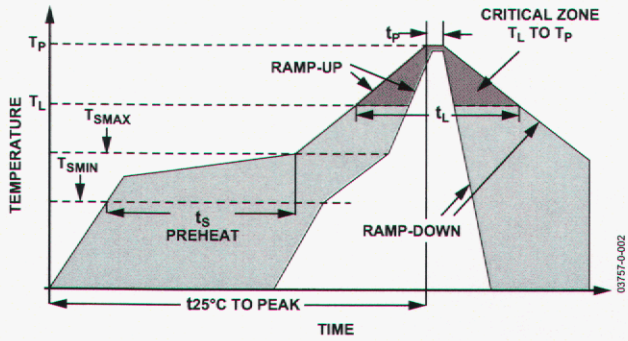


| Profile Feature | Condition | |
|---|---|---|
| | Sn63/Pb37 | Pb Free |
| Average Ramp Rate ($T_L$ to $T_P$) | 3°C/second Max | |
| Preheat | | |
| • Minimum Temperature ($T_{SMIN}$) | 100°C | 150°C |
| • Minimum Temperature ($T_{SMAX}$) | 150°C | 200°C |
| • Time ($T_{SMIN}$ to $T_{SMAX}$) ($t_S$) | 60–120 seconds | 60–150 seconds |
| $T_{SMAX}$ to $T_L$ | | |
| • Ramp-Up Rate | 3°C/second | |
| Time Maintained above Liquidous ($T_L$) | | |
| • Liquidous Temperature ($T_L$) | 183°C | 217°C |
| • Time ($t_L$) | 60–150 seconds | 60–150 seconds |
| Peak Temperature ($T_P$) | 240°C +0°C/−5°C | 260°C +0°C/−5°C |
| Time within 5°C of Actual Peak Temperature ($t_P$) | 10–30 seconds | 20–40 seconds |
| Ramp-Down Rate | 6°C/second Max | |
| Time 25°C to Peak Temperature | 6 minutes Max | 8 minutes Max |

*Figure 2. Recommended Soldering Profile*

# TYPICAL PERFORMANCE CHARACTERISTICS

($V_S$ = 5 V for all graphs, unless otherwise noted.)

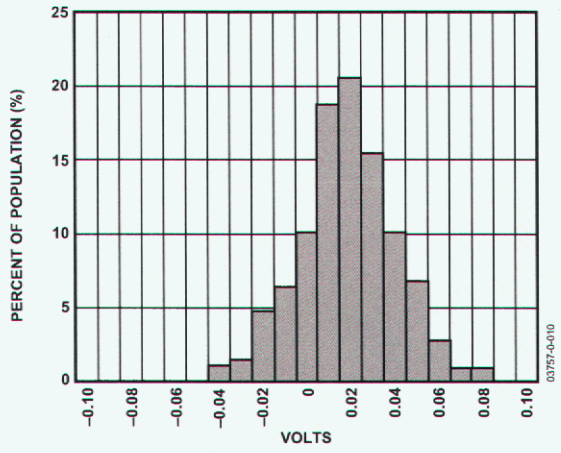


Figure 3. X Axis Zero g Bias Deviation from Ideal at 25°C

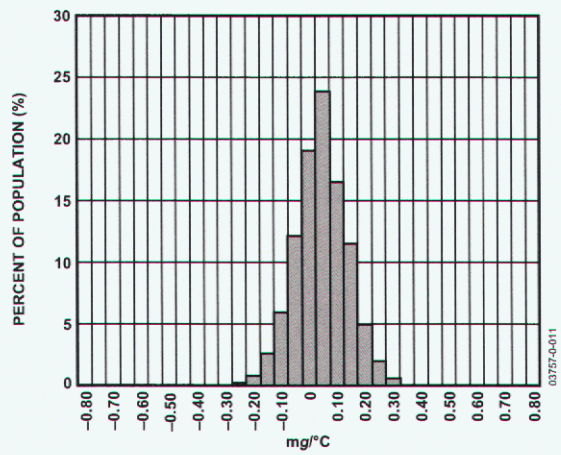


Figure 4. X Axis Zero g Bias Tempco

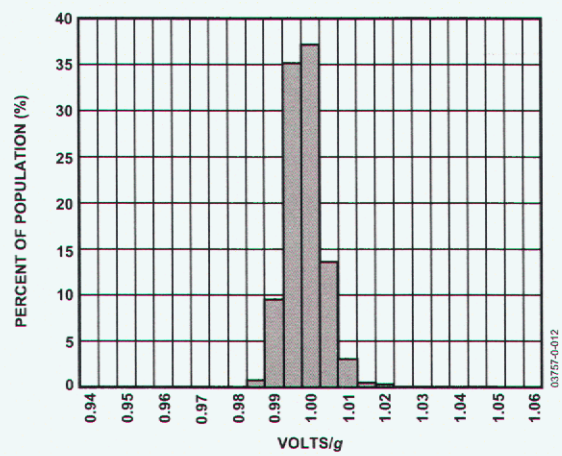


Figure 5. X Axis Sensitivity at 25°C

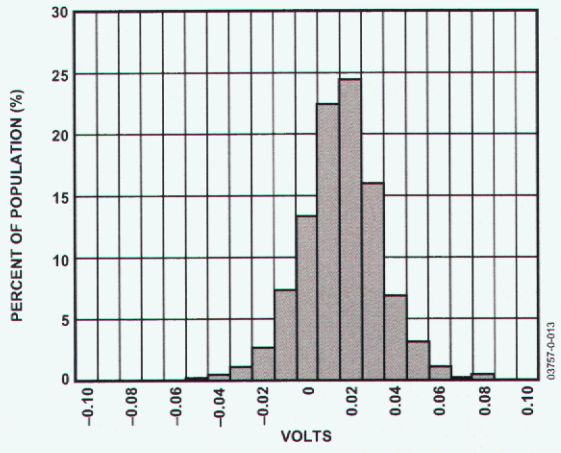


Figure 6. Y Axis Zero g Bias Deviation from Ideal at 25°C

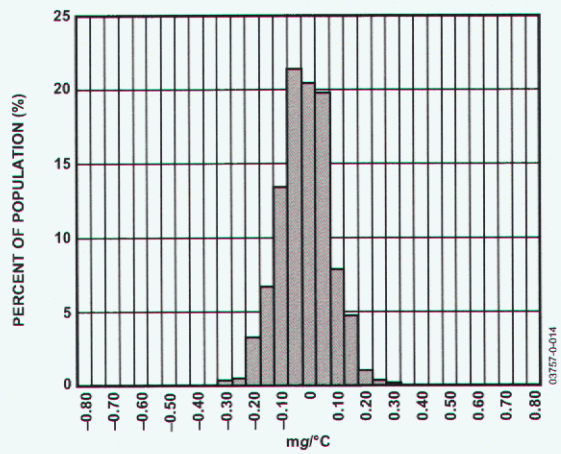


Figure 7. Y Axis Zero g Bias Tempco

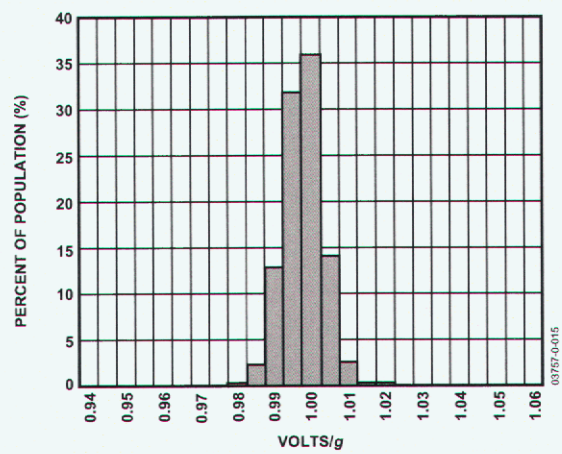


Figure 8. Y Axis Sensitivity at 25°C

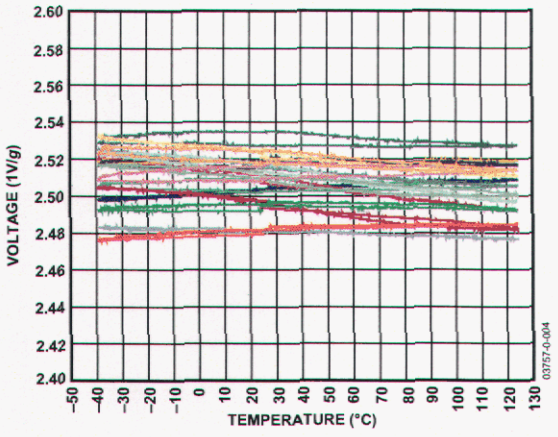


Figure 9. Zero g Bias vs. Temperature – Parts Soldered to PCB

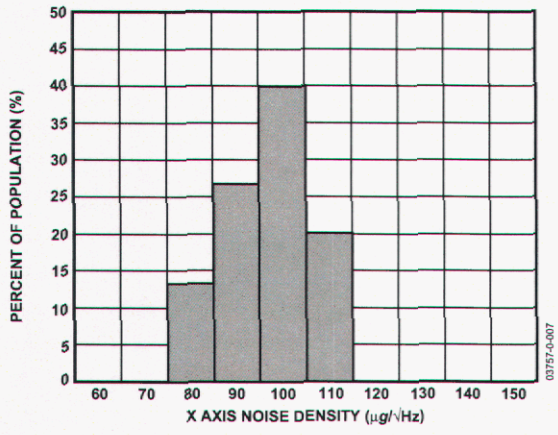


Figure 10. X Axis Noise Density at 25°C

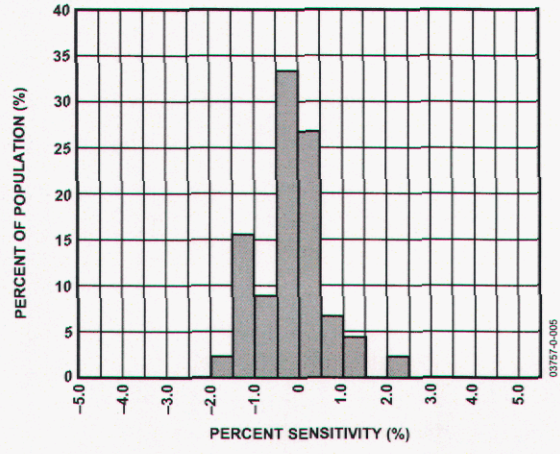


Figure 11. Z vs. X Cross-Axis Sensitivity

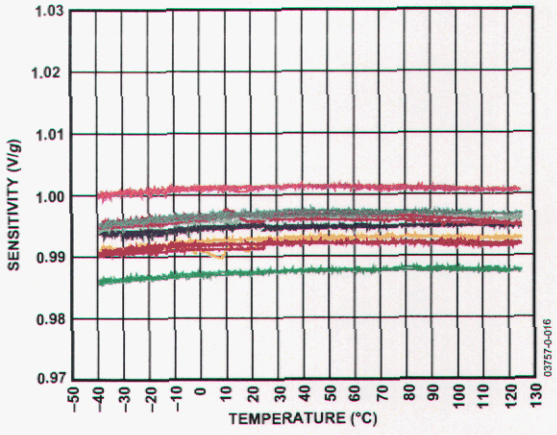


Figure 12. Sensitivity vs. Temperature – Parts Soldered to PCB

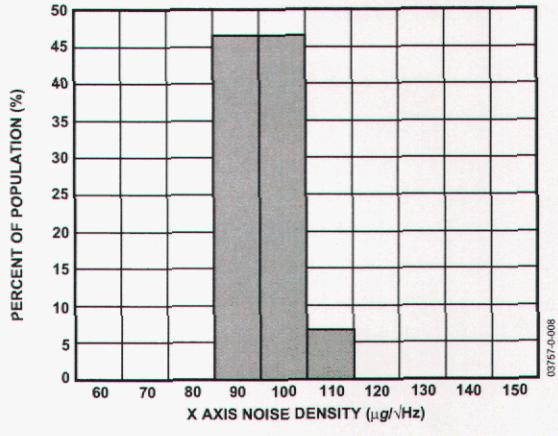


Figure 13. Y Axis Noise Density at 25°C

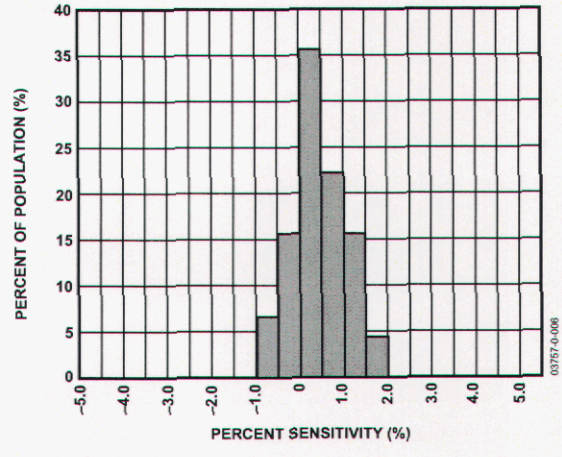


Figure 14. Z vs. Y Cross-Axis Sensitivity

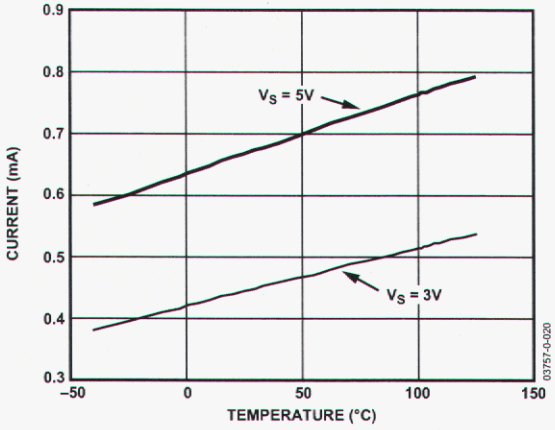


Figure 15. Supply Current vs. Temperature

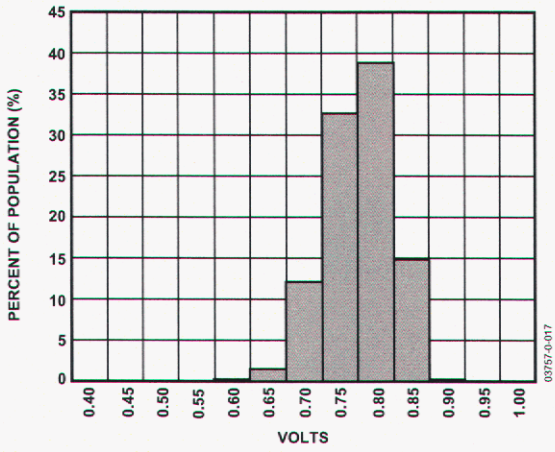


Figure 16. X Axis Self Test Response at 25°C

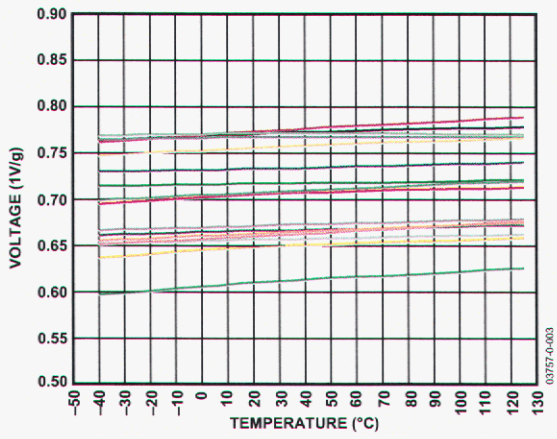


Figure 17. Self Test Response vs. Temperature

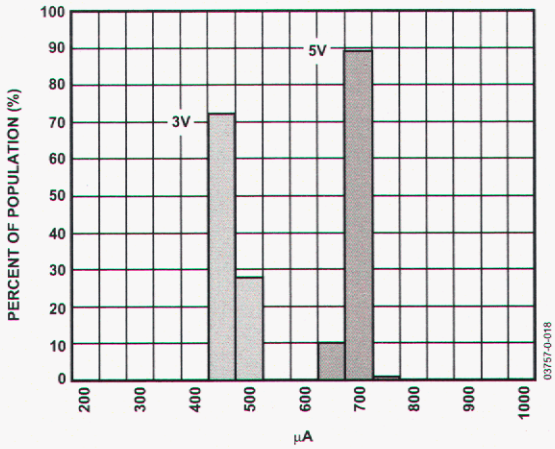


Figure 18. Supply Current at 25°C

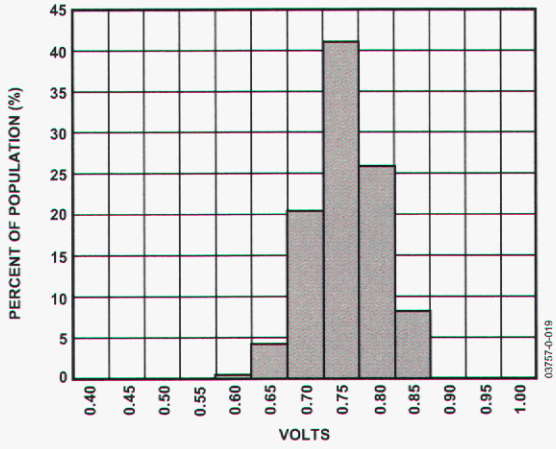


Figure 19. Y Axis Self Test Response at 25°C

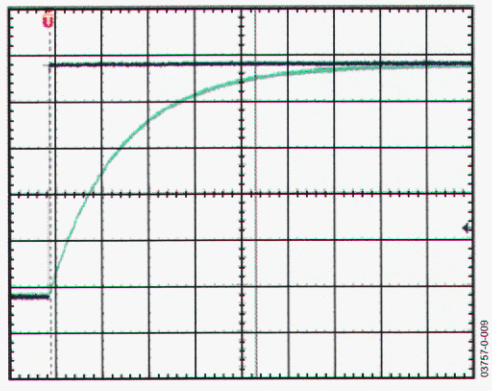


Figure 20. Turn-On Time – $C_X$, $C_Y$ = 0.1 µF, Time Scale = 2 ms/div

# THEORY OF OPERATION

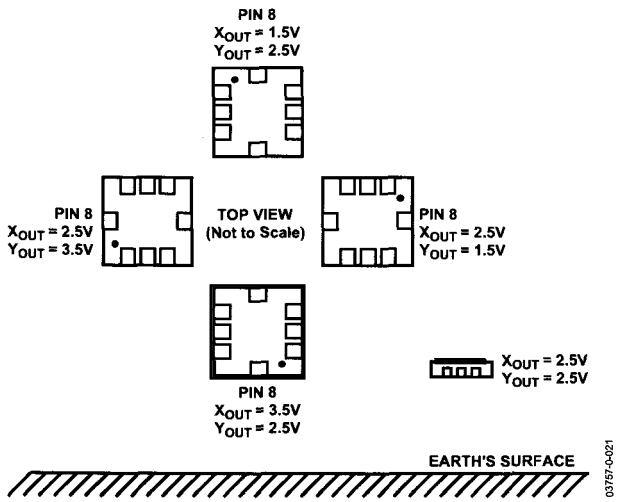


*Figure 21. Output Response vs. Orientation*

The ADXL103/ADXL203 are complete acceleration measurement systems on a single monolithic IC. The ADXL103 is a single axis accelerometer, while the ADXL203 is a dual axis accelerometer. Both parts contain a polysilicon surface-micromachined sensor and signal conditioning circuitry to implement an open-loop acceleration measurement architecture. The output signals are analog voltages proportional to acceleration. The ADXL103/ADXL203 are capable of measuring both positive and negative accelerations to at least ±1.7 *g*. The accelerometer can measure static acceleration forces such as gravity, allowing it to be used as a tilt sensor.

The sensor is a surface-micromachined polysilicon structure built on top of the silicon wafer. Polysilicon springs suspend the structure over the surface of the wafer and provide a resistance against acceleration forces. Deflection of the structure is measured using a differential capacitor that consists of independent fixed plates and plates attached to the moving mass. The fixed plates are driven by 180° out-of-phase square waves. Acceleration will deflect the beam and unbalance the differential capacitor, resulting in an output square wave whose amplitude is proportional to acceleration. Phase sensitive demodulation techniques are then used to rectify the signal and determine the direction of the acceleration.

The output of the demodulator is amplified and brought off-chip through a 32 kΩ resistor. At this point, the user can set the signal bandwidth of the device by adding a capacitor. This filtering improves measurement resolution and helps prevent aliasing.

## PERFORMANCE

Rather than using additional temperature compensation circuitry, innovative design techniques have been used to ensure high performance is built in. As a result, there is essentially no quantization error or non-monotonic behavior, and temperature hysteresis is very low (typically less than 10 m*g* over the −40°C to +125°C temperature range).

Figure 9 shows the zero *g* output performance of eight parts (X and Y axis) over a −40°C to +125°C temperature range.

Figure 12 demonstrates the typical sensitivity shift over temperature for $V_S$ = 5 V. Sensitivity stability is optimized for $V_S$ = 5 V, but is still very good over the specified range; it is typically better than ±1% over temperature at $V_S$ = 3 V.

# APPLICATIONS

## POWER SUPPLY DECOUPLING

For most applications, a single 0.1 µF capacitor, $C_{DC}$, will adequately decouple the accelerometer from noise on the power supply. However in some cases, particularly where noise is present at the 140 kHz internal clock frequency (or any harmonic thereof), noise on the supply may cause interference on the ADXL103/ADXL203 output. If additional decoupling is needed, a 100 Ω (or smaller) resistor or ferrite beads may be inserted in the supply line of the ADXL103/ADXL203. Additionally, a larger bulk bypass capacitor (in the 1 µF to 22 µF range) may be added in parallel to $C_{DC}$.

## SETTING THE BANDWIDTH USING $C_X$ AND $C_Y$

The ADXL103/ADXL203 has provisions for bandlimiting the $X_{OUT}$ and $Y_{OUT}$ pins. Capacitors must be added at these pins to implement low-pass filtering for antialiasing and noise reduction. The equation for the 3 dB bandwidth is

$$F_{-3\,dB} = 1/(2\pi(32\ \text{k}\Omega) \times C_{(X,\,Y)})$$

or more simply,

$$F_{-3\,dB} = 5\ \mu\text{F}/C_{(X,\,Y)}$$

The tolerance of the internal resistor ($R_{FILT}$) can vary typically as much as ±25% of its nominal value (32 kΩ); thus, the bandwidth will vary accordingly. A minimum capacitance of 2000 pF for $C_X$ and $C_Y$ is required in all cases.

**Table 4. Filter Capacitor Selection, $C_X$ and $C_Y$**

| Bandwidth (Hz) | Capacitor (µF) |
|---|---|
| 1 | 4.7 |
| 10 | 0.47 |
| 50 | 0.10 |
| 100 | 0.05 |
| 200 | 0.027 |
| 500 | 0.01 |

## SELF TEST

The ST pin controls the self-test feature. When this pin is set to $V_S$, an electrostatic force is exerted on the beam of the accelerometer. The resulting movement of the beam allows the user to test if the accelerometer is functional. The typical change in output will be 750 mg (corresponding to 750 mV). This pin may be left open-circuit or connected to common in normal use.

The ST pin should never be exposed to voltage greater than $V_S$ + 0.3 V. If the system design is such that this condition cannot be guaranteed (i.e., multiple supply voltages present), a low $V_F$ clamping diode between ST and $V_S$ is recommended.

## DESIGN TRADE-OFFS FOR SELECTING FILTER CHARACTERISTICS: THE NOISE/BW TRADE-OFF

The accelerometer bandwidth selected will ultimately determine the measurement resolution (smallest detectable acceleration). Filtering can be used to lower the noise floor, which improves the resolution of the accelerometer. Resolution is dependent on the analog filter bandwidth at $X_{OUT}$ and $Y_{OUT}$.

The output of the ADXL103/ADXL203 has a typical bandwidth of 2.5 kHz. The user must filter the signal at this point to limit aliasing errors. The analog bandwidth must be no more than half the A/D sampling frequency to minimize aliasing. The analog bandwidth may be further decreased to reduce noise and improve resolution.

The ADXL103/ADXL203 noise has the characteristics of white Gaussian noise, which contributes equally at all frequencies and is described in terms of µg/√Hz (i.e., the noise is proportional to the square root of the accelerometer's bandwidth). The user should limit bandwidth to the lowest frequency needed by the application in order to maximize the resolution and dynamic range of the accelerometer.

With the single pole roll-off characteristic, the typical noise of the ADXL103/ADXL203 is determined by

$$rmsNoise = (110\mu\text{g}/\sqrt{Hz}) \times (\sqrt{BW \times 1.6})$$

At 100 Hz, the noise is

$$rmsNoise = (110\mu\text{g}/\sqrt{Hz}) \times (\sqrt{100 \times 1.6}) = 1.4mg$$

Often, the peak value of the noise is desired. Peak-to-peak noise can only be estimated by statistical methods. Table 5 is useful for estimating the probabilities of exceeding various peak values, given the rms value.

**Table 5. Estimation of Peak-to-Peak Noise**

| Peak-to-Peak Value | % of Time That Noise Will Exceed Nominal Peak-to-Peak Value |
|---|---|
| 2 × RMS | 32 |
| 4 × RMS | 4.6 |
| 6 × RMS | 0.27 |
| 8 × RMS | 0.006 |

Peak-to-peak noise values give the best estimate of the uncertainty in a single measurement. Table 6 gives the typical noise output of the ADXL103/ADXL203 for various $C_X$ and $C_Y$ values.

**Table 6. Filter Capacitor Selection ($C_X$, $C_Y$)**

| Bandwidth(Hz) | $C_X$, $C_Y$ (µF) | RMS Noise (mg) | Peak-to-Peak Noise Estimate (mg) |
|---|---|---|---|
| 10 | 0.47 | 0.4 | 2.6 |
| 50 | 0.1 | 1.0 | 6 |
| 100 | 0.047 | 1.4 | 8.4 |
| 500 | 0.01 | 3.1 | 18.7 |

## USING THE ADXL103/ADXL203 WITH OPERATING VOLTAGES OTHER THAN 5 V

The ADXL103/ADXL203 is tested and specified at $V_S$ = 5 V; however, it can be powered with $V_S$ as low as 3 V or as high as 6 V. Some performance parameters will change as the supply voltage is varied.

The ADXL103/ADXL203 output is ratiometric, so the output sensitivity (or scale factor) will vary proportionally to supply voltage. At $V_S$ = 3 V the output sensitivity is typically 560 mV/*g*.

The zero *g* bias output is also ratiometric, so the zero *g* output is nominally equal to $V_S/2$ at all supply voltages.

The output noise is not ratiometric but is absolute in volts; therefore, the noise density decreases as the supply voltage increases. This is because the scale factor (mV/*g*) increases while the noise voltage remains constant. At $V_S$ = 3 V, the noise density is typically 190 µg/√Hz.

Self-test response in g is roughly proportional to the square of the supply voltage. However, when ratiometricity of sensitivity is factored in with supply voltage, self-test response in volts is roughly proportional to the cube of the supply voltage. So at $V_S$ = 3 V, the self-test response will be approximately equivalent to 150 mV, or equivalent to 270 mg (typical).

The supply current decreases as the supply voltage decreases. Typical current consumption at $V_{DD}$ = 3 V is 450 µA.

## USING THE ADXL203 AS A DUAL-AXIS TILT SENSOR

One of the most popular applications of the ADXL203 is tilt measurement. An accelerometer uses the force of gravity as an input vector to determine the orientation of an object in space.

An accelerometer is most sensitive to tilt when its sensitive axis is perpendicular to the force of gravity, i.e., parallel to the earth's surface. At this orientation, its sensitivity to changes in tilt is highest. When the accelerometer is oriented on axis to gravity, i.e., near its +1 *g* or −1 *g* reading, the change in output acceleration per degree of tilt is negligible. When the accelerometer is perpendicular to gravity, its output will change nearly 17.5 mg per degree of tilt. At 45°, its output changes at only 12.2 mg per degree and resolution declines.

### *Dual-Axis Tilt Sensor: Converting Acceleration to Tilt*

When the accelerometer is oriented so both its X axis and Y axis are parallel to the earth's surface, it can be used as a 2-axis tilt sensor with a roll axis and a pitch axis. Once the output signal from the accelerometer has been converted to an acceleration that varies between −1 *g* and +1 *g*, the output tilt in degrees is calculated as follows:

$$PITCH = ASIN(A_X/1\ g)$$

$$ROLL = ASIN(A_Y/1\ g)$$

Be sure to account for overranges. It is possible for the accelerometers to output a signal greater than ±1 *g* due to vibration, shock, or other accelerations.

# PIN CONFIGURATIONS AND FUNCTIONAL DESCRIPTIONS

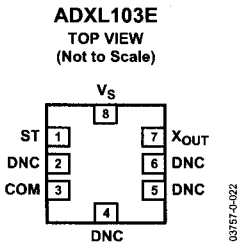


*Figure 22. ADXL103 8-Lead CLCC*

**Table 7. ADXL103 8-Lead CLCC Pin Function Descriptions**

| Pin No. | Mnemonic | Description |
|---|---|---|
| 1 | ST | Self Test |
| 2 | DNC | Do Not Connect |
| 3 | COM | Common |
| 4 | DNC | Do Not Connect |
| 5 | DNC | Do Not Connect |
| 6 | DNC | Do Not Connect |
| 7 | $X_{OUT}$ | X Channel Output |
| 8 | $V_S$ | 3 V to 6 V |

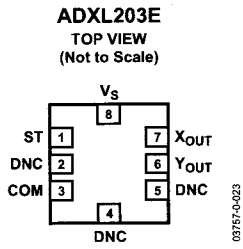


*Figure 23. ADXL203 8-Lead CLCC*

**Table 8. ADXL203 8-Lead CLCC Pin Function Descriptions**

| Pin No. | Mnemonic | Description |
|---|---|---|
| 1 | ST | Self Test |
| 2 | DNC | Do Not Connect |
| 3 | COM | Common |
| 4 | DNC | Do Not Connect |
| 5 | DNC | Do Not Connect |
| 6 | $Y_{OUT}$ | Y Channel Output |
| 7 | $X_{OUT}$ | X Channel Output |
| 8 | $V_S$ | 3 V to 6 V |

# OUTLINE DIMENSIONS

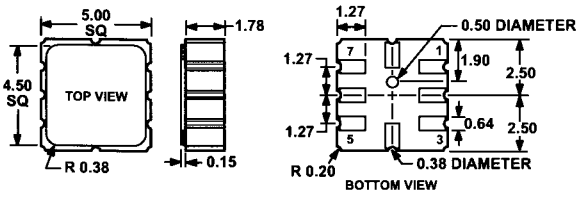


*Figure 24. 8-Terminal Ceramic Leadless Chip Carrier [LCC]*
*(E-8)*
*Dimensions shown in millimeters*

## ESD CAUTION

ESD (electrostatic discharge) sensitive device. Electrostatic charges as high as 4000 V readily accumulate on the human body and test equipment and can discharge without detection. Although this product features proprietary ESD protection circuitry, permanent damage may occur on devices subjected to high energy electrostatic discharges. Therefore, proper ESD precautions are recommended to avoid performance degradation or loss of functionality.


## ORDERING GUIDE

| ADXL103/ADXL203 Products | Number of Axes | Specified Voltage (V) | Temperature Range | Package Description | Package Option |
|---|---|---|---|---|---|
| ADXL103CE[1] | 1 | 5 | –40°C to +125°C | 8-Lead Ceramic Leadless Chip Carrier | E-8 |
| ADXL103CE–REEL[1] | 1 | 5 | –40°C to +125°C | 8-Lead Ceramic Leadless Chip Carrier | E-8 |
| ADXL203CE[1] | 2 | 5 | –40°C to +125°C | 8-Lead Ceramic Leadless Chip Carrier | E-8 |
| ADXL203CE–REEL[1] | 2 | 5 | –40°C to +125°C | 8-Lead Ceramic Leadless Chip Carrier | E-8 |
| ADXL203EB Evaluation Board | | | | Evaluation Board | |

[1] Lead finish—Gold over Nickel over Tungsten.


D03757–0–4/04(0)

ANALOG DEVICES

www.analog.com

# Improved, Ultra Low Noise ±2 *g* Dual Axis Accelerometer with Ratiometric Outputs

# MXR2312GL/ML

## FEATURES

**Resolution better than 1 milli-*g***
**Dual axis accelerometer fabricated on a monolithic CMOS IC**
**On chip mixed mode signal processing**
**No moving parts**
**50,000 *g* shock survival rating**
**17 Hz bandwidth expandable to >160 Hz**
**3.0V to 5.25V single supply continuous operation**
**Continuous self test**
**Independent axis programmability (special order)**
**Compensated for Sensitivity over temperature**
**Ultra low initial Zero-g Offset**

## APPLICATIONS

**Automotive** – Vehicle Security/Vehicle Stability control/ Headlight Angle Control/Tilt Sensing
**Security** – Gas Line/Elevator/Fatigue Sensing/Computer Security
**Information Appliances** – Computer Peripherals/PDA's/Mouse Smart Pens/Cell Phones
**Gaming** – Joystick/RF Interface/Menu Selection/Tilt Sensing
**GPS** – Electronic compass tilt correction
**Consumer** – LCD projectors, pedometers, blood pressure Monitor, digital cameras

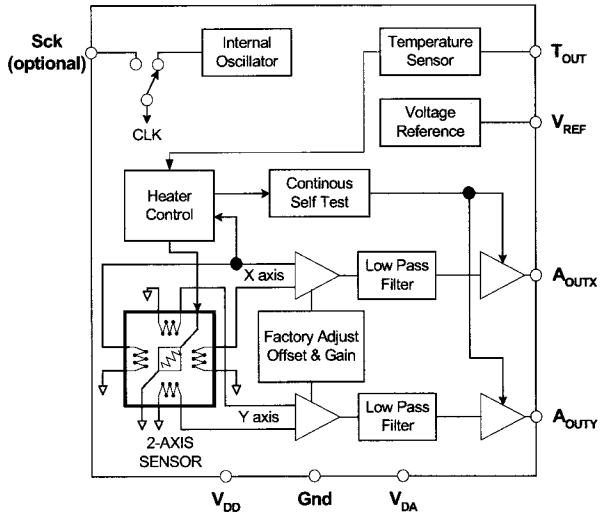


**MXR2312GL/MW FUNCTIONAL BLOCK DIAGRAM**

## GENERAL DESCRIPTION

The MXR2312GL/ML is a low cost, dual axis accelerometer fabricated on a standard, submicron CMOS process. It is a complete sensing system with on-chip mixed mode signal processing. The MXR2312GL/ML measures acceleration with a full-scale range of ±2 *g* and a sensitivity of 312mV/g. (The MEMSIC accelerometer product line extends from ±1 *g* to ±10 *g* with custom versions available above ±10 *g*.) It can measure both dynamic acceleration (e.g. vibration) and static acceleration (e.g. gravity). The MXR2312GL/ML design is based on heat convection and requires no solid proof mass. This eliminates stiction and particle problems associated with competitive devices and provides shock survival of 50,000 *g*, leading to significantly lower failure rate and lower loss due to handling during assembly.

The MXR2312GL/ML provides a ratiometric analog output that is proportional to 50% of the supply voltage at zero g acceleration. **The typical noise floor is 0.2 mg/$\sqrt{Hz}$ allowing signals below 1 milli-*g* to be resolved at 1 Hz bandwidth.** The 3dB rolloff of the device occurs at 17 Hz but is expandable to >160 Hz (reference Application Note AN-00MX-003). The MXR2312GL/ML is packaged in a hermetically sealed LCC surface mount package (5 mm x 5 mm x 2 mm height) and is operational over a -40°C to 85°C(ML) and 0°C to 70°C(GL) temperature range.



**©MEMSIC, Inc.**
**800 Turnpike St., Suite 202, North Andover, MA 01845**
**Tel: 978.738.0900 Fax: 978.738.0196**
**www.memsic.com**

**MXR2312GL/ML SPECIFICATIONS** (Measurements @ 25°C, Acceleration = 0 *g* unless otherwise noted; $V_{DD}$, $V_{DA}$ = 5.0V unless otherwise specified)

| Parameter | Conditions | MXR2312GL | | | MXR2312ML | | | Units |
|---|---|---|---|---|---|---|---|---|
| | | Min | Typ | Max | Min | Typ | Max | |
| SENSOR INPUT | Each Axis | | | | | | | |
| Measurement Range[1] | | ±2.0 | | | ±2.0 | | | *g* |
| Nonlinearity | Best fit straight line | | 0.5 | | | 0.5 | | % of FS |
| Alignment Error[2] | X Sensor to Y Sensor | | ±1.0 | | | ±1.0 | | degrees |
| Transverse Sensitivity[3] | | | ±2.0 | | | ±2.0 | | % |
| SENSITIVITY | Each Axis | | | | | | | |
| Sensitivity, Analog Outputs at pins $A_{OUTX}$ and $A_{OUTY}$[5] | | 296 | 312 | 328 | 296 | 312 | 328 | mV/*g* |
| Change over Temperature | | -10 | | +8 | -25 | | +8 | % |
| ZERO *g* BIAS LEVEL | Each Axis | | | | | | | |
| 0 *g* Offset[5] | | -0.1 | 0.0 | +0.1 | -0.1 | 0.0 | +0.1 | *g* |
| 0 *g* Voltage[5] | | 2.47 | 2.50 | 2.53 | 2.47 | 2.50 | 2.53 | V |
| 0 *g* Offset over Temperature | | | ±1.5 | | | ±1.5 | | mg/°C |
| | Based on 312 mV/g | | ±0.47 | | | ±0.47 | | mV/°C |
| NOISE PERFORMANCE | | | | | | | | |
| Noise Density, rms | Without frequency compensation | | 0.2 | 0.4 | | 0.2 | 0.4 | mg/$\sqrt{Hz}$ |
| FREQUENCY RESPONSE | | | | | | | | |
| 3dB Bandwidth - uncompensated | | 12 | 17 | | 12 | 17 | | Hz |
| 3dB Bandwidth – compensated[4] | | | >160 | | | >160 | | Hz |
| TEMPERATURE OUTPUT | | | | | | | | |
| $T_{out}$ Voltage | | 1.15 | 1.25 | 1.35 | 1.15 | 1.25 | 1.35 | V |
| Sensitivity | | 4.6 | 5.0 | 5.4 | 4.6 | 5.0 | 5.4 | mV/°K |
| VOLTAGE REFERENCE | | | | | | | | |
| $V_{Ref}$ | @3.0V-5.0V supply | 2.4 | 2.5 | 2.65 | 2.4 | 2.5 | 2.65 | V |
| Change over Temperature | | | 0.1 | | | 0.1 | | mV/°C |
| Current Drive Capability | Source | | | 100 | | | 100 | µA |
| SELF TEST | | | | | | | | |
| Continuous Voltage at $A_{OUTX}$, $A_{OUTY}$ under Failure | @5.0V Supply, output rails to supply voltage | | 5.0 | | | 5.0 | | V |
| Continuous Voltage at $A_{OUTX}$, $A_{OUTY}$ under Failure | @3.0V Supply, output rails to supply voltage | | 3.0 | | | 3.0 | | V |
| $A_{OUTX}$ and $A_{OUTY}$ OUTPUTS | | | | | | | | |
| Normal Output Range | @5.0V Supply | 0.1 | | 4.9 | 0.1 | | 4.9 | V |
| | @3.0V Supply | 0.1 | | 2.9 | 0.1 | | 2.9 | V |
| Current | Source or sink, @ 3.0V-5.0V supply | | 100 | | | 100 | | µA |
| Turn-On Time | @5.0V Supply | | 100 | | | 100 | | mS |
| | @3.0V Supply | | 40 | | | 40 | | mS |
| POWER SUPPLY | | | | | | | | |
| Operating Voltage Range | | 3.0 | | 5.25 | 3.0 | | 5.25 | V |
| Supply Current | @ 5.0V | 2.7 | 3.3 | 4.1 | 2.7 | 3.3 | 4.1 | mA |
| Supply Current[5] | @ 3.0V | 3.2 | 4.0 | 4.8 | 3.2 | 4.0 | 4.8 | mA |
| TEMPERATURE RANGE | | | | | | | | |
| Operating Range | | 0 | | +70 | -40 | | +85 | °C |

**NOTES**

[1] Guaranteed by measurement of initial offset and sensitivity.

[2] Alignment error is specified as the angle between the true and indicated axis of sensitivity.

[3] Transverse sensitivity is the algebraic sum of the alignment and the inherent sensitivity errors.

[4] External circuitry is required to extend the 3dB bandwidth (ref. Application Note: AN-00MX-003)

[5] The device operates over a 3.0V to 5.25V supply range. Please note that sensitivity and zero *g* bias level will be slightly different at 3.0V operation. For devices to be operated at 3.0V in production, they can be trimmed at the factory specifically for this lower supply voltage operation, in which case the sensitivity and zero *g* bias level specifications on this page will be met. Please contact the factory for specially trimmed devices for low supply voltage operation.

## ABSOLUTE MAXIMUM RATINGS*

Supply Voltage ($V_{DD}$, $V_{DA}$) .....-0.5 to +7.0V
Storage Temperature .....-65°C to +150°C
Acceleration .....50,000 *g*

*Stresses above those listed under Absolute Maximum Ratings may cause permanent damage to the device. This is a stress rating only; the functional operation of the device at these or any other conditions above those indicated in the operational sections of this specification is not implied. Exposure to absolute maximum rating conditions for extended periods may affect device reliability.

### Package Characteristics

| Package | $\theta_{JA}$ | $\theta_{JC}$ | Device Weight |
|---|---|---|---|
| LCC-8 | 110°C/W | 22°C/W | < 1 gram |

### Pin Description: LCC-8 Package

| Pin | Name | Description |
|---|---|---|
| 1 | $T_{OUT}$ | Temperature (Analog Voltage) |
| 2 | $A_{OUTY}$ | Y-Axis Acceleration Signal |
| 3 | Gnd | Ground |
| 4 | $V_{DA}$ | Analog Supply Voltage |
| 5 | $A_{OUTX}$ | X-Axis Acceleration Signal |
| 6 | $V_{ref}$ | 2.5V Reference |
| 7 | Sck | Optional External Clock |
| 8 | $V_{DD}$ | Digital Supply Voltage |

### Ordering Guide

| Model | Package Style | Temperature Range |
|---|---|---|
| MXR2312GL | LCC - 8 | 0 to 70°C |
| MXR2312ML | LCC - 8 | -40 to 85°C |

All parts are shipped in tape and reel packaging.

**Caution:** ESD (electrostatic discharge) sensitive device.

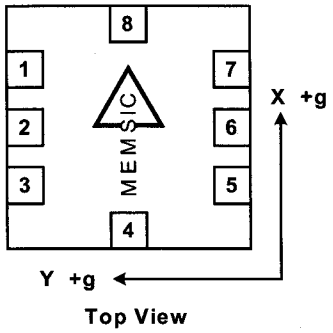


**Note:** The MEMSIC logo's arrow indicates the +X sensing direction of the device. The +Y sensing direction is rotated 90° away from the +X direction following the right-hand rule. Small circle indicates pin one(1).

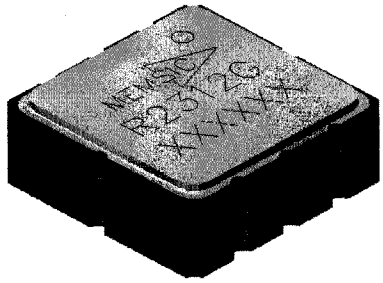

## THEORY OF OPERATION

The MEMSIC device is a complete dual-axis acceleration measurement system fabricated on a monolithic CMOS IC process. The device operation is based on heat transfer by natural convection and operates like other accelerometers having a proof mass. The stationary element, or 'proof mass', in the MEMSIC sensor is a gas.

A single heat source, centered in the silicon chip is suspended across a cavity. Equally spaced aluminum/polysilicon thermopiles (groups of thermocouples) are located equidistantly on all four sides of the heat source (dual axis). Under zero acceleration, a temperature gradient is symmetrical about the heat source, so that the temperature is the same at all four thermopiles, causing them to output the same voltage.

Acceleration in any direction will disturb the temperature profile, due to free convection heat transfer, causing it to be asymmetrical. The temperature, and hence voltage output of the four thermopiles will then be different. The differential voltage at the thermopile outputs is directly proportional to the acceleration. There are two identical acceleration signal paths on the accelerometer, one to measure acceleration in the x-axis and one to measure acceleration in the y-axis. Please visit the MEMSIC website at www.memsic.com for a picture/graphic description of the free convection heat transfer principle.

## MXR2312GL/ML PIN DESCRIPTIONS

$V_{DD}$ – This is the supply input for the digital circuits and the sensor heater in the accelerometer. The DC voltage should be between 3.0 and 5.25 volts. Refer to the section on PCB layout and fabrication suggestions for guidance on external parts and connections recommended.

$V_{DA}$ – This is the power supply input for the analog amplifiers in the accelerometer. Refer to the section on PCB layout and fabrication suggestions for guidance on external parts and connections recommended.

**Gnd** – This is the ground pin for the accelerometer.

$A_{OUTX}$ – This pin is the output of the x-axis acceleration sensor. The user should ensure the load impedance is sufficiently high as to not source/sink >100μA. While the sensitivity of this axis has been programmed at the factory to be the same as the sensitivity for the y-axis, the accelerometer can be programmed for non-equal sensitivities on the x- and y-axes. Contact the factory for additional information on this feature.

$A_{OUTY}$ – This pin is the output of the y-axis acceleration sensor. The user should ensure the load impedance is sufficiently high as to not source/sink >100μA. While the sensitivity of this axis has been programmed at the factory to be the same as the sensitivity for the x-axis, the accelerometer can be programmed for non-equal sensitivities on the x- and y-axes. Contact the factory for additional information on this feature.

$T_{OUT}$ – This pin is the buffered output of the temperature sensor. The analog voltage at $T_{OUT}$ is an indication of the die temperature. This voltage is useful as a differential measurement of temperature from ambient and not as an absolute measurement of temperature

**Sck** – The standard product is delivered with an internal clock option (800kHz). **This pin should be grounded when operating with the internal clock.** An external clock option can be special ordered from the factory allowing the user to input a clock signal between 400kHz and 1.6MHz.

$V_{ref}$ – A reference voltage is available from this pin. It is set at 2.50V typical and has 100μA of drive capability.

## DISCUSSION OF TILT APPLICATIONS AND RESOLUTION

**Tilt Applications:** One of the most popular applications of the MEMSIC accelerometer product line is in tilt/inclination measurement. An accelerometer uses the force of gravity as an input to determine the inclination angle of an object.

A MEMSIC accelerometer is most sensitive to changes in position, or tilt, when the accelerometer's sensitive axis is perpendicular to the force of gravity, or parallel to the Earth's surface. Similarly, when the accelerometer's axis is parallel to the force of gravity (perpendicular to the Earth's surface), it is least sensitive to changes in tilt.

Table 1 and Figure 2 help illustrate the output changes in the X- and Y-axes as the unit is tilted from +90° to 0°. Notice that when one axis has a small change in output per degree of tilt (in mg), the second axis has a large change in output per degree of tilt. The complementary nature of these two signals permits low cost accurate tilt sensing to be achieved with the MEMSIC device (reference application note AN-00MX-007).

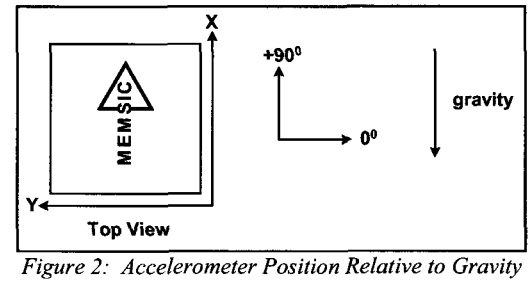


*Figure 2: Accelerometer Position Relative to Gravity*

| X-Axis Orientation To Earth's Surface (deg.) | X-Axis | | Y-Axis | |
|---|---|---|---|---|
| | X Output (g) | Change per deg. of tilt (mg) | Y Output (g) | Change per deg. of tilt (mg) |
| 90 | 1.000 | 0.15 | 0.000 | 17.45 |
| 85 | 0.996 | 1.37 | 0.087 | 17.37 |
| 80 | 0.985 | 2.88 | 0.174 | 17.16 |
| 70 | 0.940 | 5.86 | 0.342 | 16.35 |
| 60 | 0.866 | 8.59 | 0.500 | 15.04 |
| 45 | 0.707 | 12.23 | 0.707 | 12.23 |
| 30 | 0.500 | 15.04 | 0.866 | 8.59 |
| 20 | 0.342 | 16.35 | 0.940 | 5.86 |
| 10 | 0.174 | 17.16 | 0.985 | 2.88 |
| 5 | 0.087 | 17.37 | 0.996 | 1.37 |
| 0 | 0.000 | 17.45 | 1.000 | 0.15 |

*Table 1: Changes in Tilt for X- and Y-Axes*

**Resolution**: The accelerometer resolution is limited by noise. The output noise will vary with the measurement bandwidth. With the reduction of the bandwidth, by applying an external low pass filter, the output noise drops. Reduction of bandwidth will improve the signal to noise ratio and the resolution. The output noise scales directly with the square root of the measurement bandwidth. The maximum amplitude of the noise, its peak- to- peak value, approximately defines the worst case resolution of the measurement. With a simple RC low pass filter, the rms noise is calculated as follows:

$$\text{Noise (mg rms)} = \text{Noise(mg/}\sqrt{Hz}\text{)} * \sqrt{(Bandwidth(Hz)*1.6)}$$

The peak-to-peak noise is approximately equal to 6.6 times the rms value (for an average uncertainty of 0.1%).

## EXTERNAL FILTERS

**AC Coupling**: For applications where only dynamic accelerations (vibration) are to be measured, it is recommended to ac couple the accelerometer output as shown in Figure 3. The advantage of ac coupling is that variations from part to part of zero *g* offset and zero *g* offset versus temperature can be eliminated. Figure 3 is a HPF (high pass filter) with a –3dB breakpoint given by the equation: $f = 1/2\pi RC$. In many applications it may be desirable to have the HPF –3dB point at a very low frequency in order to detect very low frequency accelerations. Sometimes the implementation of this HPF may result in unreasonably large capacitors, and the designer must turn to digital implementations of HPFs where very low frequency –3dB breakpoints can be achieved.

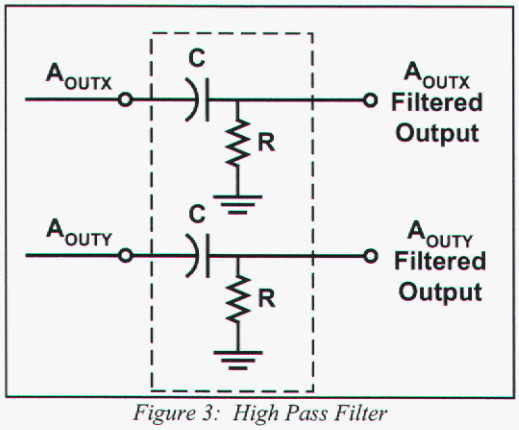


*Figure 3: High Pass Filter*

**Low Pass Filter**: An external low pass filter is useful in low frequency applications such as tilt or inclination. The low pass filter limits the noise floor and improves the resolution of the accelerometer. **When designing with MEMSIC ratiometric output accelerometers (MXRxxxx series), it is highly recommended that an external, 20 Hz low pass filter be used to eliminate internally generated periodic noise that is coupled to the output of the accelerometer.** The low pass filter shown in Figure 4 has a –3dB breakpoint given by the equation: $f = 1/2\pi RC$. For the 200 Hz ratiometric output device filter, C=0.2µF and R=39kΩ, ±5%, 1/8W.

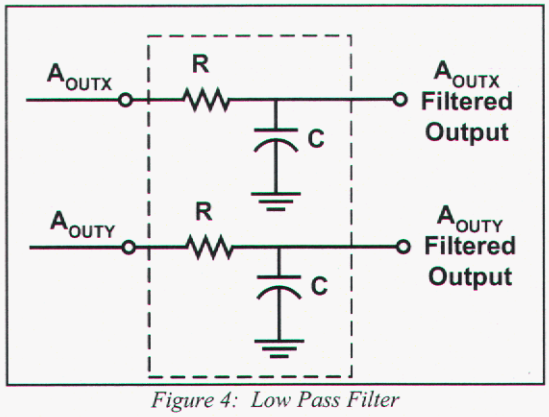


*Figure 4: Low Pass Filter*

## USING THE ACCELEROMETER IN VERY LOW POWER APPLICATIONS (BATTERY OPERATION)

In applications with power limitations, power cycling can be used to extend the battery operating life. One important consideration when power cycling is that the accelerometer turn on time limits the frequency bandwidth of the accelerations to be measured. For example, operating at 3.0V the turn on time is 40mS. To double the operating time, a particular application may cycle power ON for 40mS, then OFF for 40mS, resulting in a measurement period of 80mS, or a frequency of 12.5Hz. With a frequency of measurements of 12.5Hz, accelerations changes as high as 6.25Hz can be detected. Power cycling can be used effectively in many inclinometry applications, where inclination changes can be slow and infrequent.

## POWER SUPPLY NOISE REJECTION

Two capacitors and a resistor are recommended for best rejection of power supply noise (reference Figure 5 below). The capacitors should be located as close as possible to the device supply pins ($V_{DA}$, $V_{DD}$). The capacitor lead length should be as short as possible, and surface mount capacitors are preferred. For typical applications, capacitors C1 and C2 can be ceramic 0.1 µF, and the resistor R can be 10 Ω. In 5V applications where power consumption is not a concern, maximum supply noise rejection can be obtained by significantly increasing the values of C1, C2 and R. For example, C1 = C2 = 0.47 µF and R = 270 Ω will virtually eliminate power supply noise effects.

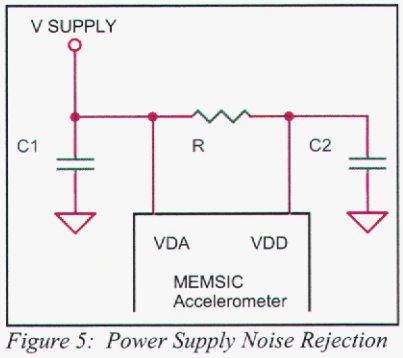


*Figure 5: Power Supply Noise Rejection*

**PCB LAYOUT AND FABRICATION SUGGESTIONS**

1. The Sck pin should be grounded to minimize noise.
2. Liberal use of ceramic bypass capacitors is recommended.
3. Robust low inductance ground wiring should be used.
4. Care should be taken to ensure there is "thermal symmetry" on the PCB immediately surrounding the MEMSIC device and that there is no significant heat source nearby.
5. A metal ground plane should be added directly beneath the MEMSIC device. The size of the plane should be similar to the MEMSIC device's footprint and be as thick as possible.
6. Vias can be added symmetrically around the ground plane. Vias increase thermal isolation of the device from the rest of the PCB.

**LCC-8 PACKAGE DRAWING**

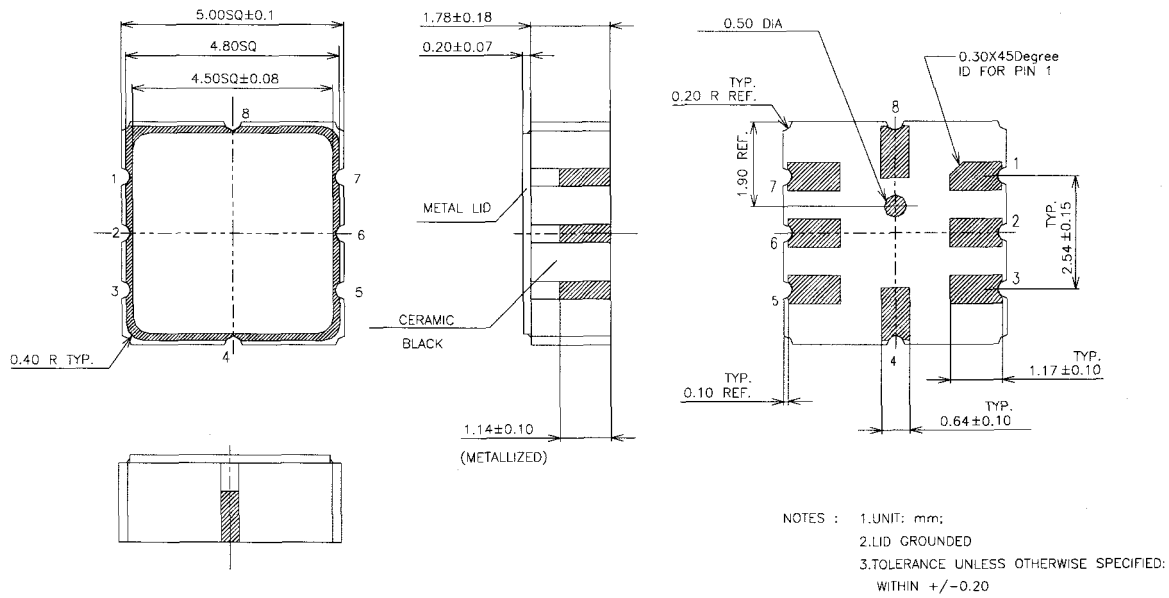


*Fig 6: Hermetically Sealed Package Outline*

# Dual Axis, Low *g*, Fully Integrated Accelerometers

By Harvey Weinberg

The *ADXL202* is the newest low-*g* (±2 *g*), dual-axis, surface-micromachined accelerometer from Analog Devices. Building on experience gained in manufacturing millions of *i*MEMS® accelerometers in the past six years, the ADXL202 is the world's first commercial dual axis, surface micromachined accelerometer to combine low-*g* sensing with lowest power, lowest noise, and digital outputs—all on a single silicon chip.

Surface micromachining, first commercialized with the ADXL50, allows for integration of the acceleration sensor with all signal conditioning electronics—tight integration of the sensor and its signal conditioning is what has made this impressive performance possible.

Lower cost was a major driver in the ADXL202 design effort. Integrating two axes resulted in a significant cost reduction per axis. In addition, while the ADXL50, ADXL150, and ADXL250 can be thought of as "acceleration to volts" transducers, the ADXL202 adds a Pulse Width Modulated (PWM) digital output capability as well. Since most accelerometers will interface with a microcontroller, a PWM output obviates the need for an A to D converter, further driving down the user's total system cost.

## Sensor Structure

As with all of our accelerometer products, the sensor element is a differential capacitor whose output is proportional to acceleration (basic sensor information can be seen in *Analog Dialogue* 27-2, 1993, and *Analog Dialogue* 30-4, 1996). Since device performance is so dependent on sensor design, a brief explanation of some of the key factors in beam design is appropriate.

The beam is made up of many interdigitated fingers. Each set of fingers can be visualized as shown in Figure 1. The differential capacitance of each finger is proportional to the overlapping area between the fixed outer plates and the moving finger, and the displacement of the moving finger. Clearly these are very small capacitors, and in order to reduce noise and increase resolution we need as large a differential capacitance as practical.

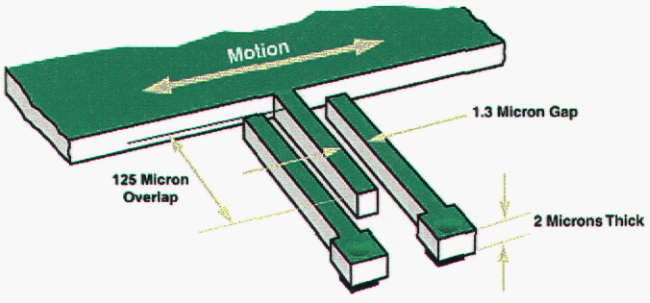


Figure 1. Beam Dimensions for a Single Finger.

The capacitor area is limited by the 2-micron height—fixed by process technology, while the (125-micron) overlap is adjustable to some extent. However longer fingers are not desirable for several reasons. Longer fingers are harder to manufacture and increased beam size translates to more expensive parts.

The movement of the beam is controlled by the polysilicon springs holding the beam. These springs and the beam's mass obey the same laws of physics we learned in high school. The force ($F$) on a mass ($m$) subject to acceleration ($a$), according to Newton's Second Law, is $F = m\,a$, and the deflection ($x$) of a restraining spring (obeying Hooke's Law) is proportional to the applied force, $F = k\,x$, and:

$$x = (m/k)\,a$$

The only two parameters under our control are the spring stiffness, or spring constant, ($k$), and mass ($m$). Reducing the spring constant seems like an easy way to improve beam sensitivity. But as usual, nothing comes for free. The resonant frequency of the beam is proportional to the spring constant, and the accelerometer must operate at frequencies below the resonant frequency. In addition, higher spring constants make for more rugged beams (higher shock survivability). So if we would like to keep the spring constant as high as possible the only parameter left to change is mass.

Adding mass normally implies a larger sensor area, resulting in more expensive parts, since the only way to add mass it to make the beam larger. In the ADXL202 a novel beam structure was invented, as shown in Figure 2. Rather than using two discrete beams placed orthogonally as in the ADXL250 (*Analog Dialogue* 30-4, 1996, page 5, Figure 5), the fingers that constitute the X and Y axis variable capacitors are integrated along the sides of a single square beam. This results in a reduction of the overall sensor area, yet the larger common beam mass enhances the resolution of the ADXL202. A spring suspension system, shown in Figure 3, situated in the corners of the beam, was designed to minimize cross-axis sensitivity (i.e., with acceleration along one axis, any tendency toward motion or outputs in the orthogonal direction is suppressed).

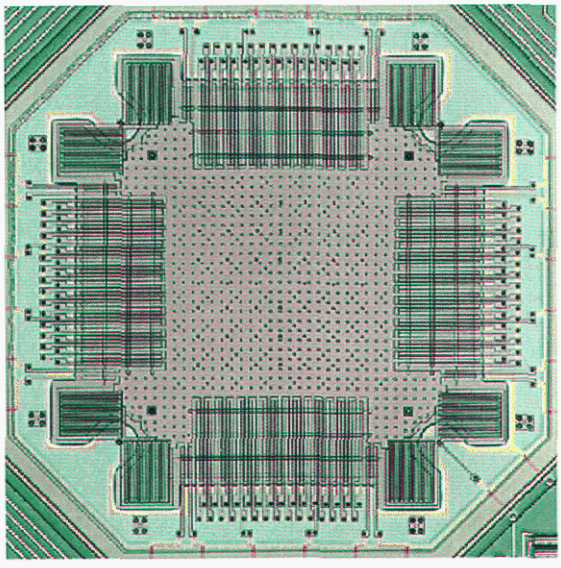

Figure 2. ADXL202 Beam Structure.

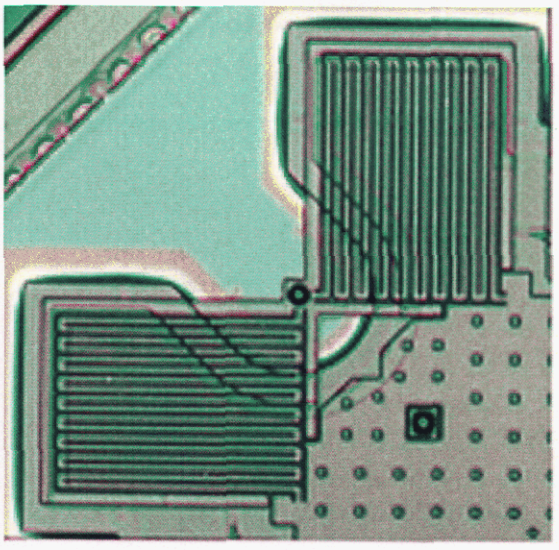

Figure 3. Detail of One Corner of the ADXL202 Beam showing springs.

### Circuit Architecture

The circuit architecture (shown in Figure 4) of the ADXL202 is similar to the ADXL250 up to the demodulator. The fixed outer plates are driven with square waves that are 180 degrees out of phase. When the movable fingers (and hence the beam) are centered between the fixed outer plates, both sides of the differential capacitor have equal capacitance and the ac voltage on the beam is zero. However, if the beam is displaced due to an applied acceleration, the differential capacitance will be unbalanced and an ac voltage of amplitude proportional to the displacement of the beam will result.

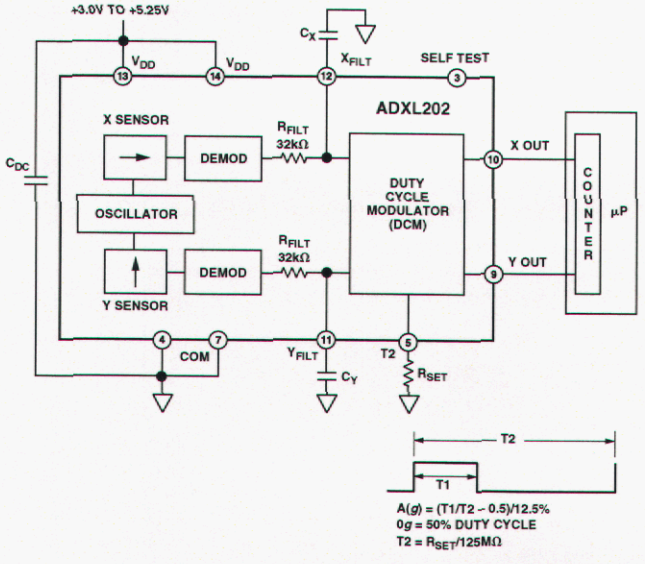


Figure 4. ADXL202 Circuit Architecture.

This ac voltage is amplified and then demodulated by a synchronous demodulator. The output of the demodulator drives the duty cycle modulator through a 32-kΩ resistor. Here a pin is available on each channel to allow the user to set the bandwidth by adding two external capacitors (one per channel) creating a simple first-order RC low pass filter. The low pass filtered signal is converted to a PWM signal by the duty cycle modulator. The period of the PWM output may be set from 0.5 to 10 ms, using a single resistor.

### Performance and Applications

Just as it was impossible 25 years ago to predict where low-cost lasers would turn up, today it's difficult to imagine the large number of applications where low-cost accelerometers will be used. The ADXL202 breaks so many performance-vs.-cost barriers that most of its really successful applications are not classically "accelerometer" (literally "acceleration-measuring") applications. They are now being used in car alarms, machine health monitoring, joysticks, game pads, and other computer input devices.

As mentioned in the introduction, the ADXL202 is the lowest noise dual axis surface micromachined accelerometer in production today. With its typical noise density of 500 mg/$\sqrt{\text{Hz}}$, it is possible to resolve inclinations of better than ±1° of tilt at bandwidths of up to 50 Hz. The high-resolution (approximately 14-bit) duty-cycle modulator allows users to take advantage of the ADXL202's capabilities in low cost systems. These capabilities have opened the door to several other non-traditional applications, such as car alarms (where they are used to sense jacking-up or towing) and automatic machine leveling.

### Support Tools

Extensive support tools are available for designers. The hardware tools available are a simple evaluation PCB with an ADXL202 in its minimum circuit configuration (part number ADXL202EB), and the ADXL202EB-232, a complete 2-axis data acquisition system that interfaces to a PC. Primarily targeted at designers who need to fully understand how acceleration measurement will enable their application or product, the ADXL202EB-232 includes software for viewing accelerometer signals and data logging.

The ADXL202 Interactive Designer is an Excel-based spreadsheet model that takes the user through the design process of selecting ADXL202 components and defining software parameters for microcontroller interface. The spreadsheet outputs component values and information about the resolution, bandwidth and acquisition rate of your design. It is available free at the Web site listed below.

Also available at that site are several hardware and software reference designs, highlighting different interface techniques and a variety of application notes. Each reference design includes flow charts and source code for various popular microcontrollers, as well as a description of where each data acquisition method is appropriate. These documents can be found at **http://www.analog.com/iMEMS/products/ADXL202_top.html.**

## Appendix B – MEMS Gyroscopes

Datasheets:

A. **ADXRS300 ±300°/sec Single Chip Yaw Rate Gyro with Signal Conditioning** by Analog Devices

Further Information:

B. **New iMEMS® Angular-Rate-Sensing Gyroscope** by John Green et. al. (from Analog Dialogue 37-03)

# ±300°/s Single Chip Yaw Rate Gyro with Signal Conditioning

# ADXRS300

## FEATURES

**Complete rate gyroscope on a single chip**
**Z-axis (yaw rate) response**
**High vibration rejection over wide frequency**
**2000 *g* powered shock survivability**
**Self-test on digital command**
**Temperature sensor output**
**Precision voltage reference output**
**Absolute rate output for precision applications**
**5 V single-supply operation**
**Ultrasmall and light (< 0.15 cc, < 0.5 gram)**

## APPLICATIONS

**Vehicle chassis rollover sensing**
**Inertial measurement units**
**Platform stabilization**

## GENERAL DESCRIPTION

The ADXRS300 is a complete angular rate sensor (gyroscope) that uses Analog Devices' surface-micromachining process to make a functionally complete and low cost angular rate sensor integrated with all of the required electronics on one chip. The manufacturing technique for this device is the same high volume BIMOS process used for high reliability automotive airbag accelerometers.

The output signal, RATEOUT (1B, 2A), is a voltage proportional to angular rate about the axis normal to the top surface of the package (see Figure 4). A single external resistor can be used to lower the scale factor. An external capacitor is used to set the bandwidth. Other external capacitors are required for operation (see Figure 5).

A precision reference and a temperature output are also provided for compensation techniques. Two digital self-test inputs electromechanically excite the sensor to test proper operation of both sensors and the signal conditioning circuits. The ADXRS300 is available in a 7 mm × 7 mm × 3 mm BGA chip-scale package.

## FUNCTIONAL BLOCK DIAGRAM

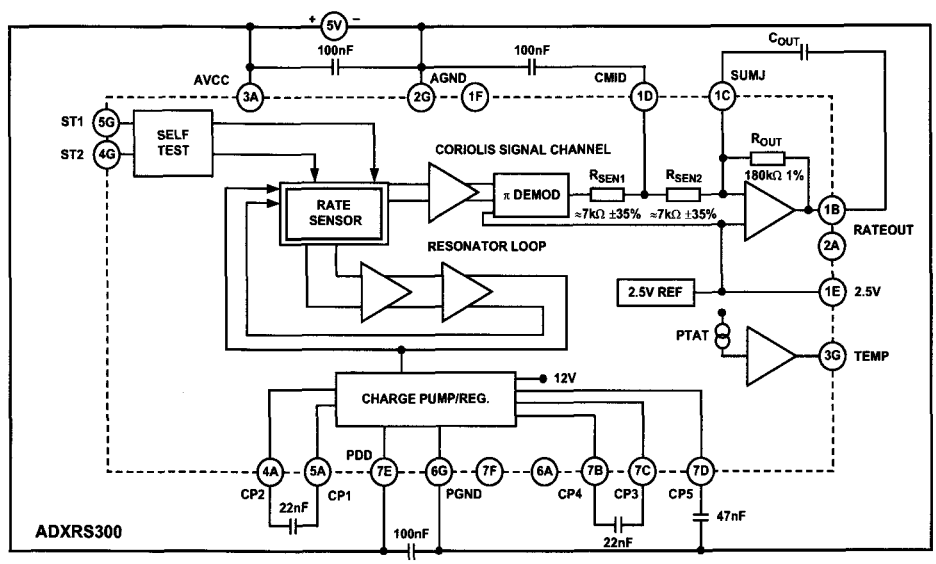


*Figure 1.*

**Rev. B**


**One Technology Way, P.O. Box 9106, Norwood, MA 02062-9106, U.S.A.**
**Tel: 781.329.4700** **www.analog.com**
**Fax: 781.326.8703** 

# TABLE OF CONTENTS



## REVISION HISTORY

**3/04—Data Sheet Changed from Rev. A to Rev. B**

Updated Format ..... Universal
Changes to Table 1 Conditions ..... 3
Added Evaluation Board to Ordering Guide ..... 8

**3/03—Data Sheet Changed from Rev. 0 to Rev. A**

Edit to Figure 3 ..... 5

# SPECIFICATIONS

@$T_A$ = 25°C, $V_S$ = 5 V, Angular Rate = 0°/s, Bandwidth = 80 Hz ($C_{OUT}$ = 0.01 µF), ±1*g*, unless otherwise noted.

**Table 1.**

| Parameter | Conditions | ADXRS300ABG | | | Unit |
|---|---|---|---|---|---|
| | | Min[1] | Typ | Max[1] | |
| SENSITIVITY | Clockwise rotation is positive output | | | | |
| Dynamic Range[2] | Full-scale range over specifications range | ±300 | | | °/s |
| Initial | @25°C | 4.6 | 5 | 5.4 | mV/°/s |
| Over Temperature[3] | $V_S$ = 4.75 V to 5.25 V | 4.6 | 5 | 5.4 | mV/°/s |
| Nonlinearity | Best fit straight line | | 0.1 | | % of FS |
| NULL | | | | | |
| Initial Null | | 2.3 | 2.50 | 2.7 | V |
| Over Temperature[3] | $V_S$ = 4.75 V to 5.25 V | 2.3 | | 2.7 | V |
| Turn-On Time | Power on to ±½°/s of final | | 35 | | ms |
| Linear Acceleration Effect | Any axis | | 0.2 | | °/s/*g* |
| Voltage Sensitivity | $V_{CC}$ = 4.75 V to 5.25 V | | 1 | | °/s/V |
| NOISE PERFORMANCE | | | | | |
| Rate Noise Density | @25°C | | 0.1 | | °/s/√Hz |
| FREQUENCY RESPONSE | | | | | |
| 3 dB Bandwidth (User Selectable)[4] | 22 nF as comp cap (see the Setting Bandwidth section) | | 40 | | Hz |
| Sensor Resonant Frequency | | | 14 | | kHz |
| SELF-TEST INPUTS | | | | | |
| ST1 RATEOUT Response[5] | ST1 pin from Logic 0 to 1 | −150 | −270 | −450 | mV |
| ST2 RATEOUT Response[5] | ST2 pin from Logic 0 to 1 | +150 | +270 | +450 | mV |
| Logic 1 Input Voltage | Standard high logic level definition | 3.3 | | | V |
| Logic 0 Input Voltage | Standard low logic level definition | | | 1.7 | V |
| Input Impedance | To common | | 50 | | kΩ |
| TEMPERATURE SENSOR | | | | | |
| $V_{OUT}$ at 298°K | | | 2.50 | | V |
| Max Current Load on Pin | Source to common | | | 50 | µA |
| Scale Factor | Proportional to absolute temperature | | 8.4 | | mV/°K |
| OUTPUT DRIVE CAPABILITY | | | | | |
| Output Voltage Swing | $I_{OUT}$ = ±100 µA | 0.25 | | $V_S$ − 0.25 | V |
| Capacitive Load Drive | | 1000 | | | pF |
| 2.5 V REFERENCE | | | | | |
| Voltage Value | | 2.45 | 2.5 | 2.55 | V |
| Load Drive to Ground | Source | | 200 | | µA |
| Load Regulation | 0 < $I_{OUT}$ < 200 µA | | 5.0 | | mV/mA |
| Power Supply Rejection | 4.75 $V_S$ to 5.25 $V_S$ | | 1.0 | | mV/V |
| Temperature Drift | Delta from 25°C | | 5.0 | | mV |
| POWER SUPPLY | | | | | |
| Operating Voltage Range | | 4.75 | 5.00 | 5.25 | V |
| Quiescent Supply Current | | | 6.0 | 8.0 | mA |
| TEMPERATURE RANGE | | | | | |
| Specified Performance Grade A | Temperature tested to max and min specifications | −40 | | +85 | °C |

[1] All minimum and maximum specifications are guaranteed. Typical specifications are not tested or guaranteed.
[2] Dynamic range is the maximum full-scale measurement range possible, including output swing range, initial offset, sensitivity, offset drift, and sensitivity drift at 5 V supplies.
[3] Specification refers to the maximum extent of this parameter as a worst-case value of $T_{MIN}$ or $T_{MAX}$.
[4] Frequency at which response is 3 dB down from dc response with specified compensation capacitor value. Internal pole forming resistor is 180 kΩ. See the Setting Bandwidth section.
[5] Self-test response varies with temperature. See the Self-Test Function section for details.

# ABSOLUTE MAXIMUM RATINGS

Table 2.

| Parameter | Rating |
|---|---|
| Acceleration (Any Axis, Unpowered, 0.5 ms) | 2000 *g* |
| Acceleration (Any Axis, Powered, 0.5 ms) | 2000 *g* |
| $+V_S$ | −0.3 V to +6.0 V |
| Output Short-Circuit Duration (Any Pin to Common) | Indefininte |
| Operating Temperature Range | −55°C to +125°C |
| Storage Temperature | −65°C to +150°C |

Stresses above those listed under the Absolute Maximum Ratings may cause permanent damage to the device. This is a stress rating only; functional operation of the device at these or any other conditions above those indicated in the operational section of this specification is not implied. Exposure to absolute maximum rating conditions for extended periods may affect device reliability.

Applications requiring more than 200 cycles to MIL-STD-883 Method 1010 Condition B (−55°C to +125°C) require underfill or other means to achieve this requirement.

Drops onto hard surfaces can cause shocks of greater than 2000 *g* and exceed the absolute maximum rating of the device. Care should be exercised in handling to avoid damage.

## RATE SENSITIVE AXIS

This is a Z-axis rate-sensing device that is also called a yaw rate sensing device. It produces a positive going output voltage for clockwise rotation about the axis normal to the package top, i.e., clockwise when looking down at the package lid.

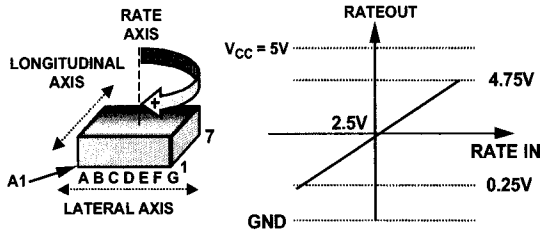


*Figure 2. RATEOUT Signal Increases with Clockwise Rotation*

## ESD CAUTION

ESD (electrostatic discharge) sensitive device. Electrostatic charges as high as 4000 V readily accumulate on the human body and test equipment and can discharge without detection. Although this product features proprietary ESD protection circuitry, permanent damage may occur on devices subjected to high energy electrostatic discharges. Therefore, proper ESD precautions are recommended to avoid performance degradation or loss of functionality.

# PIN CONFIGURATION AND FUNCTION DESCRIPTIONS

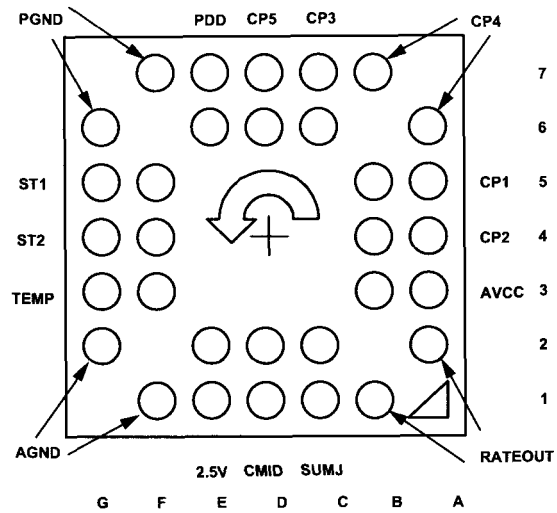


*Figure 3. 32-Lead BGA (Bottom View)*

**Table 3. Pin Function Descriptions**

| Pin No. | Mnemonic | Description |
|---|---|---|
| 6D, 7D | CP5 | HV Filter Capacitor—47 nF |
| 6A, 7B | CP4 | Charge Pump Capacitor—22 nF |
| 6C, 7C | CP3 | Charge Pump Capacitor—22 nF |
| 5A, 5B | CP1 | Charge Pump Capacitor—22 nF |
| 4A, 4B | CP2 | Charge Pump Capacitor—22 nF |
| 3A, 3B | AVCC | + Analog Supply |
| 1B, 2A | RATEOUT | Rate Signal Output |
| 1C, 2C | SUMJ | Output Amp Summing Junction |
| 1D, 2D | CMID | HF Filter Capacitor—100 nF |
| 1E, 2E | 2.5V | 2.5 V Precision Reference |
| 1F, 2G | AGND | Analog Supply Return |
| 3F, 3G | TEMP | Temperature Voltage Output |
| 4F, 4G | ST2 | Self-Test for Sensor 2 |
| 5F, 5G | ST1 | Self-Test for Sensor 1 |
| 6G, 7F | PGND | Charge Pump Supply Return |
| 6E, 7E | PDD | + Charge Pump Supply |

# THEORY OF OPERATION

The ADXRS300 operates on the principle of a resonator gyro. Two polysilicon sensing structures each contain a dither frame, which is electrostatically driven to resonance. This produces the necessary velocity element to produce a Coriolis force during angular rate. At two of the outer extremes of each frame, orthogonal to the dither motion, are movable fingers that are placed between fixed pickoff fingers to form a capacitive pickoff structure that senses Coriolis motion. The resulting signal is fed to a series of gain and demodulation stages that produce the electrical rate signal output. The dual-sensor design rejects external *g*-forces and vibration. Fabricating the sensor with the signal conditioning electronics preserves signal integrity in noisy environments.

The electrostatic resonator requires 14 V to 16 V for operation. Since only 5 V is typically available in most applications, a charge pump is included on-chip. If an external 14 V to 16 V supply is available, the two capacitors on CP1–CP4 can be omitted and this supply can be connected to CP5 (Pin 7D) with a 100 nF decoupling capacitor in place of the 47 nF.

After the demodulation stage, there is a single-pole low-pass filter consisting of an internal 7 kΩ resistor ($R_{SEN1}$) and an external user-supplied capacitor (CMID). A CMID capacitor of 100 nF sets a 400 Hz ±3 5% low-pass pole and is used to limit high frequency artifacts before final amplification. The bandwidth limit capacitor, $C_{OUT}$, sets the pass bandwidth (see Figure 5 and the Setting Bandwidth section).

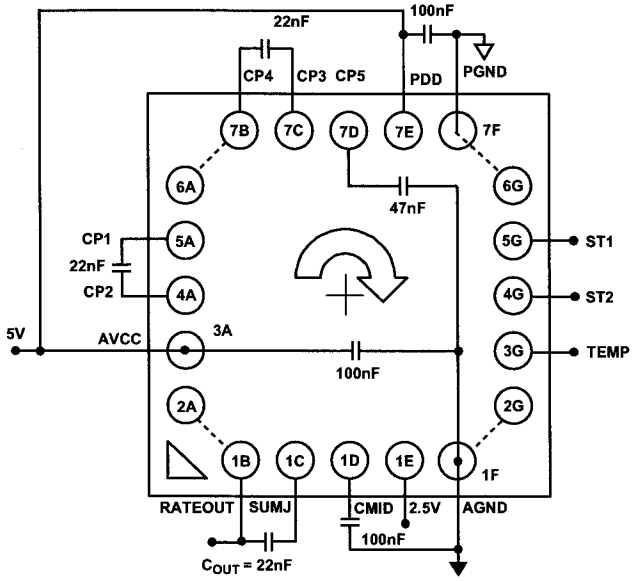


**NOTE THAT INNER ROWS/COLUMNS OF PINS HAVE BEEN OMITTED FOR CLARITY BUT SHOULD BE CONNECTED IN THE APPLICATION.**

*Figure 4. Example Application Circuit (Top View)*

## SUPPLY AND COMMON CONSIDERATIONS

Only power supplies used for supplying analog circuits are recommended for powering the ADXRS300. High frequency noise and transients associated with digital circuit supplies may have adverse effects on device operation.

Figure 4 shows the recommended connections for the ADXRS300 where both AVCC and PDD have a separate decoupling capacitor. These should be placed as close to the their respective pins as possible before routing to the system analog supply. This minimizes the noise injected by the charge pump that uses the PDD supply.

It is also recommended to place the charge pump capacitors connected to the CP1–CP4 pins as close to the part as possible. These capacitors are used to produce the on-chip high voltage supply switched at the dither frequency at approximately 14 kHz. Care should be taken to ensure that there is no more than 50 pF of stray capacitance between CP1–CP4 and ground. Surface-mount chip capacitors are suitable as long as they are rated for over 15 V.

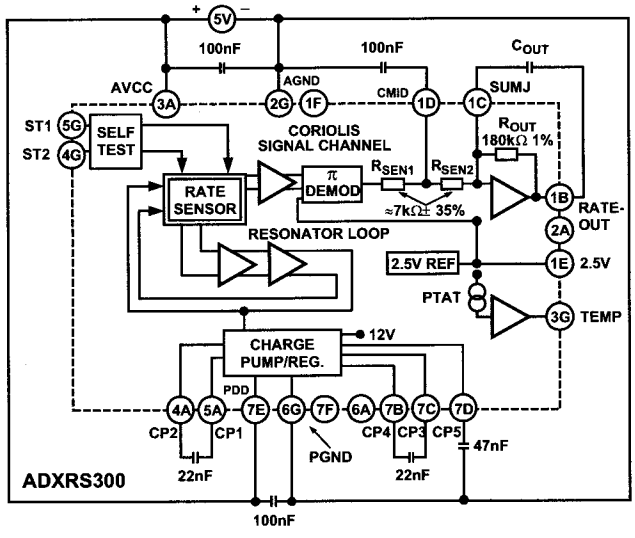


*Figure 5. Block Diagram with External Components*

## SETTING BANDWIDTH

External capacitors CMID and $C_{OUT}$ are used in combination with on-chip resistors to create two low-pass filters to limit the bandwidth of the ADXRS300's rate response. The −3 dB frequency set by $R_{OUT}$ and $C_{OUT}$ is

$$f_{OUT} = 1/(2 \times \pi \times R_{OUT} \times C_{OUT})$$

and can be well controlled since $R_{OUT}$ has been trimmed during manufacturing to be 180 kΩ ± 1%. Any external resistor applied between the RATEOUT (1B, 2A) and SUMJ (1C, 2C) pins results in

$$R_{OUT} = (180\ \text{k}\Omega \times R_{EXT}) / (180\ \text{k}\Omega \times R_{EXT})$$

The −3 dB frequency is set by RSEN (the parallel combination of $R_{SEN1}$ and $R_{SEN2}$) at about 3.5 kΩ nominal; CMID is less well controlled since $R_{SEN1}$ and $R_{SEN2}$ have been used to trim the rate sensitivity during manufacturing and have a ±35% tolerance. Its primary purpose is to limit the high frequency demodulation artifacts from saturating the final amplifier stage. Thus, this pole of nominally 400 Hz @ 0.1 µF need not be precise. Lower frequency is preferable, but its variability usually requires it to be about 10 times greater (in order to preserve phase integrity) than the well-controlled output pole. In general, both −3 dB filter frequencies should be set as low as possible to reduce the amplitude of these high frequency artifacts and to reduce the overall system noise.

## INCREASING MEASUREMENT RANGE

The full-scale measurement range of the ADXRS300 can be increased by placing an external resistor between the RATEOUT (1B, 2A) and SUMJ (1C, 2C) pins, which would parallel the internal $R_{OUT}$ resistor that is factory-trimmed to 180 kΩ. For example, a 330 kΩ external resistor will give ~50% increase in the full-scale range. This is effective for up to a 4× increase in the full-scale range (minimum value of the parallel resistor allowed is 45 kΩ). Beyond this amount of external sensitivity reduction, the internal circuitry headroom requirements prevent further increase in the linear full-scale output range. The drawbacks of modifying the full-scale range are the additional output null drift (as much as 2°/sec over temperature) and the readjustment of the initial null bias (see the Null Adjust section).

## USING THE ADXRS300 WITH A SUPPLY-RATIOMETRIC ADC

The ADXRS300's RATEOUT signal is nonratiometric, i.e., neither the null voltage nor the rate sensitivity is proportional to the supply. Rather they are nominally constant for dc supply changes within the 4.75 V to 5.25 V operating range. If the ADXRS300 is used with a supply-ratiometric ADC, the ADXRS300's 2.5 V output can be converted and used to make corrections in software for the supply variations.

## NULL ADJUST

Null adjustment is possible by injecting a suitable current to SUMJ (1C, 2C). Adding a suitable resistor to either ground or to the positive supply is a simple way of achieving this. The nominal 2.5 V null is for a symmetrical swing range at RATEOUT (1B, 2A). However, a nonsymmetric output swing may be suitable in some applications. Note that if a resistor is connected to the positive supply, then supply disturbances may reflect some null instabilities. Digital supply noise should be avoided, particularly in this case (see the Supply and Common Considerations section).

The resistor value to use is approximately

$$R_{NULL} = (2.5 \times 180{,}000)/(V_{NULL0} - V_{NULL1})$$

$V_{NULL0}$ is the unadjusted zero rate output, and $V_{NULL1}$ is the target null value. If the initial value is below the desired value, the resistor should terminate on common or ground. If it is above the desired value, the resistor should terminate on the 5 V supply. Values are typically in the 1 MΩ to 5 MΩ range.

If an external resistor is used across RATEOUT and SUMJ, then the parallel equivalent value is substituted into the preceding equation. Note that the resistor value is an estimate since it assumes $V_{CC}$ = 5.0 V and $V_{SUMJ}$ = 2.5 V.

## SELF-TEST FUNCTION

The ADXRS300 includes a self-test feature that actuates each of the sensing structures and associated electronics in the same manner as if subjected to angular rate. It is activated by standard logic high levels applied to inputs ST1 (5F, 5G), ST2 (4F, 4G), or both. ST1 causes a voltage at RATEOUT equivalent to typically −270 mV, and ST2 causes an opposite +270 mV change. The self-test response follows the viscosity temperature dependence of the package atmosphere, approximately 0.25%/°C.

Activating both ST1 and ST2 simultaneously is not damaging. Since ST1 and ST2 are not necessarily closely matched, actuating both simultaneously may result in an apparent null bias shift.

## CONTINUOUS SELF-TEST

The one-chip integration of the ADXRS300 gives it higher reliability than is obtainable with any other high volume manufacturing method. Also, it is manufactured under a mature BIMOS process that has field-proven reliability. As an additional failure detection measure, power-on self-test can be performed. However, some applications may warrant continuous self-test while sensing rate. Application notes outlining continuous self-test techniques are also available on the Analog Devices website.

# OUTLINE DIMENSIONS

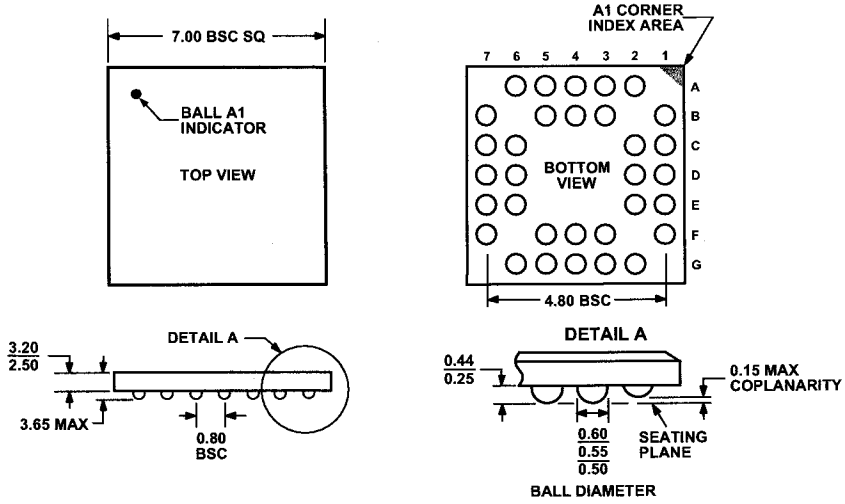


*Figure 6. 32-Lead Chip Scale Ball Grid Array [CSPBGA]*
*(BC-32)*
*Dimensions shown in millimeters*

## ORDERING GUIDE

| Model | Temperature Range | Package Description | Package Outline |
|---|---|---|---|
| ADXRS300ABG | –40°C to +85°C | 32-Lead BGA | BC-32 |
| ADXRS300ABG-Reel | –40°C to +85°C | 32-Lead BGA | BC-32 |
| ADXRS300EB | | Evaluation Board | |


C03227–0–3/04(B)

# New iMEMS® Angular-Rate-Sensing Gyroscope

by John Geen [john.geen@analog.com] and
David Krakauer [david.krakauer@analog.com]
ADI Micromachined Products Division

## INTRODUCTION

The new ADXRS150 and ADXRS300 gyros from Analog Devices, with full-scale ranges of 150°/s and 300°/s, represent a quantum jump in gyro technology. The first commercially available surface-micromachined angular rate sensors with integrated electronics, they are smaller—with lower power consumption, and better immunity to shock and vibration—than any gyros having comparable functionality. This genuine breakthrough is possible only because of the Analog Devices proprietary *integrated micro electro-mechanical system* (iMEMS) process, proven by use in millions of automotive accelerometers.

### Product Description

Gyroscopes are used to measure *angular* rate—how quickly an object turns. The rotation is typically measured in reference to one of three axes: yaw, pitch, or roll.

Figure 1 shows a diagram representing each axis of sensitivity relative to a package mounted to a flat surface. A gyroscope with one axis of sensitivity can also be used to measure other axes by mounting the gyro differently, as shown in the right-hand diagram. Here, a yaw-axis gyro, such as the ADXRS150 or ADXRS300, is mounted on its side so that the yaw axis becomes the roll axis.

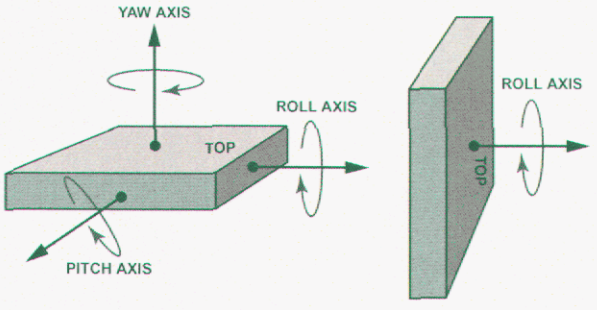


Figure 1. Gyro axes of rotational sensitivity. Depending on how a gyro normally sits, its primary axis of sensitivity can be one of the three axes of motion: yaw, pitch, or roll. The ADXRS150 and ADXRS300 are yaw-axis gyros, but they can measure rotation about other axes by appropriate mounting orientation. For example, at the right: a yaw-axis device is positioned to measure roll.

As an example of how a gyro could be used, a yaw-axis gyro mounted on a turntable rotating at 33 1/3 rpm (revolutions per minute) would measure a constant rotation of 360° times 33 1/3 rpm divided by 60 seconds, or 200°/s. The gyro would output a voltage proportional to the angular rate, as determined by its sensitivity, measured in millivolts per degree per second (mV/°/s). The full-scale voltage determines how much angular rate can be measured, so in the example of the turntable, a gyro would need to have a full-scale voltage corresponding to at least 200°/s. Full-scale is limited by the available voltage swing divided by the sensitivity. The ADXRS300, for example, with 1.5 V full-scale and a sensitivity of 5 mV/°/s, handles a full-scale of 300°/s. The ADXRS150, has a more limited full-scale of 150°/s but a greater sensitivity of 12.5 mV/°/s.

One practical application is to measure how quickly a car turns by mounting a gyro inside the vehicle; if the gyro senses that the car is spinning out of control, differential braking engages to bring it back into control. The angular rate can also be integrated over time to determine angular position—particularly useful for maintaining continuity of GPS-based navigation when the satellite signal is lost for short periods of time.

### Coriolis Acceleration

Analog Devices' ADXRS gyros measure angular rate by means of Coriolis acceleration. The Coriolis effect can be explained as follows, starting with Figure 2. Consider yourself standing on a rotating platform, near the center. Your speed relative to the ground is shown as the blue arrow lengths in Figure 2. If you were to move to a point near the outer edge of the platform, your speed would increase relative to the ground, as indicated by the longer blue arrow. The rate of increase of your tangential speed, caused by your radial velocity, is the *Coriolis* acceleration (after Gaspard G. de Coriolis, 1792-1843—a French mathematician).

If $\Omega$ is the angular rate and $r$ the radius, the tangential velocity is $\Omega r$. So, if $r$ changes at speed, $v$, there will be a tangential acceleration $\Omega v$. This is half of the Coriolis acceleration. There is another half from changing the direction of the radial velocity giving a total of $2\Omega v$ (see the Appendix). If you have mass, $M$, the platform must apply a force, $2M\Omega v$, to cause that acceleration, and the mass experiences a corresponding reaction force.

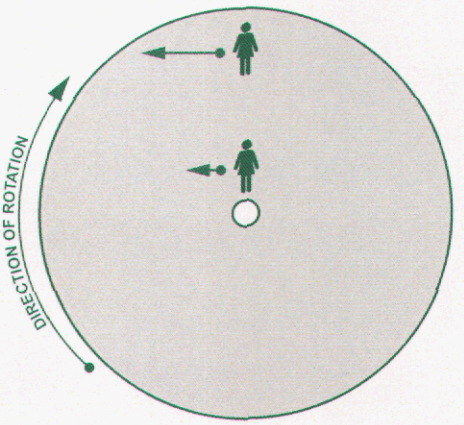


Figure 2. Coriolis acceleration example. A person moving northward toward the outer edge of a rotating platform must increase the westward speed component (blue arrows) to maintain a northbound course. The acceleration required is the *Coriolis acceleration*.

The ADXRS gyros take advantage of this effect by using a resonating mass analogous to the person moving out and in on a rotating platform. The mass is micromachined from polysilicon and is tethered to a polysilicon frame so that it can resonate only along one direction.

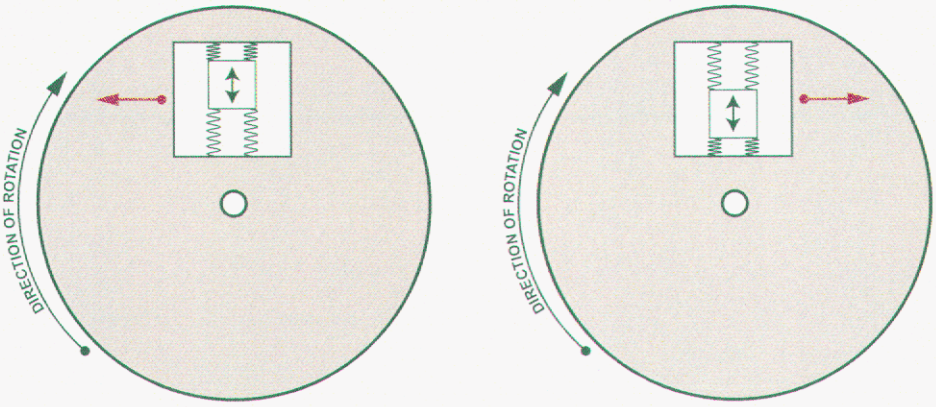


Figure 3. Demonstration of Coriolis effect in response to a resonating silicon mass suspended inside a frame. The orange arrows indicate the force applied to the structure, based on status of the resonating mass.

Figure 3 shows that when the resonating mass moves toward the outer edge of the rotation, it is accelerated to the right and exerts on the frame a reaction force to the left. When it moves toward the center of the rotation, it exerts a force to the right, as indicated by the orange arrows.

To measure the Coriolis acceleration, the frame containing the resonating mass is tethered to the substrate by springs at 90° relative to the resonating motion, as shown in Figure 4. This figure also shows the Coriolis sense fingers that are used to capacitively sense displacement of the frame in response to the force exerted by the mass, as described further on. If the springs have a stiffness, $K$, then the displacement resulting from the reaction force will be $2\ \Omega vM/K$.

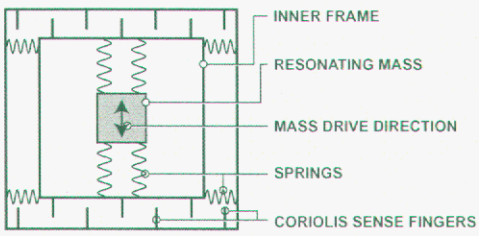


Figure 4. Schematic of the gyro's mechanical structure.

Figure 5, which shows the complete structure, demonstrates that as the resonating mass moves, and as the surface to which the gyro is mounted rotates, the mass and its frame experience the Coriolis acceleration and are translated 90° from the vibratory movement. As the rate of rotation increases, so does the displacement of the mass and the signal derived from the corresponding capacitance change.

It should be noted that the gyro may be placed anywhere on the rotating object and at any angle, so long as its sensing axis is parallel to the axis of rotation. The above explanation is intended to give an intuitive sense of the function and has been simplified by the placement of the gyro.

### Capacitive Sensing

ADXRS gyros measure the displacement of the resonating mass and its frame due to the Coriolis effect through capacitive sensing elements attached to the resonator, as shown in Figures 4, 5, and 6. These elements are silicon beams inter-digitated with two sets of stationary silicon beams attached to the substrate, thus forming two nominally equal capacitors. Displacement due to angular rate induces a differential capacitance in this system. If the total capacitance is C and the spacing of the beams is $g$, then the differential capacitance is $2\ \Omega vMC/gK$, and is directly proportional to the angular rate. The fidelity of this relationship is excellent in practice, with nonlinearity less than 0.1%.

The ADXRS gyro electronics can resolve capacitance changes as small as $12 \times 10^{-21}$ farads (12 zeptofarads) from beam deflections as small as 0.00016 Angstroms (16 femtometers). The only way this can be utilized in a practical device is by situating the electronics, including amplifiers and filters, on the same die as the mechanical sensor. The differential signal alternates at the resonator frequency and can be extracted from the noise by correlation.

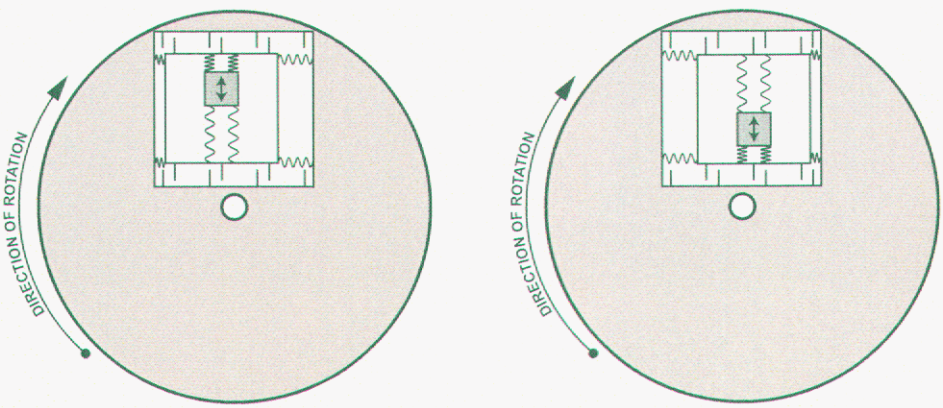


Figure 5. The frame and resonating mass are displaced laterally in response to the Coriolis effect. The displacement is determined from the change in capacitance between the Coriolis sense fingers on the frame and those attached to the substrate.

These sub atomic displacements are meaningful as the *average* positions of the surfaces of the beams, even though the individual atoms on the surface are moving randomly by much more. There are about $10^{12}$ atoms on the surfaces of the capacitors, so the statistical averaging of their individual motions reduces the uncertainty by a factor of $10^6$. So why can't we do 100 times better? The answer is that the impact of the *air molecules* causes the structure to move—although similarly averaged, their effect is far greater! So why not remove the air? The device is not operated in a vacuum because it is a very fine, thin film weighing only 4 micrograms; its flexures, only 1.7 microns wide, are suspended over the silicon substrate. Air cushions the structure, preventing it from being destroyed by violent shocks—*even those experienced during firing of a guided shell from a howitzer* (as demonstrated recently).

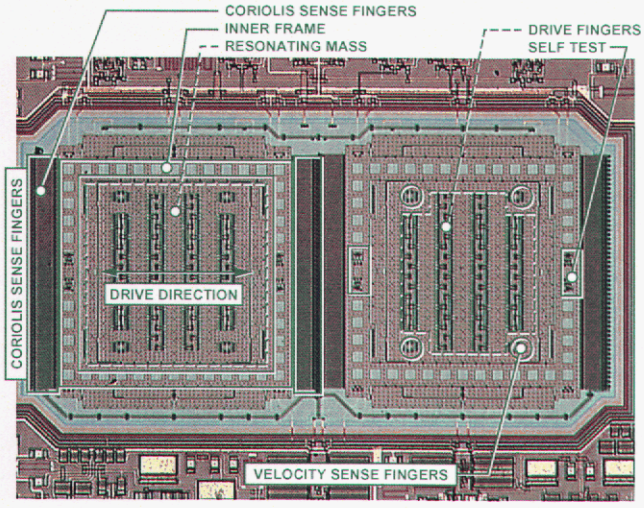


Figure 6. Photograph of mechanical sensor. The ADXRS gyros include two structures to enable differential sensing in order to reject environmental shock and vibration.

**Features**

Integration of electronics and mechanical elements is a key feature of products such as the ADXRS150 and ADXRS300, because it makes possible the smallest size and cost for a given performance level. Figure 7 is a photograph of the ADXRS die.

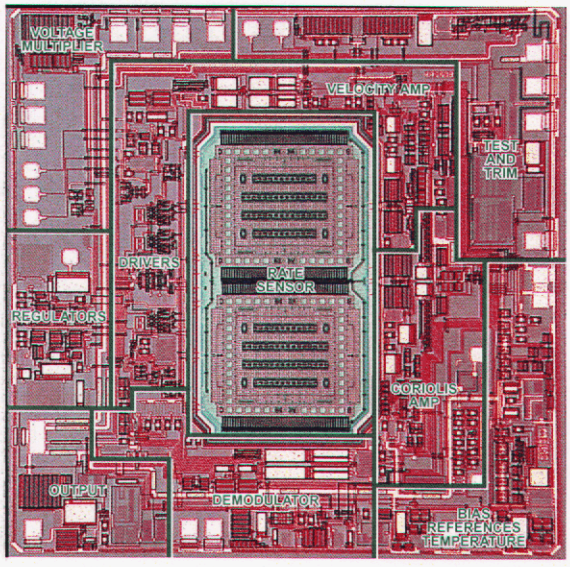


Figure 7. Photograph of ADXRS gyro die, highlighting the integration of the mechanical rate sensor and the signal conditioning electronics.

The ADXRS150 and ADXRS300 are housed in an industry-standard package that simplifies users' product development and production. The ceramic package—a 32-pin ball grid-array, (BGA)—measures 7 mm wide by 7 mm deep by 3 mm tall. It is at least 100 times smaller than any other gyro having similar performance. Besides their small size, these gyros consume 30 mW, far less power than similar gyros. The combination of small size and low power make these products ideally suited for consumer applications such as toy robots, scooters, and navigation devices.

**Immunity to Shock and Vibration**

One of the most important concerns for a gyro user is the device's ability to reliably provide an accurate angular rate-output signal—even in the presence of environmental shock and vibration. One example of such an application is automotive rollover detection, in which a gyro is used to detect whether *or not* a car (or SUV) is rolling over. Some rollover events are triggered by an impact with another object, such as a curb, that results in a shock to the vehicle. If the shock saturates the gyro sensor, and the gyro cannot filter it out, then the airbags may not deploy. Similarly, if a bump in the road results in a shock or vibration that translates into a rotational signal, the airbags might deploy when not needed—a considerable safety hazard!

As can be seen in Figures 6 and 7, the ADXRS gyros employ a novel approach to angular rate-sensing that makes it possible to reject shocks of up to 1,000*g*—they use two resonators to differentially sense signals and reject common-mode external accelerations that are unrelated to angular motion. This approach is, in part, the reason for the excellent immunity of the ADXRS gyros to shock and vibration. The two resonators in Figure 6 are mechanically independent, and they operate anti-phase. As a result, they measure the same magnitude of rotation, but give outputs in opposite directions. Therefore, the difference between the two sensor signals is used to measure angular rate. This cancels non-rotational signals that affect both sensors. The signals are combined in the internal hard-wiring ahead of the very sensitive preamplifiers. Thus, extreme acceleration overloads are largely prevented from reaching the electronics—thereby allowing the signal conditioning to preserve the angular rate output during large shocks. This scheme requires that the two sensors be well-matched, precisely fabricated copies of each other.

## SUMMARY

Analog Devices has used its iMEMS process to achieve a breakthrough with the development of the World's first fully integrated angular rate sensor. Integration yields a revolution in reliability, size, and price. The result is a gyro that is suited for a much wider range of applications than previously thought possible or affordable. The device's low power and small size will benefit small consumer and industrial products that run on batteries, such as toys, scooters, and portable instruments. The tremendous immunity to shock and vibration benefits automotive and other applications that are subject to harsh environmental conditions.

Looking forward, it is possible to exploit the iMEMS process and gyro design techniques to achieve even higher levels of integration. Just as Analog Devices has developed dual-axis accelerometers, it will be possible to produce multi-axis gyroscopes. It will even be possible to integrate both accelerometers and gyros on a single die. The resulting inertial measurement unit would enable even tiny vehicles to be stabilized and navigated autonomously.

## APPENDIX

### Motion in 2 dimensions

Consider the position coordinate, $z = r\varepsilon^{i\theta}$, in the complex plane. Differentiating with respect to time, $t$, the velocity is

$$\frac{dz}{dt} = \frac{dr}{dt}\varepsilon^{i\theta} + ir\frac{d\theta}{dt}\varepsilon^{i\theta}$$

the two terms are the respective radial and tangential components, the latter arising from the angular rate. Differentiating again, the acceleration is

$$\frac{d^2z}{dt^2} = \left[\frac{d^2r}{dt^2}\varepsilon^{i\theta} + i\frac{dr}{dt}\frac{d\theta}{dt}\varepsilon^{i\theta}\right] + \left[i\frac{dr}{dt}\frac{d\theta}{dt}\varepsilon^{i\theta} + ir\frac{d^2\theta}{dt^2}\varepsilon^{i\theta} - r\left(\frac{d\theta}{dt}\right)^2\varepsilon^{i\theta}\right]$$

The first term is the radial linear acceleration and the fourth term is the tangential component arising from angular acceleration. The last term is the familiar centripetal acceleration needed to constrain $r$. The second and third terms are tangential and are the Coriolis acceleration components. They are equal, respectively arising from the changing direction of the radial velocity and from the changing magnitude of the tangential velocity. If the angular rate and radial velocities are constant,

$$\frac{d\theta}{dt} = \Omega \text{ and } \frac{dr}{dt} = v$$

then

$$\frac{d^2z}{dt^2} = i2\Omega v\varepsilon^{i\theta} - \Omega^2 r\varepsilon^{i\theta}$$

where the angular component, $i\varepsilon^{i\theta}$, indicates a tangential direction in the sense of positive $\theta$ for the Coriolis acceleration, $2\Omega v$, and $-\varepsilon^{i\theta}$ indicates towards the center (i.e., *centripetal*) for the $\Omega^2 r$ component.

## Appendix C – Magnetometers

Datasheets:

A. **HMC2003 Three-Axis Magnetic Sensor Hybrid** by Honeywell

Further Information:

B. **Compass Heading Using Magnetometers** by Honeywell

Honeywell

SENSOR PRODUCTS

# Three-Axis Magnetic Sensor Hybrid

## HMC2003

**APPLICATIONS**

- Compassing
- Navigation Systems
- Attitude Reference
- Traffic Detection
- Proximity Detection
- Medical Devices

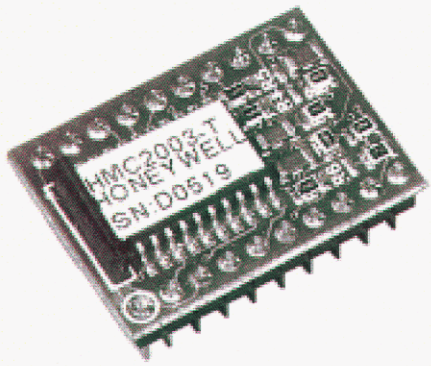


A complete 3-axis magnetometer with analog output in a 20-pin hybrid DIP package. Uses Honeywell's sensitive HMC1001 and HMC1002 MR sensors and precision instrumentation amplifiers to measure x, y and z axes. Patented integral field straps are accessible for applying offset fields or closed loop operation.

## FEATURES AND BENEFITS

| | |
|---|---|
| **Small Cost Effective Package** | DIP-20 footprint (1 in. x .75 in.) allows easy insertion into system-level boards, reducing development costs. |
| **Solid State** | All components are solid state, improving reliability and ruggedness compared to mechanical fluxgates. |
| **Wide Dynamic Range** | Accurately measures fields from 40 micro-gauss to ±2 gauss at 1V/gauss. Low noise instrumentation amplifiers with 1kHz low pass filters, reject unwanted noise. There are no flux concentrators used in this design that can lead to hysteresis and non-repeatablilty. |
| **Internal Reference** | An externally accessible +2.5V reference improves measurement accuracy and stability. An on-board excitation current source reduces temperature errors and regulates the power supply input. |
| **Offset and Set/Reset Straps** | Magnetic field offsets or closed loop circuits can be applied using the built-in straps. Output signal accuracy may be enhanced by using the integral set/reset straps. |
| **Non-Magnetic Material** | All components are especially selected and packaged in nonmagnetic material to reduce magnetic distortion and offsets. |

## GENERAL DESCRIPTION

Honeywell's three-axis magnetic sensor hybrid uses three permalloy magnetoresistive transducers and custom interface electronics to measure the strength and direction of a magnetic field. These transducers are sensitive to magnetic fields along the length, width, and height (x, y, z axis) of the 20-pin dual-in-line hybrid. Fields can be detected less than 40 microgauss and up to ±2 gauss. Analog outputs are available for each x, y, z, axis from the hybrid. With the sensitivity and linearity of this hybrid, changes can be detected in the earth's magnetic field to provide compass headings or attitude sensing. The high bandwidth of this hybrid allows anomaly detection of vehicles, planes and other ferrous objects at high speeds.

The hybrid is packaged on a small board (1 in. x 0.75 in.) and has an on-chip voltage reference that operates from a single 6 to 15 V supply. The hybrid is ideal for applications that require two- or three-axis magnetic sensing and have a very tight size constraint and/or have their own electronics and only need a magnetic transducer front-end.

Integrated with the transducer bridge circuit is a magnetically coupled strap that replaces the need for external coils and provides various modes of operation. The Honeywell patented field offset straps (Xoff+ and Xoff-, etc.) can be used to electrically apply a magnetic field to the bridge to buck, or offset an applied field. This technique can be used to cancel unwanted ambient magnetic fields or in a closed loop field nulling measurement circuit. The offset straps nominally provide a 1 gauss field along the sensitive axis per 48 mA of offset current through it.

Magnetic transducers can be affected by high momentary magnetic fields that may lead to output signal degradation. In order to eliminate this effect, and maximize the signal output, a magnetic switching technique can be applied to the bridge using the SR+ and SR- pins that eliminates the effect of past magnetic history. Refer to AN-201 for applications information on Set/Reset operation.

## CIRCUIT DIAGRAM

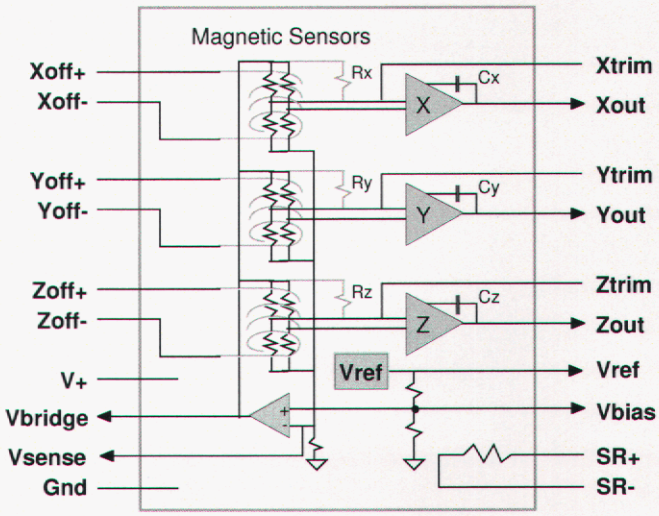


## PINOUT DIAGRAM

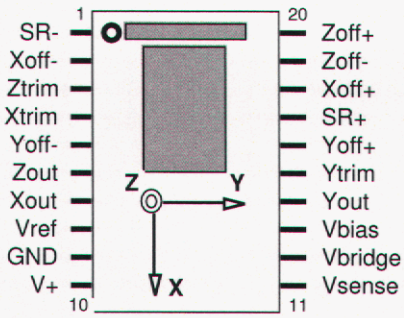


## PACKAGE DRAWING

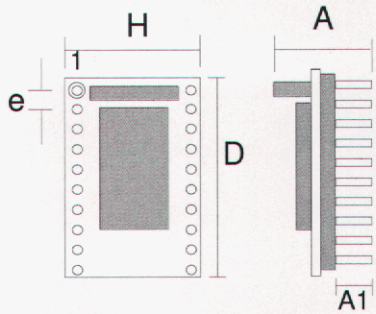


| Symbol | Millimeters | | Inches | |
|---|---|---|---|---|
| | Min | Max | Min | Max |
| A | 11.43 | 12.45 | 0.45 | 0.49 |
| A1 | 4.06 | 5.08 | 0.16 | 0.20 |
| D | 25.91 | 26.92 | 1.02 | 1.06 |
| e | 2.41 | 2.67 | 0.095 | 0.105 |
| H | 18.03 | 19.05 | 0.71 | 0.75 |

## KEY PERFORMANCE DATA

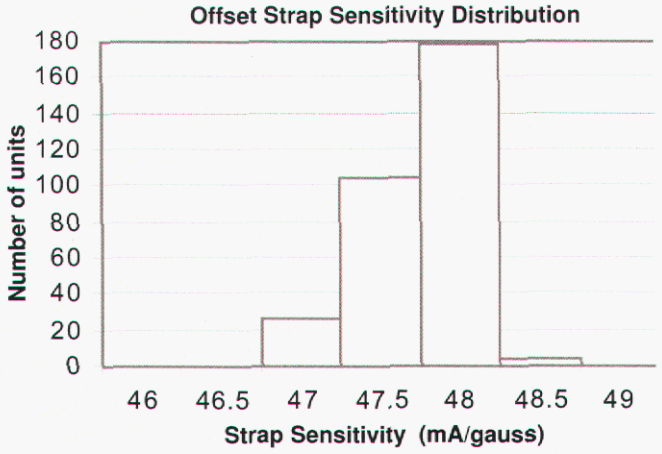


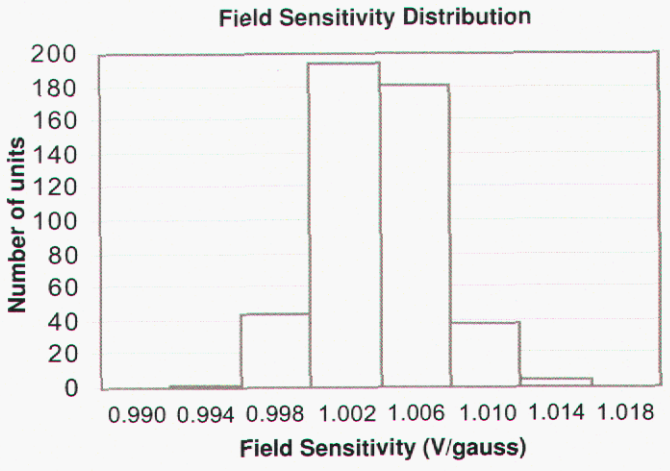


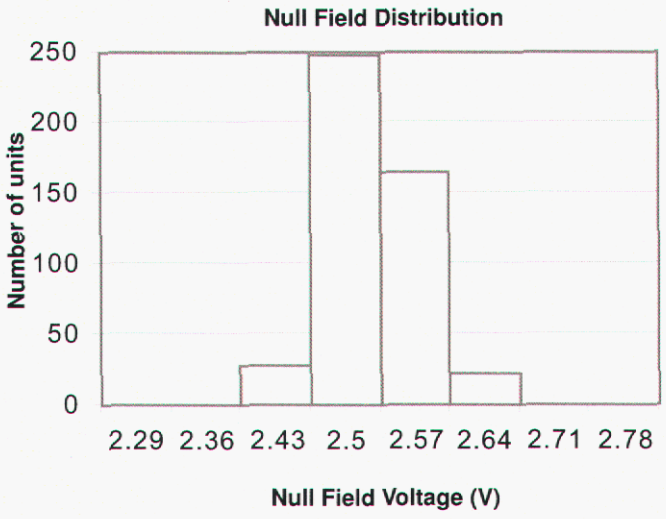


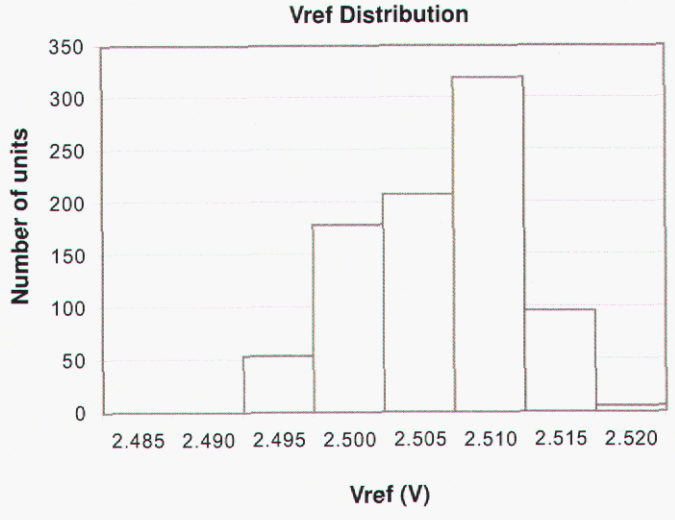


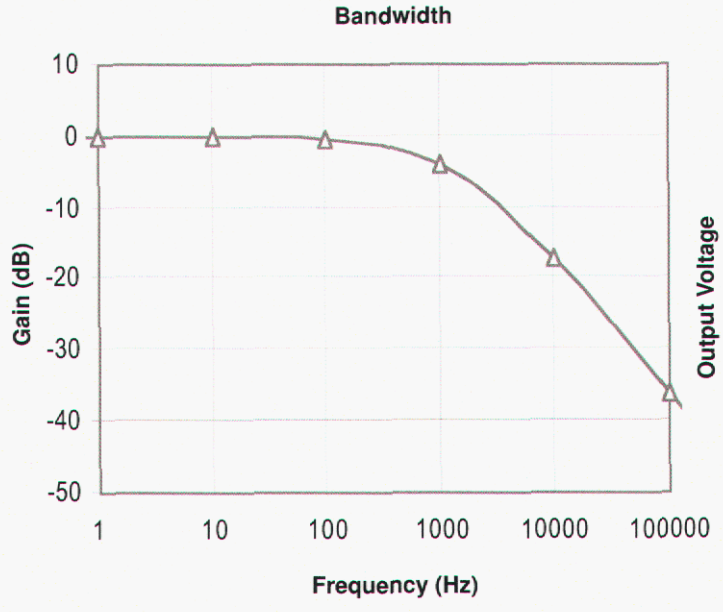


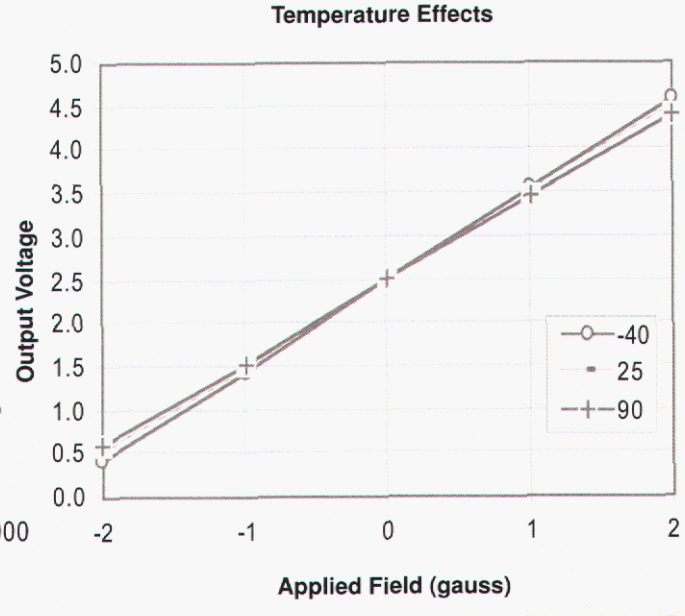

## SPECIFICATIONS

| Characteristic | Conditions (1) | Min | Typ | Max | Units (2) |
|---|---|---|---|---|---|
| Supply Voltage (3) | | 6 | | 15 | VDC |
| Supply Current | | | | 20 | mA |
| Field Range | | -2 | | 2 | gauss |
| Output Voltage | | 0.5 | | 4.5 | V |
| Resolution | | | 40 | | μgauss |
| Bandwidth | | | 1 | | KHz |
| Field Sensitivity | | 0.98 | 1 | 1.02 | V/gauss |
| Null Field Output | | 2.3 | 2.5 | 2.7 | V |
| Linearity Error | ±1 gauss Applied Field Sweep | | 0.5 | 2 | %FS |
| Linearity Error | ±2 gauss Applied Field Sweep | | 1 | 2 | %FS |
| Hysteresis Error | 3 sweeps across ±2 gauss | | 0.05 | .1 | %FS |
| Repeatability Error | 3 sweeps across ±2 gauss | | 0.05 | .1 | %FS |
| Offset Strap Resistance | | | | 10.5 | Ω |
| Offset Strap Sensitivity | | 46.5 | 47.5 | 48.5 | mA/gauss |
| Offset Strap Current | | | | 200 | mA |
| Set/Reset Strap Resistance | | | | 6 | Ω |
| Field Sensitivity Tempco | | | -600 | | ppm/° C |
| Null Field Tempco | Set/Reset not used | | ±400 | | ppm/° C |
| Null Field Tempco | Set/Reset used | | ±100 | | ppm/° C |
| Storage Temperature | | -55 | | 125 | ° C |
| Operating Temperature | | -40 | | 85 | ° C |
| Shock | | | 100 | | g |
| Vibration | | | 2.2 | | g rms |
| Power Supply Effect (shifts in Null Field Offset or Sensitivity) | Power Supply varied from 6 to 15VDC with ±1 gauss Applied Field sweep | | | 0.1 | %FS |

(1). Unless otherwise stated, test conditions are as follows: power supply = +12VDC, ambient temp = 25°C, Set/Reset switching is active.
(2). Units: 1 gauss (G) = 1 Oersted (in air), 1G = 79.58 A/m, 1G = 10E-4 Tesla, 1G = 10E5 gamma.
(3). Transient protection circuitry should be added across V+ and Gnd if an unregulated power supply is used.



**Honeywell**

*Helping You Control Your World*

Solid State Electronics Center
12001 State Highway 55
Plymouth, MN 55441
1-800-323-8295
E-Mail: clr@mn14.ssec.honeywell.com • http://www.ssec.honeywell.com
900151 Rev. C 10-97

Honeywell

# COMPASS HEADING USING MAGNETOMETERS

AN-203

Honeywell's line of magnetoresistive permalloy sensors are sensitive to magnetic fields less than 100 μgauss within a ±2 gauss range. This sensitivity can be compared to the earth's magnetic field which is roughly 0.6 gauss (48 A/m) and results in a measurement resolution of 1 part in 6,000. This applications note will discuss basic principles of compass headings and provide a method for compassing using the Honeywell Smart Digital Magnetometer.

The earth's magnetic field resembles that of a simple bar magnet. This magnetic dipole, Figure 1, has its field lines originating at a point near the south pole and terminating at a point near the north pole. These points are referred to as the magnetic poles. These field lines vary in both strength and direction about the face of the earth. In North America the field lines points downward toward north at an angle roughly 70 degrees into the earth's surface. This angle is called the magnetic angle of inclination (Ø) and is shown in Figure 2. The direction and strength of the earth's magnetic field (He) can be represented by the three axis values Hx, Hy, and Hz. The Hx and Hy information can be used to determine compass headings in reference to the magnetic poles.

Remember that it is the earth's rotational axis that defines the geographic north and south poles that we use for map references. It turns out that there is a discrepancy of ≈11.5 degrees between the geographic poles and the magnetic poles. A value can be applied to the magnetic direction to correct for this called the declination angle. This has been mapped all across the globe [1] and takes into account other factors such as large iron deposits and other natural anomalies. A declination chart of the contiguous United States is shown in Figure 3. A magnetic reading in central California, for example, would indicate 16° to the east when pointing toward true geographic north.

To determine compass headings using a magnetometer, the device must be level to the earth's surface, there should not be any ferrous materials interfering with the earth's field and the declination angle must be known. Various tilt compensation circuits and techniques can be used to normalize a magnetometer reading that is not level. There are also more sophisticated algorithms to account for nearby ferrous materials to correct for their effect on the earth's field.

A compass heading can be determined by using just the Hx and Hy component of the earth's magnetic field, that is, the directions planar with the earth's surface. Hold the magnetometer flat in an open area and note the Hx and Hy magnetic readings. These readings vary as the magnetometer is rotated in a circle as shown in Figure 4. The maximum value of Hx and Hy depend on the strength of the earth's field at that point. The magnetic compass heading can be determined (in degrees) from the magnetometer's x and y readings by using the following set of equations:

Direction (y>0) = 90 - [arcTAN(x/y)]*180/π
Direction (y<0) = 270 - [arcTAN(x/y)]*180/π
Direction (y=0, x<0) = 180.0
Direction (y=0, x>0) = 0.0

To determine true north heading, add or subtract the appropriate declination angle.

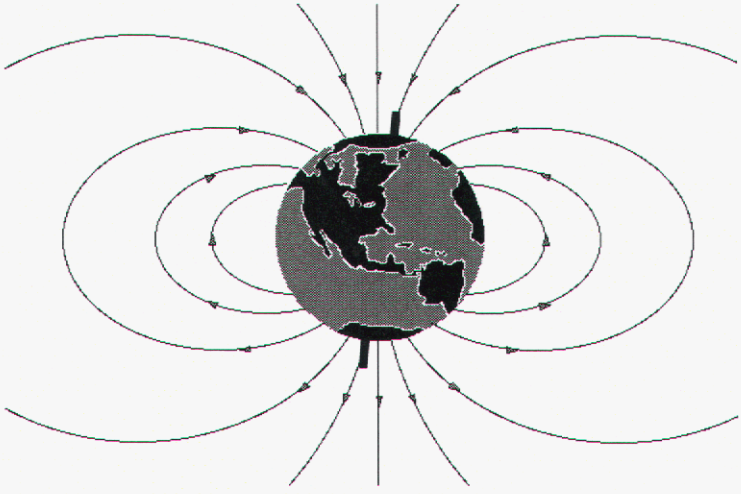

**Figure 1 - Earth's Magnetic Field**

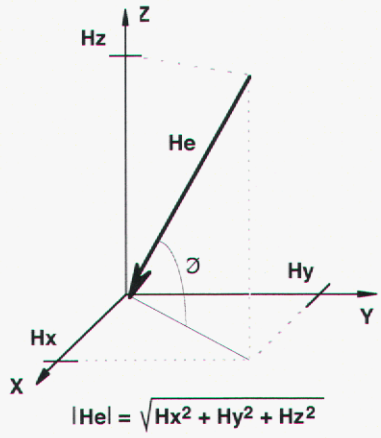


**Figure 2 - Earth's Field (He) in 3 Axis**

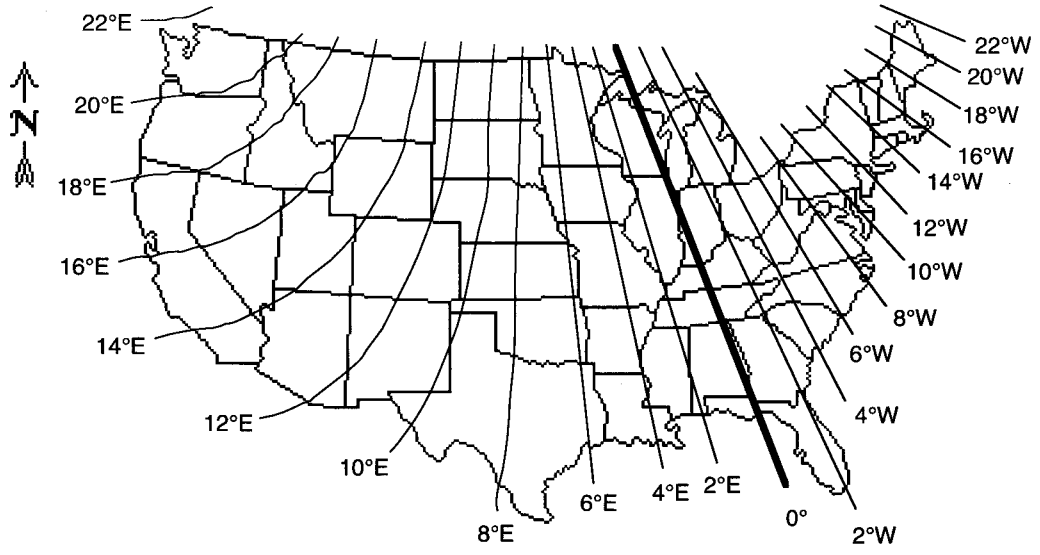


**Figure 3 - Declination (or isogonic) chart of the United States**

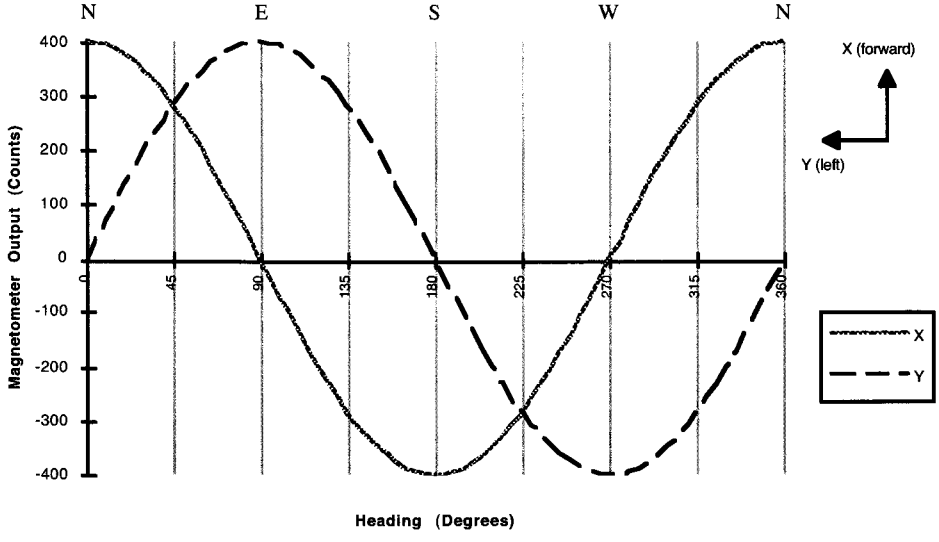


**Figure 4 - Hx and Hy Magnetometer Readings for Different Compass Headings**


## Customer Service Representative

612-954-2888 fax: 612-954-2582
E-Mail: clr@mn14.ssec.honeywell.com
Web Site: www.ssec.honeywell.com


**Magnetic Flux Density**
10,000 gauss (G) = 1 tesla (T)

**Magnetic Field**
1 oersted (Oe) = 79.58 amperes/meter (A/m)
100,000 gamma = 1 Oe = 79.58 A/m

Note: In air 1 G = 1 Oe


[1] National Geophysical Data Center, NOAA Code E/GC1, 325 Broadway, Boulder, CO 80303-3328, U.S.A. (303) 497-6478

# Appendix D – PIC Microcontroller Code

*A. IMU Code*

```
;===============================================================================
;  Travis Deyle
;  Low-Cost IMU code
;===============================================================================

    LIST P=PIC18F4320
    #include P18F4320.INC

;-------------------------------------------------------------------------------
; Program configuration settings

    __CONFIG  _CONFIG1H, _IESO_OFF_1H & _FSCM_OFF_1H & _HSPLL_OSC_1H
    __CONFIG  _CONFIG2L, _PWRT_ON_2L & _BOR_OFF_2L & _BORV_20_2L
    __CONFIG  _CONFIG2H, _WDT_OFF_2H & _WDTPS_32K_2H
    __CONFIG  _CONFIG3H, _MCLRE_ON_3H & _PBAD_DIG_3H & _CCP2MX_C1_3H
    __CONFIG  _CONFIG4L, _DEBUG_ON_4L & _LVP_OFF_4L & _STVR_OFF_4L

    __CONFIG  _CONFIG5L, _CP0_OFF_5L & _CP1_OFF_5L & _CP2_OFF_5L & _CP3_OFF_5L
    __CONFIG  _CONFIG5H, _CPB_OFF_5H & _CPD_OFF_5H
    __CONFIG  _CONFIG6L, _WRT0_OFF_6L & _WRT1_OFF_6L & _WRT2_OFF_6L & _WRT3_OFF_6L
    __CONFIG  _CONFIG6H, _WRTC_OFF_6H & _WRTB_OFF_6H & _WRTD_OFF_6H
    __CONFIG  _CONFIG7L, _EBTR0_OFF_7L & _EBTR1_OFF_7L & _EBTR2_OFF_7L & _EBTR3_OFF_7L
    __CONFIG  _CONFIG7H, _EBTRB_OFF_7H

;-------------------------------------------------------------------------------
; Constants

SPBRG_VAL       EQU     .21             ; 115200 baud for 40 MHz clock (10 MHz * 4 PLL)
TMR_COUNTS_H    EQU     0xCF            ; 800 Hz ==> 12500 counts (40MHz osc) = 30D4h
TMR_COUNTS_L    EQU     0x2C            ;   10000h - 30D4h = CF2Ch
BUFF_LEN        EQU     .200            ; must be larger than I2C_BUFF_LEN
I2C_BUFF_LEN    EQU     .128

;-------------------------------------------------------------------------------
; Variables in Data RAM

    CBLOCK  0x0000
        Buffer:BUFF_LEN                 ; I2C buffer (page size) && TX buffer
        ADchannel                       ; AD registers
        ADcount
        TempData                        ; temporary storage var (used in TX)
        StartPtrH                       ; pointer to start & end of Rx/Tx buffer
        StartPtrL
        EndPtrH
        EndPtrL
        TXEndPtrH                       ; points to end of buffer for TX to RS232
        TXEndPtrL
        I2Cslave                        ; I2C registers
        I2CaddrH
        I2CaddrL
        I2Cdata
        I2Ccount
        Flags
        Temp                            ; used in Table Lookups
    ENDC

;-------------------------------------------------------------------------------
; Bit Definitions for Flags

ReadyEEPROM     EQU     0               ; Button pressed (so init EEPROMs)
ReadyXMIT       EQU     1               ; 'T' or 't' was typed
LastChannel     EQU     2               ; indicates last channel ==> output CRLF
ReadyBUFFER     EQU     3               ; I2C_BUFF_LEN AD samples received


;-------------------------------------------------------------------------------
; ON-Board EEPROM Data

    org 0xF00000                        ; EEDATA addr for PIC18XXX devices

INTRO_MSG:  de  "Travis Deyle's IMU", 0x0D, 0x0A
```

```
INTRO_MSG_LEN   EQU     .20

;-------------------------------------------------------------------------
; Reset Vector

    org 0x0000
RESET_VEC:  goto    START


;-------------------------------------------------------------------------
; High Priority INT

    org 0x0008
HighInt:    goto    HIGH_Int_serv


;=========================================================================
;  LOW INT

    org 0x0018

LOW_Int_serv:
    btfss   PIR1,   ADIF                ; A/D interrupt occurred?
    bra     CheckNextLow                ;   no => next INT
    btfsc   PIE1,   ADIE
    rcall   AD_int

CheckNextLow:
    btfss   PIR1,   RCIF                ; RX interrupt occurred?
    bra     CheckNextLow1               ;   no => next INT
    btfsc   PIE1,   RCIE
    rcall   RX_int

CheckNextLow1:
    btfss   PIR1,   TXIF                ; TX interrupt occurred?
    bra     LOW_Int_served              ;   no => next INT
    btfsc   PIE1,   TXIE
    rcall   TX_int

LOW_Int_served:
    retfie

;=========================================================================
;   AD INT

AD_int
    movf    ADchannel,  w               ; store channel # in upper byte (bits 7-4)
    swapf   WREG                        ; swap nibbles to make channel un upper
    iorwf   ADRESH, w

    movff   WREG,   POSTINC1                ; must be even # bytes in BUFFER!!
    movff   ADRESL, POSTINC1

    movf    FSR1H,  w                   ;   I2C since we're inside INT!!
    cpfseq  EndPtrH                     ; At end of buffer?
    bra     IncChannel                  ;   no ==> keep loading
    movf    FSR1L,  w
    cpfseq  EndPtrL
    bra     IncChannel
    lfsr    1,  Buffer                  ;   yes => reset location to beginning

IncChannel:
    incf    ADchannel,  f
    movlw   .10                     ; # channels to run through
    cpfseq  ADchannel                   ; Done w/ channels 0-9?
    bra     SetChannel              ;   no ==> go to next
    clrf    ADchannel                   ;   yes => reset channel to 0 && inc count
    bcf     PIE1,   ADIE                ;   yes => stop

SetChannel:
    movlw   B'11000011'                 ; set channel!
```

```
    andwf   ADCON0, f
    movf    ADchannel,  w
    rlncf   WREG
    rlncf   WREG
    iorwf   ADCON0, f

    bcf     PIR1,   ADIF                ; clear flag for next sample
    bsf     ADCON0, GO_DONE             ; Begin next A/D Sample

endAD_int:
    incf    ADcount,    f               ; two bytes per sample stored in BUFF
    incf    ADcount,    f
    movlw   I2C_BUFF_LEN
    cpfseq  ADcount
    bra     FinishAD_int
    clrf    ADcount
    bsf     Flags,      ReadyBUFFER     ; initiate xmission

FinishAD_int:
    return


;=============================================================================
;   TX INT

TX_int:
    movff   POSTINC0,   TempData        ; get data & inc position in array

    movf    FSR0H,  w                   ; At last element?
    cpfseq  TXEndPtrH
    bra     PutTXREG                    ;    no ==> continue
    movf    FSR0L,  w
    cpfseq  TXEndPtrL
    bra     PutTXREG                    ;    no ==> continue
    lfsr    0,  Buffer                  ;    yes => replace start @ beginning,
    bcf     PIE1,   TXIE                ;           xmit last, then quit

PutTXREG:
    movff   TempData,   TXREG
    return

;=============================================================================
;   RX INT

RX_int:
    btfsc   RCSTA,  OERR                ; overrun ERR?
    bra     ErrOERR                     ;   yes => handle
    btfsc   RCSTA,  FERR                ; framing ERR?
    bra     ErrFERR                     ;   yes => handle

    movf    RCREG,  w                   ; get input char (clears RCIF)
    xorlw   'T'
    btfsc   STATUS, Z                   ; was character 'T'?
    bra     SetTXforXmit                ;   yes => handle
    xorlw   'T'                         ; restore received val
    xorlw   't'
    btfsc   STATUS, Z                   ; was character 't'?
    bra     SetTXforXmit                ;   yes => handle
    bra     endRX_int                   ;   no ==> ignore

ErrOERR:
    bcf     RCSTA,  CREN                ; reset the logic (on > off > on)
    bsf     RCSTA,  CREN
    bra     endRX_int

ErrFERR:
    movf    RCREG,  w                   ; discard data
    bra     endRX_int

SetTXforXmit:                           ; enable Xmit & set TX buffer len
    bsf     Flags,      ReadyXMIT
```

```
    bcf     PIE1,   RCIE                ; disable RX INTs

endRX_int:
    return

;=============================================================================
; HIGH INT

HIGH_Int_serv:
    btfss   INTCON, INT0IF              ; BUTTON interrupt occurred?
    bra     CheckNextHigh               ;   no => next INT
    btfsc   INTCON, INT0IE
    rcall   BUTTON_int

CheckNextHigh:
    btfss   INTCON, TMR0IF              ; TMR0 interrupt occurred?
    bra     HIGH_int_served             ;   no ==> finish
    btfsc   INTCON, TMR0IE
    rcall   TMR0_int

HIGH_int_served:
    retfie                              ; re-enable ints and return


;=============================================================================
;   BUTTON INT

BUTTON_int:
    movf    PORTD,  w
    xorlw   0x03                        ; Toggle LEDs
    movwf   PORTD

    call    SetupTIMERS                 ; enables 800 Hz timer
    bsf     Flags,  ReadyEEPROM         ; enable writing...
    bcf     Flags,  ReadyBUFFER
    lfsr    2,      Buffer              ; setup I2C FSR
    lfsr    1,      Buffer              ; setup AD FSR
    bcf     INTCON, INT0IF
    bcf     INTCON, INT0IE              ; disable further button presses
    return


;=============================================================================
;   TMR0 INT

TMR0_int:
    movlw   TMR_COUNTS_H                ; must set TMR0H first!
    movwf   TMR0H
    movlw   TMR_COUNTS_L
    movwf   TMR0L

    clrf    ADchannel                   ; BEGIN A/D at channel 0
    bcf     PIR1,   ADIF                ; clear flag
    bsf     PIE1,   ADIE                ; enable AD
    bsf     ADCON0, GO_DONE             ; begin sampling!

    bcf     INTCON, TMR0IF
    return


;=============================================================================
; MAIN

START:
; Overall Configuration (Enable Interrupts now)
    bsf     RCON,   IPEN                ; Enable priorities
    movlw   0xC0                        ; Enable global High & Low INTs
    iorwf   INTCON, f

; Individual Configuration
    call    SetupBUTTON
```

```
    call    SetupLED
    call    SetupBUFFER
    call    SetupUSART
    call    SetupAD
    call    SetupI2C
    call    StartupMSG


; Begin actual MAIN
MainLoop:
    btfss   Flags,  ReadyEEPROM         ; ready to send start bit?
    goto    MainLoop                    ;   no ==> keep waiting

    call    SetupI2C                    ; easier than rewriting code here...

WrEEPROM:
    btfss   Flags,      ReadyBUFFER
    bra     WrEEPROM

    movf    PORTD,  w                   ; turn on RED & GREEN
    iorlw   0x03
    movwf   PORTD

    bcf     Flags,      ReadyBUFFER
    clrf    I2Ccount

    bcf     I2Cslave,   0               ; write enabled
    call    SendSlaveAddr               ; send start + addr
    call    SendAddrH
    call    SendAddrL

SendDataI2C:
    movff   POSTINC2,   I2Cdata         ; send data
    call    SendData

    movf    FSR2H,  w                   ; rotate to start of buffer?
    cpfseq  EndPtrH
    bra     AdjI2Ccount
    movf    FSR2L,  w
    cpfseq  EndPtrL
    bra     AdjI2Ccount
    lfsr    2,  Buffer

AdjI2Ccount:
    incf    I2Ccount                    ; xmit I2C_BUFF_LEN bytes
    movlw   I2C_BUFF_LEN
    cpfseq  I2Ccount
    bra     SendDataI2C
    call    SendStop

    movlw   I2C_BUFF_LEN                ; adjust I2C address
    addwf   I2CaddrL,   f
    movlw   0x00
    addwfc  I2CaddrH,   f
    btfss   STATUS,     C
    bra     WrEEPROM
    movlw   0x02
    addwf   I2Cslave,   f
    movf    I2Cslave,   w
    andlw   B'00001110'
    xorlw   B'00001010'
    btfss   STATUS,     Z
    bra     WrEEPROM

    bcf     PIE1,       ADIE
    bcf     INTCON,     TMR0IE

    movf    PORTD,      w               ; make LED green
    iorlw   0x02
    andlw   0xFE
    movwf   PORTD
```

```
WaitForXMIT:
    btfss   Flags,      ReadyXMIT       ; 't' or 'T' received?
    goto    WaitForXMIT                 ;   no ==> keep waiting

    movf    PORTD,      w               ; turn on RED & GREEN
    iorlw   0x03
    movwf   PORTD

    clrf    I2CaddrH                    ; setup I2C @ start
    clrf    I2CaddrL
    movlw   0xA0
    movwf   I2Cslave

BeginReadingEEPROM:
    lfsr    2,  Buffer
    bcf     Flags,      LastChannel
    bcf     I2Cslave,   0               ; setup for read @ location
    call    SendSlaveAddr
    call    SendAddrH
    call    SendAddrL
    call    SendStop

    bsf     I2Cslave,   0               ; READ and store 1st byte
    call    SendSlaveAddr
    call    ReceiveData
    movf    I2Cdata,    w
    swapf   WREG
    call    HEXtoASCIITable
    movff   Temp,   POSTINC2
    movf    Temp,   w
    xorlw   0x39
    btfsc   STATUS,     Z               ; channel == '8'?
    bsf     Flags,      LastChannel     ;   yes => set flag
    movlw   ':'                         ; CHANNEL:VALUE,CRLF?
    movwf   POSTINC2
    movf    I2Cdata,    w               ; 2nd nibble
    call    HEXtoASCIITable
    movff   Temp,   POSTINC2

    call    ReceiveDataNOACK            ; READ 2nd byte
    call    SendStop
    movf    I2Cdata,    w
    swapf   WREG
    call    HEXtoASCIITable
    movff   Temp,   POSTINC2            ; 1st nibble
    movf    I2Cdata,    w
    call    HEXtoASCIITable
    movff   Temp,   POSTINC2            ; 2nd nibble
    movlw   ','
    movwf   POSTINC2

    btfss   Flags,      LastChannel
    bra     UpdateAndNew
    movlw   0x0D
    movwf   POSTINC2
    movlw   0x0A
    movwf   POSTINC2

UpdateAndNew:
    incf    I2CaddrL,   f               ; we read 2 bytes...
    incfsz  I2CaddrL,   f               ; Low Addr rolled over?
    bra     XMITsample                  ;   no ==> update buffer addr
    incf    I2CaddrH,   f               ;   yes => Wait for next
    bnc     XMITsample                  ; High Addr rolled over?
    movlw   0x02                        ;   yes => inc chip #
    addwf   I2Cslave,   f

XMITsample:
    lfsr    0,          Buffer
    movff   FSR2H,      TXEndPtrH
```

```
    movff   FSR2L,      TXEndPtrL
    bsf     PIE1,   TXIE
    nop
    nop
    nop
WaitForTXtoComplete:
    nop
    nop
    nop
    btfsc   PIE1,   TXIE                ; TXIE will be cleared when whole buffer TXed
    bra     WaitForTXtoComplete

    movf    I2Cslave,   w
    andlw   B'00001110'
    xorlw   B'00001010'
    btfss   STATUS,     Z               ; I2C has gone through all 5 EEPROMs?
    bra     BeginReadingEEPROM          ;   no ==> start new page write

    movf    PORTD,  w                   ; turn off LEDs
    andlw   0xFC
    movwf   PORTD

INFLOOP:
    goto    INFLOOP


;=============================================================================
; SetupBUTTON
;   --Button contained on RB0
;   --Negative edge triggered
;   --Automatic High Priority INT

SetupBUTTON:
    bsf     INTCON, INT0IE              ; Enable int0
    bcf     INTCON2,INTEDG0             ; neg edge trig
    return

;=============================================================================
; SetupLED
;   --Red LED on RD0
;   --Green LED on RD1
;   --Active HIGH

SetupLED:
    movlw   0xFC                        ; Setup RD0-1 as outputs
    andwf   TRISD,  f
    movlw   0x01                        ; Make LED red initially
    movwf   PORTD
    return


;=============================================================================
; SetupBuffer
;   --sets the start & end pointers for our buffer.

SetupBUFFER:
    movlw   HIGH Buffer                 ; store location of buffer start
    movwf   StartPtrH
    movlw   LOW Buffer
    movwf   StartPtrL
    movlw   HIGH (Buffer+BUFF_LEN)      ; store location of buffer end
    movwf   EndPtrH
    movlw   LOW (Buffer+BUFF_LEN)
    movwf   EndPtrL
    return


;=============================================================================
; SetupUSART
;   --RX & TX on RC7 & RC6
;   --Both set as Low Priority INT
```

```
;   --Setup HS Baud gen

SetupUSART:
    movff   StartPtrH,  FSR0H           ; FSR0 reserved for TX
    movff   StartPtrL,  FSR0L

    movlw   0x80                        ; RC7 is input (RX)
    iorwf   TRISC,  f
    movlw   0xBF                        ; RC6 is output (TX)
    andwf   TRISC,  f
    movlw   SPBRG_VAL                   ; set BAUD rate
    movwf   SPBRG
    movlw   0x24                        ; set TXEN & BRGH (mode async)
    movwf   TXSTA
    movlw   0x90                        ; enable serial and continuous receive
    movwf   RCSTA

    movlw   0xCF                        ; TX & RX both LOW priority
    andwf   IPR1,   f
    bsf     PIE1,   RCIE                ; enable RX INTs
    return

;=============================================================================
; SetupTIMERS

SetupTIMERS:
    movlw   TMR_COUNTS_H                ; must set TMR0H first!
    movwf   TMR0H
    movlw   TMR_COUNTS_L
    movwf   TMR0L

    bsf     INTCON2,    TMR0IP          ; set TMR0 as high priority INT
    bcf     INTCON,     TMR0IF          ; clear flag if it was already set

    movlw   B'10001000'                 ; enable 16-bit timer w/ no prescaler
    movwf   T0CON

    bsf     INTCON,     TMR0IE          ; enable interrupt
    return


;=============================================================================
; SetupAD
;   --Displays startup message to serial Terminal

SetupAD:
    movff   StartPtrH,  FSR1H           ; FSR1 reserved for AD
    movff   StartPtrL,  FSR1L

    movlw   B'11110100'                 ; setup IO ports as inputs for AD0-11
    iorwf   TRISA,  f
    movlw   B'01111000'
    iorwf   TRISB,  f
    movlw   B'11100000'
    iorwf   TRISE,  f

    clrf    ADchannel                   ; start at channel 0, count 0
    clrf    ADcount

    movlw   B'00000001'                 ; channel 0 && enable AD module
    movwf   ADCON0

    movlw   B'00000011'                 ; AN0 - 11 enabled
    movwf   ADCON1

    movlw   B'10110110'                 ; Right justified, 12 TAD setup
    movwf   ADCON2                      ;   Clk = Fosc/64

    bcf     IPR1,   ADIP                ; set AD as low priority
    bsf     PIE1,   ADIE
```

```
    return


;===============================================================================
; SetupI2C

SetupI2C:
    movlw   0x18                    ; set TrisC<3:4> as inputs
    iorwf   TRISC,  f
    lfsr    2,  Buffer              ; FSR2 reserved for I2C

    bsf     SSPSTAT,    SMP         ; slew rate control disabled
    movlw   0x28                    ; enable I2C in master mode
    movwf   SSPCON1
    movlw   0x18                    ; Clock rate of 400 kHz
    movwf   SSPADD

    movlw   0xA0                    ; setup registers & flags
    movwf   I2Cslave
    clrf    I2CaddrH
    clrf    I2CaddrL
    clrf    I2Cdata
    bcf     Flags,  ReadyEEPROM
    bcf     Flags,  ReadyXMIT
    return

;-------------------------------------------------------------------------------

SendSlaveAddr:
    bsf     SSPCON2,    SEN         ; START BIT
WaitStartSent:
    btfsc   SSPCON2,    SEN         ; start sent?
    bra     WaitStartSent           ;   no ==> keep waiting

rSendSlaveAddr:
    bcf     PIR1,   SSPIF           ; clear flag from SEN
    movf    I2Cslave,   w           ; SLAVE ADDR
    movwf   SSPBUF
SlaveAddr:
    btfss   PIR1,       SSPIF       ; finished sending slave addr?
    bra     SlaveAddr               ;   no ==> keep waiting

    btfss   SSPCON2,    ACKSTAT     ; ACK received from slave...?
    return                          ;   yes => good, it worked

    bsf     SSPCON2,    RSEN        ; send repeated start bit
restartSent
    btfsc   SSPCON2,    RSEN        ; repeat start sent?
    bra     restartSent

    bra     rSendSlaveAddr


;-------------------------------------------------------------------------------

SendAddrH:
    bcf     PIR1,       SSPIF
    movff   I2CaddrH,   SSPBUF      ; ADDR HIGH
AddrH:
    btfss   PIR1,       SSPIF       ; finished sending addrH?
    bra     AddrH                   ;   no ==> keep waiting
AddrHAck:
    btfsc   SSPCON2,    ACKSTAT     ; ack received?
    bra     AddrHAck                ;   no ==> keep waiting
    bcf     PIR1,       SSPIF
    return

;-------------------------------------------------------------------------------

SendAddrL
```

```
    movff   I2CaddrL,   SSPBUF          ; ADDR LOW
AddrL:
    btfss   PIR1,       SSPIF           ; finished sending addrL?
    bra     AddrL                       ;   no ==> keep waiting
AddrLAck:
    btfsc   SSPCON2,    ACKSTAT         ; ack received?
    bra     AddrLAck                    ;   no ==> keep waiting
    bcf     PIR1,       SSPIF
    return

;-------------------------------------------------------------------------

SendData:
    bcf     PIR1,       SSPIF
    movff   I2Cdata,    SSPBUF          ; DATA
DataSent:
    btfss   PIR1,       SSPIF           ; finished sending addrH?
    bra     DataSent                    ;   no ==> keep waiting
DataSentAck:
    btfsc   SSPCON2,    ACKSTAT         ; ack received?
    bra     DataSentAck                 ;   no ==> keep waiting
    bcf     PIR1,       SSPIF
    return

;-------------------------------------------------------------------------

SendStop:
    bsf     SSPCON2,    PEN             ; STOP BIT
StopSent:
    btfsc   SSPCON2,    PEN
    bra     StopSent
    bcf     PIR1,       SSPIF
    return

;-------------------------------------------------------------------------

ReceiveData:
    bcf     PIR1,       SSPIF
    bsf     SSPCON2,    RCEN            ; RECEIVE (enable)
WaitReceive:
    btfss   PIR1,       SSPIF           ; has SSP received a data byte?
    bra     WaitReceive                 ;   no ==> wait

    bcf     SSPCON2,    ACKDT           ; ACK
    bsf     SSPCON2,    ACKEN           ; send ACK bit

SendACKDT:
    btfsc   SSPCON2,    ACKEN           ; has ACKDT bit been sent yet?
    bra     SendACKDT                   ;   no ==> wait

    movff   SSPBUF,     I2Cdata         ; save data to I2Cdata reg
    return


ReceiveDataNOACK:
    bcf     PIR1,       SSPIF
    bsf     SSPCON2,    RCEN            ; RECEIVE (enable)
WaitReceiveNOACK:
    btfss   PIR1,       SSPIF           ; has SSP received a data byte?
    bra     WaitReceiveNOACK            ;   no ==> wait

    bsf     SSPCON2,    ACKDT           ; ACK
    bsf     SSPCON2,    ACKEN           ; send ACK bit

SendACKDTNOACK:
    btfsc   SSPCON2,    ACKEN           ; has ACKDT bit been sent yet?
    bra     SendACKDTNOACK                  ;   no ==> wait

    movff   SSPBUF,     I2Cdata         ; save data to I2Cdata reg
    return
```

```
;*****************************************************************************
; StartupMSG
;   --Displays startup message to serial Terminal

StartupMSG:
    movlw   HIGH (Buffer+INTRO_MSG_LEN) ; Set Length of string...
    movwf   TXEndPtrH
    movlw   LOW (Buffer+INTRO_MSG_LEN)
    movwf   TXEndPtrL

    movlw   LOW INTRO_MSG
    movwf   EEADR                       ; Start @ INTRO_MSG
    bcf     EECON1, EEPGD               ; Read from Data EEPROM (not flash)
    bcf     EECON1, CFGS

ReadONchipEEPROM:
    bsf     EECON1, RD                  ; EEDATA now valid
    movff   EEDATA, POSTINC0
    incf    EEADR,  f
    movlw   LOW (INTRO_MSG+INTRO_MSG_LEN)
    cpfseq  EEADR                       ; Read less than length of msg
    bra     ReadONchipEEPROM            ;   yes => keep reading into buffer

    movff   StartPtrH,  FSR0H           ; restore FSR0 reserved for TX
    movff   StartPtrL,  FSR0L
    bsf     PIE1,   TXIE                ; enable Xmit
    return

;*****************************************************************************
; HEX to ASCII table

HEXtoASCIITable:
    andlw   0x0F                        ; only deal with lower nibble
    movwf   Temp
    movlw   0x09
    cpfsgt  Temp                        ; nibble > 09h?
    bra     ZeroThruNine                ;   no ==> adjust for 0-9
    movlw   0x37                        ;   yes => adjust for A-F
    addwf   Temp,   f
    bra     EndHEXtoASCII

ZeroThruNine:
    movlw   0x30
    addwf   Temp,   f

EndHEXtoASCII:
    return

    end
```

*B. Test Bench Code*

```
;===============================================================================
;  Travis Deyle
;  Test Setup Code (Tilting via servo motor)
;===============================================================================

    LIST P=PIC18F4320
    #include P18F4320.INC

;-------------------------------------------------------------------------------
; Program configuration settings

    __CONFIG  _CONFIG1H, _IESO_OFF_1H & _FSCM_OFF_1H & _HS_OSC_1H
    __CONFIG  _CONFIG2L, _PWRT_ON_2L & _BOR_OFF_2L & _BORV_20_2L
    __CONFIG  _CONFIG2H, _WDT_OFF_2H & _WDTPS_32K_2H
    __CONFIG  _CONFIG3H, _MCLRE_ON_3H & _PBAD_DIG_3H & _CCP2MX_C1_3H
    __CONFIG  _CONFIG4L, _DEBUG_OFF_4L & _LVP_OFF_4L & _STVR_OFF_4L

    __CONFIG  _CONFIG5L, _CP0_OFF_5L & _CP1_OFF_5L & _CP2_OFF_5L & _CP3_OFF_5L
    __CONFIG  _CONFIG5H, _CPB_OFF_5H & _CPD_OFF_5H
    __CONFIG  _CONFIG6L, _WRT0_OFF_6L & _WRT1_OFF_6L & _WRT2_OFF_6L & _WRT3_OFF_6L
    __CONFIG  _CONFIG6H, _WRTC_OFF_6H & _WRTB_OFF_6H & _WRTD_OFF_6H
    __CONFIG  _CONFIG7L, _EBTR0_OFF_7L & _EBTR1_OFF_7L & _EBTR2_OFF_7L & _EBTR3_OFF_7L
    __CONFIG  _CONFIG7H, _EBTRB_OFF_7H


;-------------------------------------------------------------------------------
; Variables in Data RAM

    CBLOCK  0x0000
        COUNT                       ; used to count for 2 seconds (100 servo pulses)
    ENDC

;-------------------------------------------------------------------------------
; Reset Vectors

    org 0x0000
    goto    START
    org 0x0008
    goto    START


;===============================================================================
; MAIN

START:
    clrf    TRISB                   ; Let my Debug LED's start up
    movlw   0x01
    movwf   PORTB


    clrf    TRISC                   ; set PortC as outputs
    clrf    PORTC
    movlw   b'10000111'             ; TMR0 on, 256 prescale
    movwf   T0CON
    movlw   b'00110001'             ; TMR1 on, 8 prescaler
    movwf   T1CON

    movlw   .256
    movwf   COUNT
ONE:
    bcf     INTCON, TMR0IF          ; clear flags and setup timers
    bcf     PIR1,   TMR1IF
    movlw   0xFF
    movwf   TMR0H
    movlw   (.256 - .78)            ; 20 ms
    movwf   TMR0L
    movlw   0xFF
    movwf   TMR1H
    movlw   (.256 - .200)           ; constant determined by laser & yardstick for angle
    movwf   TMR1L
```

```
    bsf     PORTC,  0               ; turn on
    btfss   PIR1,   TMR1IF
      goto  $ - 2
    bcf     PORTC,  0               ; turn off
    btfss   INTCON, TMR0IF
      goto  $ - 2

    decfsz  COUNT
      goto  ONE

    movlw   .100                    ; 2 seconds at current position
    movwf   COUNT
    movlw   0x02
    movwf   PORTB
TWO:
    bcf     INTCON, TMR0IF          ; clear flags and setup timers
    bcf     PIR1,   TMR1IF
    movlw   0xFF
    movwf   TMR0H
    movlw   (.256 - .78)            ; 20 ms
    movwf   TMR0L
    movlw   0xFF
    movwf   TMR1H
    movlw   (.256 - .210)           ; constant determined by laser & yardstick for angle
    movwf   TMR1L

    bsf     PORTC,  0               ; turn on
    btfss   PIR1,   TMR1IF
      goto  $ - 2
    bcf     PORTC,  0               ; turn off
    btfss   INTCON, TMR0IF
      goto  $ - 2

    decfsz  COUNT
      goto  TWO

    movlw   .100                    ; 2 seconds at current position
    movwf   COUNT
    movlw   0x03
    movwf   PORTB
THREE:
    bcf     INTCON, TMR0IF          ; clear flags and setup timers
    bcf     PIR1,   TMR1IF
    movlw   0xFF
    movwf   TMR0H
    movlw   (.256 - .78)            ; 20 ms
    movwf   TMR0L
    movlw   0xFF
    movwf   TMR1H
    movlw   (.256 - .220)           ; constant determined by laser & yardstick for angle
    movwf   TMR1L

    bsf     PORTC,  0               ; turn on
    btfss   PIR1,   TMR1IF
      goto  $ - 2
    bcf     PORTC,  0               ; turn off
    btfss   INTCON, TMR0IF
      goto  $ - 2

    decfsz  COUNT
      goto  THREE

    movlw   .100                    ; 2 seconds at current position
    movwf   COUNT
    movlw   0x04
    movwf   PORTB
FOUR:
    bcf     INTCON, TMR0IF          ; clear flags and setup timers
    bcf     PIR1,   TMR1IF
    movlw   0xFF
    movwf   TMR0H
```

```
    movlw   (.256 - .78)            ; 20 ms
    movwf   TMR0L
    movlw   0xFF
    movwf   TMR1H
    movlw   (.256 - .230)           ; constant determined by laser & yardstick for angle
    movwf   TMR1L

    bsf     PORTC,  0               ; turn on
    btfss   PIR1,   TMR1IF
      goto  $ - 2
    bcf     PORTC,  0               ; turn off
    btfss   INTCON, TMR0IF
      goto  $ - 2

    decfsz  COUNT
      goto  FOUR
    movlw   0x05
    movwf   PORTB
FIVE:
    bcf     INTCON, TMR0IF          ; clear flags and setup timers
    bcf     PIR1,   TMR1IF
    movlw   0xFF
    movwf   TMR0H
    movlw   (.256 - .78)            ; 20 ms
    movwf   TMR0L
    movlw   0xFF
    movwf   TMR1H
    movlw   (.256 - .240)           ; constant determined by laser & yardstick for angle
    movwf   TMR1L

    bsf     PORTC,  0               ; turn on
    btfss   PIR1,   TMR1IF
      goto  $ - 2
    bcf     PORTC,  0               ; turn off
    btfss   INTCON, TMR0IF
      goto  $ - 2

    goto    FIVE
    end
```

# Appendix E – MatLab Code

```
function IMU(InFile, PlotAccel, PlotGyro, PlotMagnet, PlotAll)

% Constants & Device Info (used during scaling/plotting)
    % Accelerometer
        % Vcc is 5V
        % linear output centered about 2.5V
        % range +- 2g
        % sensitivity is 312 mV/g

    % Gyroscopes
        % Vcc is 5V
        % linear output centered about 2.5V
        % range is +- 300 degrees/sec
        % sensitivity is 5 mV/(degree/sec)

    % 3-Axis Magnetometer
        % Vcc is 12V
        % linear output centered about 2.5V
        % range +- 2 gauss
        % sensitivity is 1 V/gauss

    SampPerSec = 800;

% Open File & Read Data In

    [fid message] = fopen(InFile,   'r');      % open input file as READ-ONLY
    if (fid == -1)
        fprintf(1,  'Could not open %s\n   Error Message: %s\n\n'  , InFile, message);
        return;
    end

    [Data, count] = fscanf(fid,   '%x:%x,');  % read in all the data (which is in HEX)
    samples = count / (2 * 10);               % 2*10 is the # of values per sample

% Partition & Scaling
    % Channel 0 -- Magnetometer Z Axis  (physical AN0)
        MagnetometerZ = Data(20*[0:samples-1] + 2);
        MagnetometerZ = ((MagnetometerZ * 5 / 1024) - 2.5) / 1.0;
    % Channel 1 -- Magnetometer Y Axis  (physical AN1)
        MagnetometerY = Data(20*[0:samples-1] + 4);
        MagnetometerY = ((MagnetometerY .* 5 / 1024) - 2.5) / 1.0;
    % Channel 2 -- Magnetometer X Axis  (physical AN2)
        MagnetometerX = Data(20*[0:samples-1] + 6);
        MagnetometerX = ((MagnetometerX * 5 / 1024) - 2.5) / 1.0;
    % Channel 3 -- Accelerometer Z Axis  (physical AN3)
        AccelerometerZ = Data(20*[0:samples-1] + 8);
        AccelerometerZ = ((AccelerometerZ * 5 / 1024) - 2.5) / 0.312;
    % Channel 4 -- Accelerometer X Axis  (physical AN4)
        AccelerometerX = Data(20*[0:samples-1] + 10);
        AccelerometerX = ((AccelerometerX .* 5 / 1024) - 2.5) / 0.312;
    % Channel 5 -- Accelerometer Y Axis  (physical AN5)
        AccelerometerY = Data(20*[0:samples-1] + 12);
        AccelerometerY = ((AccelerometerY .* 5 / 1024) - 2.5) / 0.312;
    % Channel 7 -- Gyroscope X Axis  (physical AN7)
        GyroscopeX = Data(20*[0:samples-1] + 16);
        GyroscopeX = ((GyroscopeX .* 5 / 1024) - 2.5) / 0.005;
    % Channel 8 -- Gyroscope Y Axis  (physical AN8)
        GyroscopeY = Data(20*[0:samples-1] + 18);
        GyroscopeY = ((GyroscopeY .* 5 / 1024) - 2.5) / 0.005;
    % Channel 9 -- Gyroscope Z Axis  (physical AN9)
        GyroscopeZ = Data(20*[0:samples-1] + 20);
        GyroscopeZ = ((GyroscopeZ .* 5 / 1024) - 2.5) / 0.005;

    % Time
        Time = [0:samples - 1] / SampPerSec;
        endTime = (samples - 1) / SampPerSec;

% Plotting
    if (PlotAccel == 1 | PlotAccel == 2)
        figure;
        hold on;

        if (PlotAccel == 2)                                          % X-axis Testing?
            subplot(3,1,1);
            plot(Time, AccelerometerX,   'R');                       % yes, lets play with this a bit
            legend( 'X Axis Unfiltered' );
            ylabel( 'Linear Acceleration (g)' );
            xlabel( 'Time (sec)' );
            title( 'Accelerometer' );

            subplot(3,1,2);
            for (i = 1:(samples-16))                                     % yes create running average filter
                avgX(i) = 1/16 .* sum(AccelerometerX(i:(i+16)));
            end
            plot(Time(1:samples-16), avgX,   'B');                   % plot the filtered values
            legend( 'X Axis 8-Point Running Filter' );
            ylabel( 'Linear Acceleration (g)' );
            xlabel( 'Time (sec)' );
            title( 'Accelerometer (Filtered)' );
```

```
            subplot(3,1,3);
            tilt = asin(avgX)*180/pi;                                   % A = sin(theta) ==> theta = asin(A
) in radians
            plot(Time(1:samples-16), tilt,   'B');
            legend( 'X Axis Tilt (using Filtered)' );
            ylabel( 'Tilt (degrees)' );
            xlabel( 'Time (sec)' );
            title( 'Tilt');

            figure;
            plot(Time(1:samples-16), tilt,   'B');
            legend( 'X Axis Tilt (using Filtered)' );
            ylabel( 'Tilt (degrees)' );
            xlabel( 'Time (sec)' );
            title( 'Tilt');
        else                                                            % nope, just finish plotting
            plot(Time, AccelerometerX,   'R');
            plot(Time, AccelerometerY,   'G');
            plot(Time, AccelerometerZ,   'B');
            legend( 'X Axis', 'Y Axis', 'Z Axis');
            ylabel( 'Linear Acceleration (g)' );
            xlabel( 'Time (sec)' );
            title( 'Accelerometer Tilt Measurement' );
        end
    end

    if (PlotMagnet == 1)
        figure;
        hold on;
        plot(Time, MagnetometerX,   'R');
        plot(Time, MagnetometerY,   'G');
        plot(Time, MagnetometerZ,   'B');
        ylabel( 'Magnetic Field Strength (gauss)' );
        xlabel( 'Time (sec)' );
        legend( 'X Axis', 'Y Axis', 'Z Axis');
        title( 'Magnetometers' );
    end


    if (PlotGyro == 1)
        figure;
        hold on;
        plot(Time, GyroscopeX,   'R');
        plot(Time, GyroscopeY,   'G');
        plot(Time, GyroscopeZ,   'B');
        ylabel( 'Angular Velocity (degrees/sec)' );
        xlabel( 'Time (sec)' );
        legend( 'X Axis', 'Y Axis', 'Z Axis');
        title( 'Rate Gyroscopes' );
    end

    if (PlotAll == 1)
        figure;

        subplot(3,1,1);
        hold on;
        plot(Time, AccelerometerX,   'R');
        plot(Time, AccelerometerY,   'G');
        plot(Time, AccelerometerZ,   'B');
        ylabel( 'Linear Acceleration (g)' );
        xlabel( 'Time (sec)' );
        legend( 'X Axis', 'Y Axis', 'Z Axis');
        title( 'Accelerometers' );

        subplot(3,1,2);
        hold on;
        plot(Time, GyroscopeX,   'R');
        plot(Time, GyroscopeY,   'G');
        plot(Time, GyroscopeZ,   'B');
        ylabel( 'Angular Velocity (degrees/sec)' );
        xlabel( 'Time (sec)' );
        legend( 'X Axis', 'Y Axis', 'Z Axis');
        title( 'Rate Gyroscopes' );

        subplot(3,1,3);
        hold on;
        plot(Time, MagnetometerX,   'R');
        plot(Time, MagnetometerY,   'G');
        plot(Time, MagnetometerZ,   'B');
        ylabel( 'Magnetic Field Strength (gauss)' );
        xlabel( 'Time (sec)' );
        legend( 'X Axis', 'Y Axis', 'Z Axis');
        title( 'Magnetometers' );
    end

return
```